**Universidade de Aveiro** Departamento de Ciências Médicas
**2021**

**ANA SOFIA MARQUES JOAQUINITO**

# APLICAÇÕES BIOMÉDICAS DE MATERIAIS FOTOATIVOS À BASE DE AMIDO

# BIOMEDICAL APPLICATIONS OF STARCH-BASED PHOTOACTIVE MATERIALS

Universidade de Aveiro Departamento de Ciências Médica
2021

**ANA SOFIA MARQUES JOAQUINITO**

# APLICAÇÕES BIOMÉDICAS DE MATERIAIS FOTOATIVOS À BASE DE AMIDO

# BIOMEDICAL APPLICATIONS OF STARCH-BASED PHOTOACTIVE MATERIALS

Dissertação apresentada à Universidade de Aveiro para cumprimento dos requisitos necessários à obtenção do grau de Mestre em Biomedicina Molecular, realizada sob a orientação científica da Professora Doutora Maria do Amparo Ferreira Faustino, Professora Auxiliar do Departamento de Química da Universidade de Aveiro, Professora Doutora Maria Adelaide de Pinho Almeida, Professora Catedrática do Departamento de Biologia da Universidade de Aveiro, e da Professora Doutora Susana Cecília de Brito Gomes Guerreiro, Professora Convidada da Faculdade de Medicina da Universidade do Porto e Instituto de Investigação e Inovação em Saúde da Universidade do Porto.

Dedico este trabalho a todos os que fazem os meus dias felizes e coloridos, e a todos os que de uma maneira ou de outra me ajudaram na concretização desta jornada no meu percurso académico.

**o júri**

presidente

Professora Doutora Ana Margarida Domingos Tavares de Sousa
professora auxiliar em regime laboral, da Universidade de Aveiro

Professora Doutora Maria do Amparo Ferreira Faustino
professora auxiliar da Universidade de Aveiro

Doutora Francesca Giuntini
lecturer of Liverpool John Moores University

**agradecimentos**

É impossível realizar qualquer trabalho ambicioso sem ajuda e colaboração, e portanto só tenho muitos a quem agradecer.

À Dr.ª Amparo Faustino, o meu profundo obrigado por me ter recebido na sua equipa e no seu laboratório, por todo o apoio e motivação, e pela extraordinária e admirável capacidade de resolução de problemas.

À Dr.ª Adelaide Almeida, por me ter recebido no seu laboratório mesmo numa altura complicada e de restrições, e me ter ajudado a prosseguir o meu caminho.

À Dr.ª Susana Guerreiro, por me ter acolhido e acompanhado, e me ter ensinado a olhar para células.

À Dr.ª Idalina Gonçalves e o seu grupo, pela disponibilização do material usado.

À Cristina Dias, ao Carlos Monteiro, e à Ana Rita Monteiro, por todo o auxílio nesta viagem pelo mundo das porfirinas.

À Maria Bartolomeu, pelo interesse, pela ajuda, pela companhia, e por sempre se assegurar que nada me falte.

Aos meus pais, pelo apoio e por estarem sempre presentes mesmo não podendo estar presentes.

Aos meus avós, por me ajudarem em tudo o que podem mesmo quando eu digo que não é preciso.

Ao Alexandre Rocha e à Snu, por me aturarem com uma paciência invejável, mesmo nos dias mais stressantes, e como uma pitada de magia tornar tudo um pouco melhor.

Não teria sido possível sem qualquer um destes, obrigado.

**palavras-chave**

Terapia fotodinâmica, biomateriais, amido, atividade antimicrobiana, viabilidade celular, regeneração de feridas, diabetes;

**resumo**

A centralidade que a luz apresenta na vida do ser Humano desde a antiguidade até à sua utilização em aplicações industriais e biomédicas faz com que esta continue a ser objeto de intensa investigação.
O conhecimento das suas propriedades e da forma como afeta o ambiente e os seres vivos permite encontrar novas aplicações nomeadamente biomédicas. A terapia fotodinâmica é reconhecida desde finais da década de 70 como uma abordagem promissora no tratamento de neoplasias. Esta abordagem terapêutica tira partido da interação da luz com compostos fotossensíveis designados de fotosensibilizadores que na presença de oxigénio molecular produzem espécies reativas de oxigénio capaz de levar à morte celular de células tumorais. Das células tumorais às células microbianas foi um passo, e esta abordagem fotodinâmica tem sido muito bem sucedida nomeadamente utilizando porfirinas como fotosensibilizadores, na inativação de microorganismos incluindo estirpes microbianas multi-resistentes aos agentes antimicrobianos convencionais (eg. antibióticos, antifúngicos, etc). Com o aumento da resistência microbiana aos antimicrobianos convencionais e o surgimento crescente de condições crónicas como diabetes e as suas complicações, torna-se imperativo encontrar novas terapias que permitam tratar e melhorar a qualidade de vida dos pacientes. Este estudo teve como objetivo avaliar a possibilidade de utilizar materiais baratos, como seja o amido, para suportar derivados porfirínicos e desta forma produzir materiais fotoactivos com capacidade de atuar como fotosensibilizadores e inactivarem comuns infeções de pele como sejam as provocadas por *Staphylococcus aureus* resistente à meticilina (MRSA) e *Pseudomonas aeruginosa* e que surgem em úlceras de diabéticos, e mais do que isso, avaliar a sua capacidade de promoverem a regeneração de tecidos. As porfirinas selecionadas para incorporar no amido foram a porfirina catiónica 5,10,15,20-tetraquis(1-metilpiridinium-4-il)porfirina (TMPyP) e porfirina neutra 5,10,15,20-tetraquis(pentafluorofenil)porfirina (TPP5F) que foram preparadas e posteriormente imobilizadas nos materiais à base de amido. Os filmes fotoactivos preparados por incorporação de porfirina em amido, foram então testados e as suas propriedades antimicrobianas em estudos *in vitro* e *ex vivo* avaliadas. O filme à base de amido com a TMPyP incorporada revelou promissora atividade antimicrobiana sendo que conseguiu inativar a *S. aureus* (MRSA), tanto *in vitro* como *ex vivo*, após exposição a luz branca com uma irradiância de 50 mW $cm^{-2}$ por 60 min e 24h, respetivamente. Utilizando pele de porco como um modelo de infeção de pele, este filme contendo TMPyP revelou potencial em prevenir a instalação de infeções bacterianas.
Para avaliar a biocompatibilidade dos filmes de amido-porfirina preparados e possíveis efeitos estimulantes na regeneração de tecidos, foram realizados estudos *in vitro* em linhas celulares de fibroblastos (HDF) e células endoteliais (HMEC), dois componentes importantes da regeneração de tecido e cura de feridas. Quatro parâmetros diferentes foram testados: viabilidade celular,

migração celular, formação de ROS e adesão celular. Para tal os filmes à base de amido-porfirinas foram aplicados e irradiados com luz vermelha proveniente de um sistema LED com uma irradiância de 5 mW $cm^{-2}$ por 15 min. Os filmes de dimensões 7.06 $mm^2$ revelaram os melhores resultados nos ensaios de viabilidade celular, e as células nestas condições apresentam elevada quantidade de ROS celular. A aplicação de luz parece ter influenciado todos os parâmetros exceto a formação de ROS. A luz vermelha em baixa dose parece influenciar positivamente a viabilidade e regeneração em células endoteliais, revelando-se um potencial promotor de vascularização. Os resultados obtidos com os filmes amido-porfirina permitem perspetivar a sua potencial aplicação no tratamento de feridas/úlceras de diabéticos.

**keywords**

Photodynamic therapy, biomaterials, starch, antimicrobial activity, cellular viability, diabetes

**abstract**

The centrality that light presents in the human being's life since antiquity to its use in industrial and biomedical applications makes it a topic of intense research. The knowledge of its properties and the way it affects the environment and living beings allows us to find new applications, namely biomedical. Photodynamic therapy is known since the end of the 1970's as a promising approach in the treatment of neoplasia. This therapeutic approach takes advantage of light's interaction with photosensitive compounds, named photosensitizers, which in the presence of molecular oxygen produce reactive oxygen species capable of leading tumoral cells to cellular death. From tumoral cells to microbial cells was only a step, and this photodynamic approach has proved very successful, more specifically using porphyrins as photosensitizers, in inactivating microorganisms, including microbial strains multi-resistant to conventional antimicrobial agents (e.g., antibiotics, antifungals). With the rise of microbial resistance to conventional antimicrobials and increasing emergence of chronical conditions such as diabetes and its complications, it becomes imperative to find new therapies which allow to treat and help meliorate patients' quality of life.

The goal of this study was to evaluate the possibility of using cost-friendly materials, such as starch, to support porphyrinic derivatives and in this way to produce photoactive materials with the ability to act as photosensitizers and inactivate common skin infections such as the ones incited by methicillin-resistant *Staphylococcus aureus* and *Pseudomonas aeruginosa*, and which arise in diabetic ulcers, and furthermore to evaluate its ability to promote tissue regeneration. The porphyrins selected to incorporate in starch were cationic porphyrin 5,10,15,20-tetrakis(1-methylpyridinium-4-yl)porphyrin (TPP5F) and neutral porphyrin 5,10,15,20-tetrakis(pentafluorophenyl)porphyrin (TMPyP) which were prepared and later immobilized in the starch-based materials. The photoactive films prepared by incorporation of porphyrin in starch were then tested and their antimicrobial properties evaluated in *in vitro* and *ex vivo* studies.

The TMPyP incorporated starch-based film revealed promising antimicrobial activity as it was able to inactivate *S.aureus* (MRSA), both *in vitro* and *ex vivo,* after white light exposure with an irradiance of 50 mW $cm^{-2}$ for 60 min and 24h, respectively. Using porcine skin as skin infection model, this TMPyP film revealed potential in preventing the onset of bacterial infections. To evaluate the biocompatibility and possible stimulating effects in tissue regeneration of the starch/ porphyrin films, *in vitro* studies were conducted in cell lines of fibroblasts (HDF) and endothelial cells (HMEC), two important components of tissue regeneration and wound healing. Four different parameters were tested: cellular viability, cellular migration, ROS formation and cellular adhesion. For that, the starch/porphyrin-based materials were applied and irradiated with a red light from a LED system with an irradiance of 5 mW $cm^{-2}$ for 15 min. The films of 7.06 $mm^2$ revealed the best results in viability and at these conditions

the cells present high levels of cellular ROS. The application of light seems to have influenced all parameters except ROS formation. Low dose red-light seems to positively influence viability and wound healing in endothelial cells, revealing itself as a potential promoter of vascularization. The results obtained with the starch/porphyrin films allow for a perspective of their potential application in the treatment of diabetics' wounds/ulcers.

## Table of Contents

## Table of Figures

### Chapter 1.



### Chapter 2.

**Table of Tables**

**Chapter 1**



**Chapter 3**

**Abbreviation List**

**ALT** Alanine Amino Transferase

**aPDT** Antimicrobial Photodynamic Therapy

**ATP** Adenosine Triphosphate

**AzA** Azure A

**CD** Carbon Dot

**CFU** Colony Forming Units

**Cu(II)TCPP** 5,10,15,20-tetrakis(4-carboxyphenyl)porphyrinatecopper(II)

**DCFDA** 2',7'-dichlorofluorescein diacetate

**DFI** Diabetic Foot Infection

**DFU** Diabetic Foot Ulcer

**DM** Diabetes Mellitus

**DNA** Deoxyribonucleic Acid

**DPP4** Dipeptidyl Peptidase-4

**ECM** Extracellular Matrix

**ECSOD** Extracellular Superoxide Dismutase

**FDA** Food and Drug Administration

**Ga-PP-IX** Galium-Protoporphyrin-IX

**HA** Hyaluric Acid

**HDF** Human Dermal Fibroblasts

**hiPSC** Human Induced Pluripotent Stem Cell

**HMEC** Human Microvascular Endothelial Cells

**HO-1** Heme Oxygenase-1

**I/R** Ischemia and Reperfusion

**IL-1** Interleukin -1

**ISC** Intersystem Crossing

**KS** Keratin Sponges

**LED** Light Emitting Diode

**LLLT** Low-Level Laser Light Therapy

**MB** Methylene Blue

**MBC** Minimum Bactericidal Concentration

**MDA** Malondialdehyde

**MIC** Minimum Inhibitory Concentration

**Mn(III)TMPyP** 5,10,15,20-tetrakis(1-methylpyridinium-4-yl)porphyrinatemanganese(III) chloride

**MnTBAP** 5,10,15,20-tetrakis(4-carboxyphenyl)porphyrinatemanganese(III) chloride

**MOF** Metal-Organic Framework

**MPS** Methylprednisolone

**MRSA** Methicillin Resistant *Staphylococcus aureus*

**MTS** 3-(4,5-dimethylthiazol-2-yl)-5-(3-carboxymethoxyphenyl)-2-(4-sulfophenyl)-2H-tetrazolium

**NIR** Near Infrared

**NO** Nitric Oxide

**NPWT** Negative Pressure Wound Therapy

**NSC** Neural Stem Cells

**PB** Prussian Blue

**PBM** Photobiomodulation

**PBP2a** Penicilin-binding Protein

**PBS** Phosphate Buffer Saline

**Pcs** Phthalocyanines

**PDE5** Phosphodiesterase 5

**PDT** Photodynamic Therapy

**Pheo *a*** Pheophorbide *a*

**PP-IXArg$_2$** Protoporphyrin IX Diarginate

**PS** Photosensitizer

**QD** Quantum Dot

**ROS** Reactive Oxygen Species

**SA** Serum Albumin

**SB** Stratum Basale

**SGLT2** Sodium-Glucose Co-Transporter-2

**SGr** Stratum Corneum

**SOD** Superoxide Dismutase

**SS** Stratum Spinosum

**TBO** Toluidine Blue

**TGF-β1** Transforming growth factor Beta 1

**TMPyP** 5,10,15,20-tetrakis(1-methylpyridinium-4-yl)porphyrin

**TNF-α** Tumour Necrosis Factor Alpha

**TPP5F** 5,10,15,20-tetrakis(pentafluorophenyl)porphyrin

**TPS** Thermoplastic Starch

**TriMPyP** 5-phenyl-10,15,20-tris(1-methylpyridinium-4-yl)porphyrin trichloride

**TTFAP** 5,10,15,20-tetrakis [4-[2-(*N,N,N*-trimethylammonium)ethyl]thio]-2,3,5,6-tetrafluorophenyl]porphyrin tetraiodide

**TZDs** Thiazolidinediones

**WHO** World Health Organization

# Chapter 1. Introduction

## *1. Diabetes Mellitus*

### 1.1. A Brief Overview

What we now call Diabetes mellitus (DM) has been around for long enough to have been once characterized as 'the honey urine' disease and described in ancient Egyptian manuscripts as a 'too great emptying of urine' [1]. Nowadays, it is defined as a clinical condition marked by the deficiency of insulin secretion or action in the body, resulting in high levels of blood glucose [2][3]. In 2016, the World Health Organization (WHO) has attributed 1.6 million deaths worldwide to DM and it is considered one of the largest global health emergencies of the 21$^{st}$ century [4][3]. Insulin, a small globular protein containing two chains with 21 and 30 amino acid residues, is a hormone normally produced by pancreatic β-cells, which functions are intimately linked with energy availability for the body [5], [6]. There are three main types of DM: type 1, type 2 and gestational DM. Type 1 DM typically manifests in early childhood and adolescence and is characterized by an absolute insulin deficiency caused by T-cell-mediated autoimmune destruction of pancreatic β-cells [7]. Type 2 DM is characterized by insulin insensitivity as a result of insulin resistance, declining insulin production, and eventual pancreatic β-cell failure [8]. This the most common DM type and accounts for about 90-95% of the diagnosed cases of DM [3]. Lastly, gestational DM is a pregnancy complication in which hyperglycemia develops spontaneously during the second or third trimester [9]. This condition constitutes a serious risk for the women with gestational DM and for the offspring to develop type 2 DM, in the future [3]. A combination and interaction of genetic factors, environmental (including obesity, and pollution) and lifestyle can contribute to the development of DM [10]. According to the International Diabetes Federation the number of diabetes cases will increase in next years, predicting 592 million total cases and 175 million undiagnosed cases in 2035 [11]. These values are sufficiently scarring to require the improvement understanding of the pathology and new therapies for it and its complications so that a better quality of life can be provided for the DM affected.

### 1.2. Complications of Diabetes Mellitus: The diabetic foot

The Diabetes Mellitus disease leads to imbalance and a number of physiological complications due to the consistently high levels of glucose in the blood. Hypoglycemia, ketoacidosis or chronic, debilitating complications affecting multiple organ systems, like retinopathy, nephropathy, neuropathy, and

cardiovascular disease are some of the acute to life-threatening conditions found in DM patients [12]. Left uncontrolled, the problems can achieve even more serious proportions. The end-stage consequences of diabetic complications can include severe vision loss, severe renal disease (with need for dialysis or transplant), myocardial infarction and stroke and amputations [12]. Though consistent and persistent hyperglycemia is the main responsible for DM complications, a lot of them are found to be exacerbated by other co-pathologies [12]. In fact, most researchers find clinical evidence pointing to a higher prevalence of infectious diseases among individuals with DM than non-diabetic individuals [2].

From the various complications of diabetes, the diabetic foot is perhaps one of the most devastating. The diabetes foot becomes affected by ulceration that is associated with neuropathy and/or peripheral arterial disease of the lower limb [13]. The nerve dystrophy acquired by diabetic patients causes, among others, muscle weakness, atrophy and loss of protective sensation of pain, pressure and heat. Coupled with an inadequate blood supply to the lower limbs these constitute ideal conditions for foot ulcerations to occur [13]. About 4-10% of the diabetic population develops diabetic foot ulceration, and 5-24% of foot ulcers will eventually lead to limb amputation [13]. According to the available data provided by International Diabetes Federation, every 30 s a lower limb or part of a lower limb is lost to amputation somewhere in the world as a consequence of DM [14]. Once an amputation has taken place, it is reported a 50% chance of developing an ulcer in the contralateral limb within 5 years [15]. An infection of the ulcer can ultimately increase the chances of an amputation, especially in patients with peripheral arterial disease [13]. The severity of this condition on patients includes not only financial burdens but also serious psychological stress and quality of life decrease.

Diabetic foot infections (DFI) are of one of the most common consequences of DM that lead to hospitalization and are the most common precipitating event leading to lower limb amputation [16]. It seems that most mild infections are usually monomicrobial, with gram-positive *cocci* as culprits, such as *Streptococcus* species and *Staphylococcus aureus,* while the more severe and more complicated to treat forms of DFIs (often found in deep or chronic wounds) are polymicrobial and caused by gram-negative *bacilli* (such as *Klebsiella* species, *Escherichia coli,* and *Pseudomonas* species), aerobic gram-positive *cocci* and anaerobes [17]. There is an increase in prevalence of resistant strains, due partly to over-use of antibiotics and broad-spectrum antibiotics, which poses a large concern for these already difficult to treat conditions. Machado *et al.* report a prevalence of 40% of Methicillin Resistant *Staphylococcus aureus* strain

(MRSA), in their study of diabetic foot infections in a Portuguese tertiary center, for 2016 [16].

### 1.3. Current Treatments and Therapy Strategies

After a DM diagnosis, a treatment is required for a balanced and controlled life. To maintain a steady metabolic control over the disease, are required, besides the pharmacological treatment, changes in lifestyle, such as an adequate sleep time, controlled diet, alcohol consumption and structured exercise [18]. The pharmacological drug approach sees insulin injection as a main treatment for Type 1 DM, where an insulin deficiency is seen, and often as a monotherapy or combined with hypoglycemic drugs for Type 2 DM when these are not being successful in regularizing glucose levels by themselves. Moreover, Metformin and Thiazolidinediones (TZDs) (Fig. 1) are commonly prescribed antidiabetic drugs, working to increase insulin sensitivity, while Dipeptidyl peptidase-4 (DPP4) inhibitors and sodium-glucose co-transporter-2 (SGLT2) inhibitors can be prescribed to increase insulin production and boost glucose elimination. Often a combination therapy is needed to adequately control blood glucose, and is implemented when monotherapy is no longer sufficient [5].

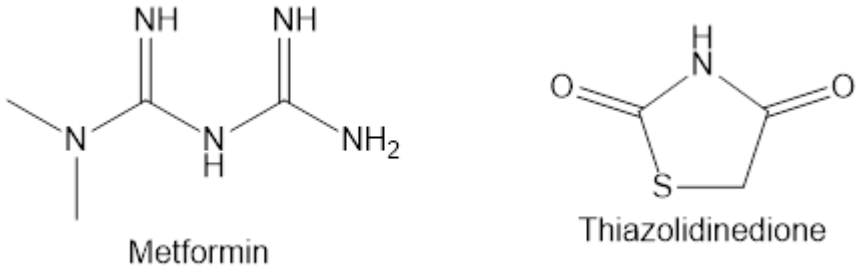


**Fig. 1.1** – Structures of Metformin and Thiazolidinedione, common antidiabetic drugs.

In the case where a foot ulcer develops and is diagnosed, treatment generally includes debridement of the wound (eliminating necrotic tissues and surface debris), management of any infection, revascularization procedures, and off-loading of the ulcer (readjusting the pressure, weight, and balance of the foot) [13]. Debridement of the wound is usually a key step in diabetic foot ulcers' management, but there still seems to be some debate as to the best methodology to follow. Maggot debridement therapy has been suggested as a selective method for the diabetic chronic ulcers [19]. This entails the application of live maggots on wounds as a way to get rid of the necrotic tissue. The maggot has been found to not only help debridement but also stimulate wound healing (through the production of granulation tissue) and disinfect [19]. In another important aspect of diabetic foot ulcer management, the need for

revascularization of the diabetic foot stems from a vascular inefficiency which then reduces tissue oxygenation and can be achieved through procedures such as bypass surgery or hyperbaric oxygen treatment. Recently, a therapy using phosphodiesterase 5 (PDE5) inhibitors, a common treatment for pulmonary hypertension, cardiac insufficiency and erectile dysfunction, has been proposed for the same purpose [20].

Often, the open and chronic foot wounds are infected by bacteria. The presence of an infection, or DFI, requires a management wound healing through the use of antimicrobial agents, optimization of glycemic control and possibly effective surgery. Surgery provides a way to control infection, prevent it from spreading and preserve functionality of the limb. This means that amputation may be needed to save a patient's life as a serious infection treatment [21]. As previously mentioned, the misuse of antibiotics and large use of broad-spectrum ones have contributed to the rise of resistant strains of bacteria. This, in turn, makes antibiotic treatment ineffective in curing DFIs and increases the probability of resorting to amputation as infection control. The options to treat DFUs and DFIs seem to have limited efficacy and are not tailored to each patient. Often the patient's poor vascularization issues result in difficulty for the antimicrobial to reach the infected area, making treatment even more challenging. Overall, the management of diabetic foot ulcers remains a therapeutic challenge which requires further investigation for efficient and cost-effective ways to promote healing. The rise of problems such as multidrug-resistant bacteria, the inherent complicated nature of the condition and the times which we live in, with pandemics slowing research and interfering with the normal therapy routines of patients, posing further risks and complications to their recovery, the need to provide new insight and treatment options is paramount.

## 2. Photodynamic Therapy

### 2.1. General Concept

Photodynamic therapy (or PDT) has been used for many years as a cancer therapy and is already an approved approach to treat some oncologic and non-oncological conditions although the first evidence of the photodynamic action was in the presence of a paramecia. Nevertheless, PDT has been gaining popularity for its antimicrobial properties.

Microorganisms have the ability to evolve and select for immunity to antimicrobial drugs that target them and some strains have done so from the beginning of the “antibiotic era” including to most antibiotics available from the 1970s until the present [22][23]. It is estimated that by 2050, deaths due to antimicrobial resistance will exponentially rise above 10 million deaths per year, surpassing the current number of 700,000 deaths per year [22]. Therefore, alternate methods and treatments against resistant microorganisms are needed and antimicrobial photodynamic therapy (or aPDT) may prove to be an available solution. Photodynamic action can be described as a photochemical reaction used to selectively destroy cells [24]. The principle of aPDT is based on three major components: the photosensitizer (PS), light, and dioxygen. In the singlet ground state, the PS molecule has two electrons with opposite spins which absorb a photon with the appropriate quantum energy (wavelength) and is promoted from the ground singlet state ($S_0$) to an unstable, excited singlet state ($S_n$). When in this unstable state it can then lose energy and return to the ground state ($S_0$) by fluorescence light emission (radiative process) or by heat via internal conversion (non-radiative process) as demonstrated by the simplified Jablonski

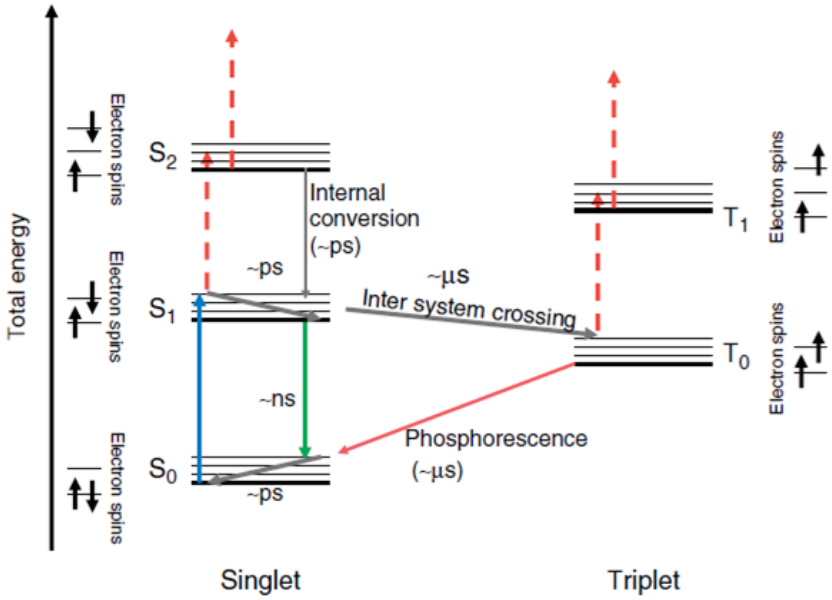


**Fig. 1.2-** The Modified Jablonski diagram of states (adapted from [25]).

diagram Fig. 1.2 [25]. Instead of these two decay processes it can also convert to a longer-living and more stable excited triplet state ($T_1$) through an intersystem crossing (ISC process), and return from here to the ground state ($S_0$) through a radiative process of phosphorescence emission or interact with surrounding molecules by two mechanisms (Type I and Type II) generating reactive oxygen species (ROS) (free radicals and singlet oxygen).

In a Type I reaction, the excited state PS ($T_1$) undergoes an electron transfer reaction for surrounding substrates (e.g. amino acid residues), that eventually leads to the formation of ROS. These electron transfer reactions can involve either donation or acceptance of electrons to form radical anions or cations. A superoxide radical anion ($O_2^{\cdot -}$) can be produced by the reaction of the radical anion with dioxygen, or dismutation can occur forming hydrogen peroxide ($H_2O_2$), a precursor to free hydroxyl radicals ($HO^{\cdot}$), highly reactive radicals and powerful oxidants [26][23]. In a Type II reaction, energy is transferred to the ground state molecular oxygen forming singlet oxygen ($^1O_2$). Singlet oxygen is a highly electrophilic entity and can interact with various enzymes. All these different ROS can oxidize various biological molecules, such as proteins, nucleic acid and lipids, leading to cell death and destruction of the microorganisms [27]. The lifetime of $^1O_2$ is very short (~10-320 ns), limiting its diffusion to only approximately 10-55 nm in cells, and so, photodynamic damage is likely to only occur at very close proximities to the intracellular location of the PS where the $^1O_2$ is produced [26].

**Type I Reaction**

$PS\ (T_1) + Biomolecule \rightarrow PS^{-}\bullet + Biomolecule^{+}\bullet$

$PS^{-}\bullet + O_2 \rightarrow PS\ (S_0) + O_2^{-}\bullet$

**Type II Reaction**

$PS\ (T_1) + {}^3O_2 \rightarrow PS\ (S_0) + {}^1O_2$

**Fig. 1.3 –** Representative equations of Type I and Type II photosensitized reactions.

## 2.2. Photosensitizers

The photodynamic effects depend on a multitude of variables which include the structural features of the PS, its aggregation state in solution, PS concentration, contact time with cell, dioxygen concentration, and the parameters of the light used. A change in any of these conditions will result in a different rate of photoinactivation [28], [29]. Over the years, a large number of PS, with varying structures, have been found and designed to target and kill a broad range of microorganisms, including bacteria, fungi, viruses and parasites [30]. The ideal PS (for clinical purposes, non-tumoral) must have some key requirements, among them not be toxic or create new toxic byproducts, not be mutagenic or carcinogenic, to have some selectivity or targetability to the target cells, to have a reliable activation, a versatile and easy administration procedure, to be available , not expensive and to be biocompatible [31].

Among the known PS structures, the most used PS comprise the group of tetrapyrrole structures in which are included the porphyrins, chlorins, corroles, phthalocyanines, bacteriochlorins and isobacteriochlorins. (Shown in Fig. 2 and Fig. 3). Porphyrins are highly colored aromatic macrocycles that occur abundantly in nature and play many important roles in biological systems, such as the heme, the prosthetic group (a porphyrin iron complex), of hemoglobin and myoglobin and involved in dioxygen transport and storage, respectively, or in chlorophylls (chlorin magnesium complex), essential to plants for the photosynthesis process (Fig. 4) [26], [32].

Porphyrins absorb in the visible region, which makes them adequate candidates for photochemical reactions in living tissues. They are pH-dependent photoactive chromophores, typically with an intense absorption band between 380-500 nm (Soret band) corresponding to a $S_0 \rightarrow S_2$ transition and absorption bands between 500-750 nm (Q band) corresponding to a weak transition ($S_1 \rightarrow S_0$) [33] [34]. Chlorins are reduced porphyrinic macrocycles, also called dihydro-type porphyrins, and so they exhibit similar photophysical properties, but have enhanced red-shifted Q bands [35]. Their photophysical and biological properties offer many advantages for PDT, including red absorption, which allows deeper penetration into tissues, high $^1O_2$ quantum yield, rapid body clearance and low dark toxicity. Their main limitation being their poor water solubility, which lowers their biocompatibility [36].

Bacteriochlorins and isobacteriochlorins resemble chlorins in structure, once they are reduced macrocycles they have two reduced pyrroles when compared with the full oxidized system of the porphyrin (Fig. 2) [37]. They can be naturally occurring, in the form of bacteriochlorophylls, for instance, or prepared in the lab synthetically, and they can absorb NIR photons in the range of 700-900 nm. They reveal, in general, low cytotoxicity in the dark and their ability to absorb in the near-infrared region conveys them the potential to deeply penetrate living tissues. However, the naturally occurring bacteriochlorins are found to be the least stable of the group of tetrapyrrolic structures, being very sensitive to oxidation, and, so, much effort is put into designing synthetic stable bacteriochlorins [38]. Similarly, isobacteriochlorins are almost identical to bacteriochlorins, except their two reduced pyrrolic units are in adjacent rather than opposing positions (Fig. 2) Considering among the tetrapyrrolic PS, that porphyrins are perhaps the most studied group, having demonstrated efficacy in many applications, and easily structurally modulated envisaging their potential application in new areas, they are the PS of interest in this work. Phthalocyanines (Pcs), like the other structures here discussed, are symmetrical macrocycles, with intense absorption in the visible range of ~650-750 nm [39]. In fact, Pcs have some advantages when

compared to porphyrins, such as their strong absorption in the red region, and by coordinating them with metals like Zn, Al and Si, it seems to yield a higher $^1O_2$ generation quantum yield [40]. Also, their four fused benzenoid aromatics grants them excellent thermal and chemical stability, making them desirable for many applications such as organic solar cells, cancer PDT, and near-IR imaging [39], [41].

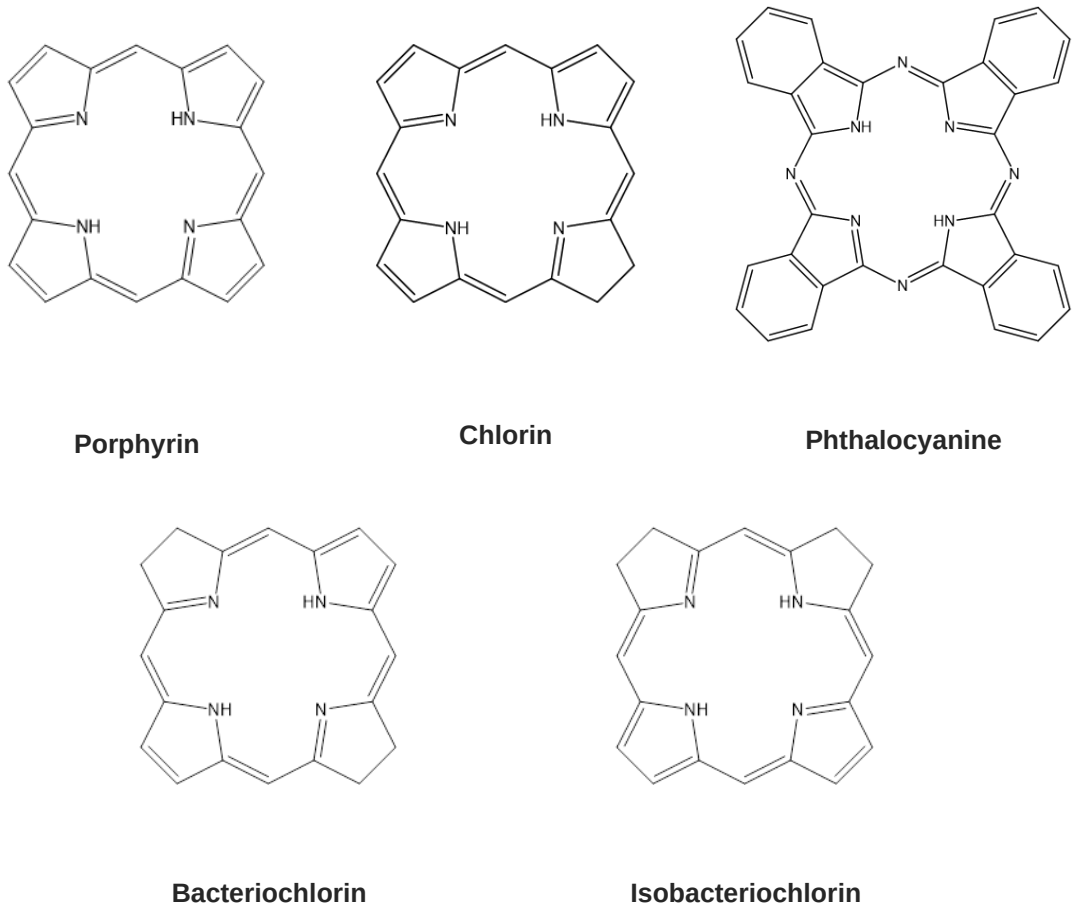


**Fig. 1.4**- Chemical structures of porphyrin, chlorin, phthalocyanine, bacteriochlorin and isobacteriochlorin.

## 2.3. Photosensitizer Delivery

The delivery of the PS in the biological system may be done in various ways. It can be administered in solution or conjugated with a support. The PS can also be immobilized on a solid support, which confers him surface photoactivity, or loaded into a delivery system [42]. Porphyrins have been known to be grafted onto natural polymers, such as chitosan, cellulose and dextran, and other solid supports, such as polyester isophtalic resin, silicone, cationic nylon, and polyethylene [29], [43]–[45]. It is mostly a question of designing a functional porphyrin support for the envisioned application. For instance, loading the PS into

nanostructures could result in higher local PS concentration, which consequently translates into more effective $^1O_2$ generation and enhanced targeting by light activation [42]. Furthermore, combining semiconductor quantum dots (QD) with porphyrin seems to create functional materials for PDT [46]. In fact, coupling QDs with PS can introduce advantages since they may enable the use of wavelengths at which the PS does not absorb and improve its delivery [47][48]. Among these, photoluminescent carbon dots (CDs) are an emerging carbonaceous nanomaterial that have interesting properties such as water solubility, high photostability and benign biocompatibility. The preparation of porphyrin based carbon dots with good solubility and small size might offer an advantageous alternative way for the application of porphyrins in PDT [49].

## 2.4. PDT in the Healing Process

Besides cancer treatment, inactivation of microorganisms or water disinfection, another possible application for PDT is found in wound healing. By administering a PS topically or systemically and irradiating a wound with light of appropriate wavelength, an effective wound healing can be achieved. This may prove promising, especially in treatment of chronic wounds such as diabetic foot ulcers [50]. The healing of a wound requires a well-orchestrated integration of the complex biological and molecular events of cell migration, cell proliferation, and extracellular matrix deposition. The whole process of wound healing consists of four phases: hemostasis, inflammation, proliferation, and tissue remodeling or resolution. These stages are not to be seen as a linear succession of separate events with well-defined periods of time, but instead as stages that may overlap over time. Generally, the wounds that demonstrate an impaired healing, including delayed acute wounds and chronic wounds, have failed to progress through these normal stages of healing and may have become stalled in one or more [51][52][53][54]. Most chronic wounds are ulcers, resulting from illnesses or conditions such as ischemia, DM mellitus, venous stasis disease, or high pressure [52]. In the case of DM, there is an impairment of vascular flow, creating a setting of poor tissue oxygenation. This poor perfusion leads to a disrupted healing process and an hypoxic wound [52]. ROS such as hydrogen peroxide ($H_2O_2$) and superoxide anion ($O_2^-$) are thought to act as cellular messengers to stimulate key processes associated with wound healing, including cell motility, cytokine action and angiogenesis. This happens in a normally healing wound, though an increased level of ROS may cause additional tissue damage [52]. Inflammation is a normal part of the wound-healing process and important to remove microorganisms from the affected area. The inflammatory response

involves the activation of immune cells, such as mastocytes, gamma-delta cells, and Langerhans cells, and leads to the release of leukocytes and neutrophils to the site of lesion, which are known for expressing many pro-inflammatory cytokines and highly active antimicrobial substances. However, if an effective decontamination is not achieved, the inflammation may be prolonged since bacteria and endotoxins can lead to a prolonged elevation of pro-inflammatory cytokines such as interleukin -1 (IL-1) and tumour necrosis factor alpha (TNF-α). If this condition persists, the wound may enter a chronic state and fail to heal [53][52]. As the antimicrobial action of aPDT is based on releasing ROS, it has the potential of both enhancing wound healing and decontamination of the site.

## 3. Light therapies in Diabetes

The application of light to treat health conditions is an ancient approach but updated since. Many efforts are done to identify which conditions and disorders it may help, and how. In fact, the use of light, in particular, Low-Level Laser Light Therapy (LLLT), also named PhotoBiomodulation (PBM) is used to increase the health conditions. This approach takes advantage of photons and non-thermal irradiance to alter biological activity by exposing cells or tissue to low-levels of red and near infrared (NIR) light [55]. This means that a low powered laser of 1-1000 mW is used to promote biological reactions at wavelengths from 632 to 1064 nm [56]. Currently, this technique is used in a wide range of applications (e.g. dentistry, orthodontics), [57][58] and has also been found to have beneficial effects on pain, inflammation, and wound healing [59]. The photobiomodulation (PBM) is generated by the absorption of light energy by endogenous photoreceptors in the mitochondria, leading to a production of ROS and ATP and a decrease in oxidative stress [59]. The application of light is usually performed by a low powered laser or LED [60]. Wavelengths used in the range of 390 nm to 600 nm are used to treat superficial tissue, and longer wavelengths in the range of 600 m, to 1100 nm, which penetrate further, are used to treat deeper-seated tissues [55]. Indeed, PBM has been found to enhance cellular proliferation of several cell types such as fibroblasts, endothelial cells and keratinocytes, as well as enhance neovascularization, promote angiogenesis and increase collagen synthesis, aiding in the healing of acute and chronic wounds and decreasing the time of recovery [60][61][62][63].

This approach has already been started for DM. Some authors report having combined these light therapies with classical treatments, such as pharmacological, others have evaluated the effects of an independent treatment. Whether influencing the main disorder of DM or its derived complications, light

therapies, here focusing mainly on PDT and PBM, seem to leave their mark. PBM, for example, has already been shown to positively impact wound healing in diabetic cases, as it seems to decrease the number and the degranulation of mast cells [64], [65], provide shielding for glucose neurotoxicity by inducing anti-apoptotic effects [66], enhance migration and survival of diabetic wounded fibroblasts [67] as well as stimulate their differentiation [68], and even influence and regulate lipid metabolism in insulin-resistant adipocytes. [69] The use of PDT using methylene blue has also been studied for treatment of periodontitis, however the different reported results are somewhat contradictory [70]–[72].

To fully comprehend the extent to which PBM and PDT affect DM, is perhaps the realization of a novel way of treating diabetic patients.

### 3.1. Light as an Adjuvant for Pharmacological Therapy

Some studies have evaluated the effects of photobiomodulation combined with pharmacological therapy terms of wound healing, such as the combination of metformin and photobiomodulation. Reportedly, the addition of PBM to metformin treatment proves a synergistic effect, and results in decreased colony forming units (CFU) of bacteria, accelerated wound healing process, and hastened repair at inflammation and proliferation stages of skin injury repair [73], [74]. Alternatively Chengnan *et al.* proposes a light activatable hydrogel for metformin delivery, to avoid the common side effects reported by patients associated with the oral administration of the drug, which include nausea, abdominal pain and indigestion [75]. The hydrogel permitted to release metformin in a transdermal fashion by intermittent cycles of near-infrared light, demonstrating another example of how light can benefit treatment.

Other combined treatments with either PBM or PDT have been described, such as with adipose derived stem cells [76], mesenchymal stem cells [77], and curcumin [78]–[81], reporting positive effects. However, more and more, the benefits of these light treatments on their own have been brought to attention.

### 3.2. Retinopathy and Neuropathy

The microvascular defects associated with DM result in complications such as diabetic retinopathy and neuropathy. Diabetic retinopathy is marked by the ophthalmological vascular lesions which may result in blindness [82], [83], while in neuropathy there is a progressive degeneration of nerve fibers reaching the sensory, motor and autonomic nerves due to damage of the small blood vessels that supply the nerves [56], [84]. Cheng *et al.* have reported beneficial effects of PBM on the retina, having found that it protected against the reduction of visual

function caused by diabetes in their study with diabetic mice, showing the potential of this therapy as an adjuvant treatment of retinopathy. [85] PBM has also shown its promise in treating neuropathy and benefit nerve regeneration as Anju *et al.* reviews. [56] A reduction in pain seems to be the main effect noted in patients with neuropathy receiving PBM treatment, improving their quality of life [84]. However, other parameters should be further evaluated, as the way PBM specifically modulates nerves and neuron regeneration is not yet fully understood and may provide useful insight into the condition and the ways this therapy may improve it.

### 3.3. Diabetic Wounds (Diabetic Foot Ulcers)

As previously mentioned, it is often the case where DM patients suffer from poor circulation, and in a DFI setting, this poses as an obstacle for drugs to reach the infected area. An option where a treatment could be localized in the affected tissue without the need to resort to the blood stream would be ideal, which is where light therapies such as PDT and PBM gain their appeal.

PBM has more and more been appointed as an effective therapy to reduce pain and benefit tissue repair. In treating the diabetic foot with PBM, some authors have found that the tissue repair process of the foot ulcers is expedited [86], [87] while some even report benefits in the regain of sensitivity in the feet [88]. At the very least, most authors find that the use of red light increases the chance of a positive outcome for the patient and reduce the chance of amputation [89], [90]. Besides the therapeutic advantages, the simplicity of the procedure enables patients to apply them at home, allowing them to take more control of their own health and relieving the burden of health care facilities [91], [92].

Regarding PDT, there are already some reported cases of diabetic ulcers being treated with PDT. A treatment with methylene blue (MB) has revealed effective in reducing the area of diabetic ulcers and accelerated their closure using laser therapy (red light, 660 nm and power ~30 mW) [93]. Using either MB or toluidine blue (TBO), Tardivo *et al.* found excellent results in treating DFUs, even pointing out that classical debridement might not be necessary for patients which undergo PDT [94]. The Zn(II) phthalocyanine RLP068 has also already been tested to treat DFUs, having been found to reduce the microbial load of species most typically found in DFUs and facilitate ulcer healing. [95] Furthermore, it is reported that the combination of PDT and PBM has revealed promising in the treatment of ulcers, as Rosa *et al.* demonstrate. Their study reports the use of curcumin as PS for PDT and PBM (blue light, 450 nm, 30 mW $cm^{-2}$, 12 min, 22 J $cm^{-2}$ and red light, 660 nm, 10 J $cm^{-2}$, respectively), also adding a cellulose membrane to coat

the wound, promoting wound healing, and maintaining favorable conditions. This combination showed positive results as it sped up the healing of pressure ulcers in diabetic patients [96].

The processes and mechanisms of action by which these light therapies work to improve a biological wound setting are complex. This because they may affect many parameters. Fekrazad *et al.,* for example, have found a correlation between the application of red and/or infrared light in tissue wounds and the activation of TGF-β1, which can influence the acceleration, in an early stage, of healing phases [97]. It is also known that the light intensity and laser type/ wavelength used can affect the outcome of the therapy and how the system responds [98], [99]. There is much yet to be studied to define a standardized protocol, regardless, overall, these phototherapies show promise in the treatment of the diabetic foot, as low-cost treatments, with no known adverse effects and which most authors report having a beneficial influence.

## 4. Porphyrins in Wound Healing and Regeneration

The ability to structurally manipulate porphyrins and conjugate them to other molecules or to solid supports provides a versatile multitude of possible applications [100]. Particularly, the *meso*-tetrasubstituted porphyrin derivatives can be very interesting platforms, due to their shape, symmetry and possibility to periphery functionalization. They can be tailored in their optical, electronic or biochemical properties to serve many desired applications [101]. The photophysical and photosensitizing properties of porphyrins and their derivatives show great potential for applicability in fields such as chemistry, biology, medicine, optics, and electronics. They can be used as mentioned above as PS for PDT, for DNA binding and cleavage, or as catalysts for oxidation and reduction chemical reactions. In the medicinal field, they have been tested for imaging [102]–[104], diagnosis and cancer therapy [105], [106], while in the sensors field, taking advantage of their optical and electronic properties, they have been involved with signal transduction, fluorescence, electrical resistance, and capacitance [107]–[110]. Furthermore, metalloporphyrins, being able to coordinate gas molecules such as $CO_2$, and NO, are also used as organic-sensing entities [33],[111],[112].

In Figure 1.5 are represented the structure of the different porphyrinic derivatives contemplated in this review.

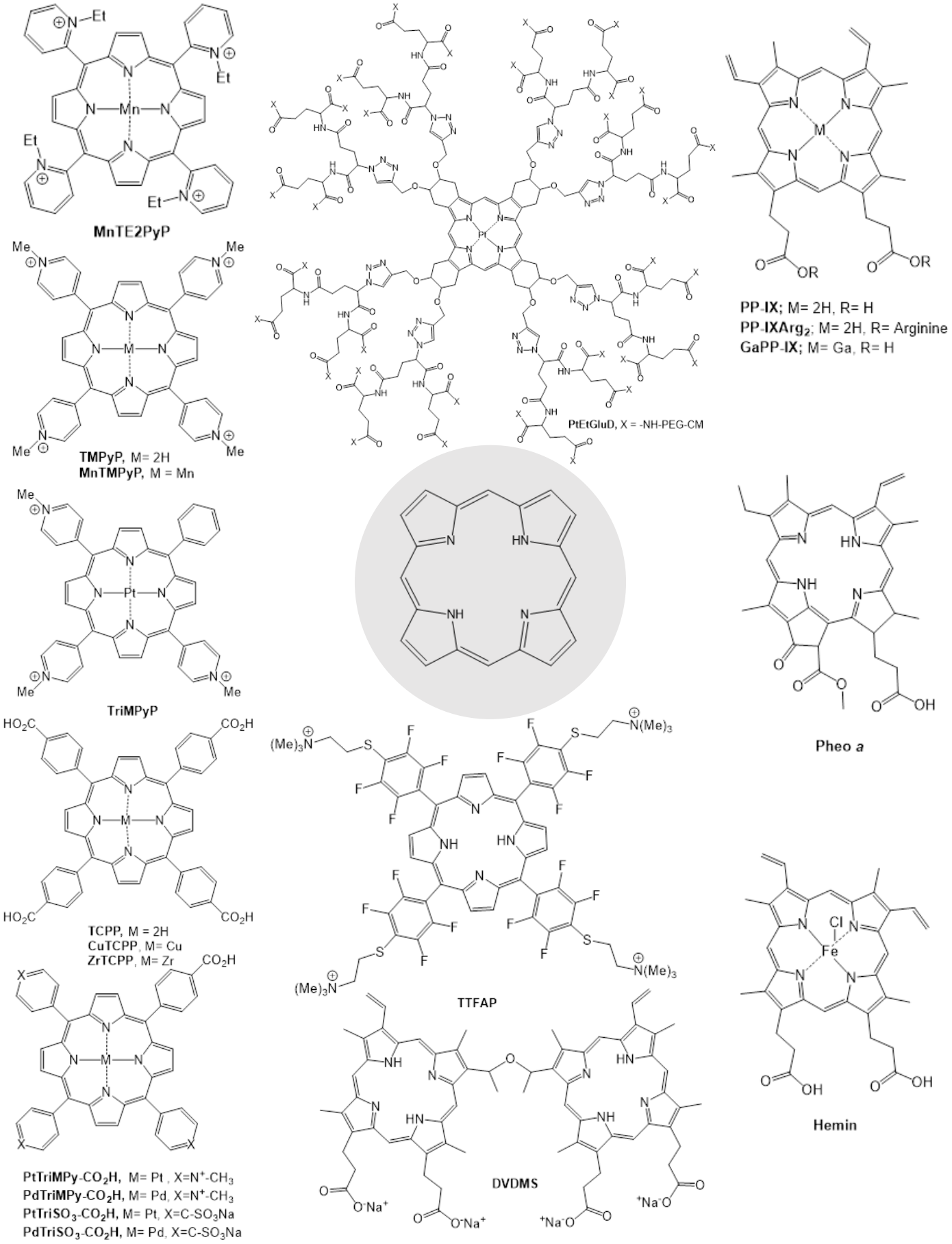


**Fig. 1.5**- Chemical structures of porphyrin derivatives used for wound healing purposes.

## 4.1. Applications of Supported Porphyrins

### *4.1.1. Gels*

To apply a compound in clinical practices, some adaptations may be required in the delivery system, as the compound by itself may not have the required properties for an effective application. Such is the case with Sinoporphyrin sodium (DVDMS), a dimeric porphyrinic PS that produces a high $^1O_2$ quantum yield, fluorescence imaging and antibacterial efficiency, however it is not very stable under physiological conditions and not effectively deposited in a wound setting [113]. Mai *et al.* went around this problem by using a hydrogel-based delivery.

Hydrogels are hydrophilic, environmentally-friendly polymers with three-dimensional polymeric networks, similar to the natural extracellular matrix, which are considered promising biomaterials for wound dressings, drug-delivery and other biomedical applications [114],[113]. Hydrogels can be natural polymer-based, such as chitosan and hyaluronic acid (HA) or synthetic, with poly(vinyl alcohol), for example [115]. In this particular case, Mai *et al.* used a chitosan-based hydrogel delivery aiming to magnify the photodynamic antibacterial effect and accelerate the wound healing process of burn wound infections. Chitosan, a partially *N*-deacetylated chitin, is a hydrophilic biopolymer which has been used for purposes of wound dressing and tissue regeneration because of its biocompatibility, biodegradability and antimicrobial activity [116],[117]. Here, the hydrogel (a carboxymethyl chitosan- sodium alginate, or CSDP hydrogel) improved the physiological stability of DVDMS and enhanced the treatment effectiveness. Furthermore, the authors report that the hydrogel formulation used displayed excellent biocompatibility, desirable mechanical properties, imaging capabilities and high $^1O_2$ quantum yields. In an *in vivo* burn model, the hydrogel-DVDMS formulations are reported to have augmented wound healing along with photodynamic antimicrobial chemotherapy against *S. aureus* by inhibition of bacterial growth, controlled inflammation, higher collagen deposition and rapid epithelialization [113].

Richter *et al.* also delved into the hydrogels as delivery systems, having preferred, however, a combination of an iron-chelator deferiprone (Def) and the heme-analog gallium-protoporphyrin-IX (Ga-PP-IX) to incorporate in a surgical wound gel (composed of a mixture of dextran-aldehyde, succinyl-chitosan and buffer solution) and assess its activity against *S. aureus* planktonic and biofilm-associated small colony variants (SCVs). Chitosan/dextran-based hydrogels have been developed to aid in post surgeries, reducing the number of adhesions, and having good haemostatic, mucoadhesive, and antimicrobial properties [118]. In their *in vitro* wound model, the Def-GaPP-IX gel formulation showed antibiofilm

effectiveness effect, seeming to complement the wound healing properties of the chitosan/dextran-based gel with antibacterial and antibiofilm activity [119].

**Table 1.1** – Porphyrins in hydrogels used for antibacterial and healing applications.

| PS | Support | Purpose | Conditions | Result | Ref |
|---|---|---|---|---|---|
| **DVDMS** | Hydrogel-based DVDMS/bFGF nanohybrids | Antibacterial activity and accelerate wound healing | [DVDMS] of 2, 5 and 10 µg/mL; Irradiation of 0-30 J $cm^{-2}$ in *S. aureus* Irradiation of 30 J $cm^{-2}$ in mice. | Effective antibacterial effect; Inhibition of biofilm formation; Improvement of wound healing. | Mai *et al.* (2020) [113] |
| **Def-GaPP-IX** | Dextran-aldehyde succinyl-chitosan gel | Potentiate activity of antibiotics | [GaPP] of 100 and 500 µg/mL Not irradiated | Antibacterial and antibiofilm activity against *S.aureus* SCVs Complementation of gel's wound healing properties. | Richter *et al.* (2017) [119] |

### *4.1.2. 3D Scaffolds*

The application of 3D scaffolds has been a huge asset for the tissue engineering field. Regardless of tissue type, the materials designed for use must follow some basic ideal characteristics such as biocompatibility and biodegradability, well summarized by *O'Brien* in his 2011 review [120]. Keratin, the major component of hair, wool, feathers, horns and nails, seems to improve the production of anti-inflammatory cytokines and reduce the amount of pro-inflammatory cytokines, promoting a remodeling response, which can grant some potential for regenerative medicine to this support. Moreover, wool keratin demonstrates an ability to support PSs, conferring the possibility of designing photoactive scaffolds. Thus, Ferroni *et al.* took advantage of this characteristic, designed a photo-activable porous sponge made of wool keratin loaded with two different PSs, Azure A (AzA) (a phenothiazine dye), and 5,10,15,20-tetrakis [4-[2-(*N,N,N*-trimethylammonium)ethyl]thio]-2,3,5,6-tetrafluorophenyl]porphyrin tetraiodide (TTFAP), and evaluated its physico-chemical properties, antibacterial activity and ability to function as a scaffold for fibroblasts growth *in vitro*. The results showed a stronger interaction of keratin to TTFAP than AzA. On the other hand, TTFAP loaded sponges exhibited effective bactericide effect towards gram-positive bacteria (*S. aureus*), while AzA loaded sponges were effective

upon white light activation against both gram-positive (*S. aureus)* and negative bacteria (*Pseudomonas aeruginosa*), demonstrating a higher photoactivity. Neither PS-loaded sponge negatively impacted the proliferation of human fibroblasts, demonstrating no *in vitro* photocytotoxicity [121].

On the neural field, it has been reported the development of a porphyrin-protein based scaffold aimed to guide nerve repair and neural regeneration. Damage to the nervous system may result in a partial inability to transmit neural impulses. To restore functionality to the damaged neural pathways one can try to regrow neuronal axons that have been damaged, restore damaged nerve cells or generate new neurons to replace those lost [122]. Using serum albumin (SA) as their scaffold biomaterial doped with hemin, an oxidized form of iron protoporphyrin IX, to source growth factors, Hsu *et al.* tested the ability of this scaffold for neural tissue engineering of human induced pluripotent stem cell (hiPSC)-derived neural stem cells (NSC). Pluripotent stem cells have developed a large interest in the field of neuronal regeneration, since they can be cultured and expanded indefinitely and can differentiate into any cell type of the body [122]. This biocompatible scaffold, who was able to incorporate and release growth factors, was able to promote cell engraftment, proliferation and differentiation. The authors noted a higher current passing through the hemin-doped SA scaffolds when an electrical stimulus was applied than non-doped SA scaffolds and controls. This enables a better neuronal conductivity and results in a stimulation of neuronal maturation and neurite outgrowth and branching. The authors postulate that the electrostatic interactions between hemin and SA affect the substrate-dependent differences in peptide and protein adsorption, which make the hemin a regulator in this scaffold's action [123].

**Table 1.2** – Porphyrins in scaffolds used for antibacterial and healing applications.

| PS | Support | Purpose | Conditions | Result | Ref |
|---|---|---|---|---|---|
| **TTFAP and AzA** | Photo-functionalized keratin sponges | Antibacterial activity and function as scaffolds for fibroblasts growth | Sponges loaded with 10 mg/mL of PS; KS- TTFAP sponge with 78 µm pores, and KS-AzA with 39 µm pores; Irradiated with 9- 346 J $cm^{-2}$. | KS- TTFAP showed bactericidal effect for *S. aureus*;; KS-AzA showed bactericidal effect towards *S. aureus* and *P. aeruginosa*; Promotion of proliferation of human fibroblasts. | Ferroni *et al.* (2016) [121] |

| | | | | | |
|---|---|---|---|---|---|
| **Hemin** | Hemin-doped SA fibrous scaffold | Neural Tissue Engineering Applications | Scaffold doped with 130 μM of hemin Electrical stimulation with cyclic potential in the ±0.75 V bias range at a scan rate of 40 mV/s. | Scaffold can provide supportive microenvironment, bioactive molecule incorporation and electrical stimulation to promote cell engraftment, proliferation, and differentiation; Scaffold is biocompatible and can incorporate and release growth factors. | Hsu *et al.* (2018) [123] |

### *4.1.3. Lipid-based Delivery*

Lipid-based drug delivery systems have gained importance in recent years due to their ability to improve solubility and bioavailability of drugs with poor water solubility [124]. Ben-Mordechai *et al.*, reported in 2017 an example of how lipid-based drug carriers may be used to treat acute myocardial infarction. Their hypothesis states that activation of heme oxygenase-1 (HO-1) in macrophages may improve infarct healing and repair, and to test it they chose to load a hyaluronan-coated lipid-based drug carrier with hemin, a potent HO-1 inducer. In their study, the targeting of infarct macrophages resulted in improved healing and repair after myocardial infarction. Furthermore, the authors postulated that the strategy used may be applicable to other cardiovascular diseases associated with macrophage activation [125].

**Table 1.3** – Porphyrins in lipid-based carriers used for antibacterial and healing applications.

| PS | Support | Purpose | Conditions | Result | Ref |
|---|---|---|---|---|---|
| **Hemin** | Hyaluronan-coated lipid-based drug carrier | Improve cardiac remodeling and function | Mice injected with 2 mg $kg^{-1}$ of hemin/HA-LP; Not irradiated. | Improvement of healing and repair after myocardial infarction | Ben-Mordechai *et al.* (2017) [125] |

### *4.1.4. Metal-Organic Frameworks (MOFs)*

Metal-Organic Frameworks (MOFs) are a class of porous solids with ultrahigh porosity and great internal surface areas. They are formed by joining metal-containing units with organic linkers, creating open crystalline frameworks

with permanent porosity [126]. The MOFs composition is gifted with flexibility on its geometry, size and functionality, which makes it a candidate for a variety of applications [127],[128]. Han *et al.* took advantage of this versatility for accelerating wound healing purposes. Using PCN-224, a 5,10,15,20-tetrakis(4-carboxyphenyl)porphyrinatecopper (Cu(II)TCPP) with $Zr_6$ clusters, the goal was to rid the bacteria of infected wounds. The introduction of $Cu^{2+}$ in the correct amount seemed to improve the MOF's ability to transport carriers, enhancing its photocatalytic properties. The copper MOF is reported to have shown an antibacterial efficacy of 99.71% against *S.aureus* and 97.14% against *E.coli* after 20 min of red light irradiation (660 nm). This, joined with the fact that good biocompatibility was found in animal rat models, makes this kind of framework a potential candidate for treating bacteria-infected wounds. In their *in vivo* wound healing study, 8 days after treatment, the wounds in the MOF group were significantly improved while those in the control group were still quite serious. Their postulation is that this ability to accelerate wound healing might be a result of a $Cu^{2+}$ release [128]. Indeed, copper(II) has been found to have beneficial effects in the skin, seeing as copper(II) stimulates dermal fibroblasts proliferation, upregulates certain types of collagen and fibroblasts' production of elastin fiber components, and serves as a cofactor of superoxide dismutase, (an enzyme important for protection against free radicals), among others [129]. On the other hand, the exposure of microorganisms to copper(II) ions has been found to cause significant damage or direct contact killing, as it harms their envelope phospholipids, microbial envelope or intracellular proteins and nucleic acids [129]. Overall, this capacity to harm microorganisms but benefit the human dermal cells, may prove that Han *et al.* had the right idea using a $Cu^{2+}$ metalloporphyrin for their PDT approach to wound healing.

Similarly, Ximing *et al.* had previously prepared Cu(II)TCPP MOFs and evaluated its bactericidal properties, however they encapsulated Ag nanoparticles to prepare composite materials of Ag(I)-Cu(II)TCPP MOFs and introduced them *in vitro* and *in vivo. In vitro*, the scratch wound assay revealed a faster recovery speed for wounds treated with Ag(I)-Cu(II)TCPP MOFs, when compared to the blank control group (physiological saline). *In vivo,* the authors compared the treatment with their composite and with penicillin on infected mice wounds. Again, a faster healing rate was evidenced in models treated with Ag-CuTCPP MOFs than that treated with penicillin or physiological saline, being that the ones treated with the latter had the slowest healing rates [130].

These approaches using Cu(II)TCPP MOFs, however promising, are not the only approaches reported in the literature. In fact, the Prussian Blue (PB) MOF is a kind of photothermal material clinically ratified by the US Food and Drug

Administration (FDA), which has good photothermal effect, simple preparation, low biotoxicity, and biodegradability. PB crystals consist of iron ions coordinated by CN bridges, and are common coordination polymers with high surface area which exhibit high peroxidase-like catalytic activity [127]. A core-shell dual MOF heterostructure was synthesized by Luo *et al.* in order to achieve a synergetic effect of photothermal and photodynamic properties and eradicate bacteria, using a PB MOF as a core and a porphyrin-doped UIO-66-TCPP MOF as a shell (PB@MOF). Antibacterial rates of more than 99% were found for *S.aureus* and 98% for *E.coli* when treated with PB@MOF under dual illumination (808 nm NIR, and 660 nm red light), as the authors report a rupture on the bacteria's membrane, after irradiation. Moreover, on their *in vivo* animal experiment, Luo *et al.* tested how this antibacterial effect might facilitate wound healing and found that the best wound healing rate was exhibited by the dual light illumination group. In the first week of healing, vast inflammatory cells were found at the injured site in the control group, when compared to the dual illumination group where fewer are reported [131].

Although the bactericidal effects of MOFs have now been established, Wang *et al.* bring us to another potential application, in ophthalmology regeneration. The authors study the effect of a zirconium-porphyrin (ZrTCPP) MOF (NPMOF) in treating photoreceptor degeneration. For this, methylprednisolone (MPS), a glucocorticoid medication, was loaded in the NPMOF (MPS-NPMOF), hoping to develop a new therapeutic approach with NPMOF-based intraocular delivery system. Lesions to the retinas can be a result of traumatic injury or the consequence of a retinal degenerative disease, which both may result in permanent loss of retinal neurons and sight. In industrialized countries, the progressive dysfunction and death of retinal photoreceptors is the leading cause for adult blindness [132]. Among the therapies available today, are transplantation of photoreceptors (rods and cones) and retinal pigment epithelium, and bionic retinal implants [133]. Studies such as these, are, therefore, a step forward in finding new therapies that may stimulate a natural regeneration of photoreceptors and preserve the visual sense. The results appeared promising, as the nanoparticle NPMOF exhibited *in vivo* biocompatibility and low biotoxicity. MPS-NPMOF was able to release MPS continuously and exert its therapeutic effects at the lesion site. This meant an improved defense against stress-induced apoptosis in the retina after injury, and a promotion of photoreceptor regeneration. The authors postulate that this might be a promising approach to treat conditions of the ocular posterior segment, such as solar retinopathy, diabetic retinopathy and age-related macular degeneration [134].

These four studies, apart from using MOFs for regeneration purposes, also have in common porphyrin choice, TCPP. In fact, porphyrinic macrocycles can be viewed as attractive bridging ligands in MOFs structure building, due to their rigid molecular structure, tunable peripheral substituents, and the metalation site in their core. TCPP-based MOFs offer two distinct metal binding sites, one functional metal binding site in the porphyrin core and another at the carboxyl ligand [135]. Furthermore, the conjugation with porphyrins may enhance intersystem crossing, increasing $^1O_2$ generation efficiency while the porous structure of the MOF may facilitate the diffusion of ROS which benefits studies which apply PDT [136].

**Table 1.4** – Porphyrins in MOFs used for antibacterial and wound healing applications.

| PS | Support | Purpose | Conditions | Result | Ref |
|---|---|---|---|---|---|
| **TCPP** | $Zr_6$ cluster with TCPP ligand (PCN 224), Cu-doped ($Cu_n$MOF) | Enhance photocatalytic activity and photothermal effects of Cu-doped MOFs for rapid treatment of Bacteria-Infected Wounds | 40 mg of $H_2$TCPP used in MOF preparation<br>MOF, $Cu_{10}$MOF and $Cu_{25}$MOF solutions of (0.5, 1.5, 2.5 mg/mL)<br>Irradiation of 20 min under red light (660 nm, 0.4 W $cm^{-2}$ (80 J $cm^{-2}$) | $Cu_{10}$MOF showed antibacterial efficacy against *S. aureus* and *E.coli;*<br>Acceleration of wound healing;<br>No toxicity to major organs. | Han *et al.* (2019) [128] |
| **Cu (II) TCPP** | Ag-CuTCPP MOFs | Antibacterial Activity and Promotion of Wound Healing | 20 mg (0.025 mmol) of CuTCPP used in nanoparticles preparation;<br>Tested in a range of concentrations to determine IC50, MIC and MBC<br>Not irradiated | Antibacterial effect better than penicillin, (*in vitro)*<br>Cytotoxicity was lower than naked Ag nanoparticles and ions<br>*In vivo,* excellent antibacterial effect, extremely low cytotoxicity and promoted wound healing | Ximing *et al.* (2017) [130] |

| | | | | | |
|---|---|---|---|---|---|
| **TCPP** | Core-shell dual MOF heterostructure (porphyrin doped shell) | Enhance photothermal and photodynamic synergy with dual MOF to sterilize wounds | Three different TCPP concentrations tested in materials (with 0 mg, 0.5 mg and 1.5 mg added)<br>Irradiation of 10 min by 808 nm + 660 nm light (dual light) | Poor antibacterial effect under single illumination;<br>Improved antibacterial effect under dual light irradiation;<br>(against *S. aureus* and *E. coli*) | Luo *et al.* (2019) [131] |
| **ZrTCPP** | MPS-NPMOF | Treatment of Photoreceptor Degeneration | 10 mg of TCPP used in MOF preparation<br>2 mg/mL MPS-NPMOF administered to fish | Good *in vivo* biocompatibility and low biotoxicity<br>Defense of stress-induced apoptosis of retina<br>Promotion of photoreceptor regeneration | Wang *et al.* (2019) [134] |

### *4.1.5. Nanoparticles and membranes*

One of the many factors involved in wound healing is the production of nitric oxide (NO). Production of NO metabolites, nitrite ($NO_2$) and nitrate ($NO_3$), are elevated early in the fluid of subcutaneous wounds, and their presence seems to correlate with collagen deposition in dermal fibroblasts as well as angiogenesis and inflammation [137],[138]. Irregular NO levels have also been associated with impaired wound healing in conditions such as DM [139]–[141], chronic steroid treatment [142], [143] and malnutrition [144], [145], among others [137], [146], [147]. Su *et al.* demonstrate a way to topically deliver NO supply to wound sites, making use of Prussian Blue (PB) nanocubes, conjugated with hemin, which can carry NO. Nanocubes are an assembly of nanoparticles formed from collective linear chains to a cubical shape, and which may present many potential applications in functional nanomaterials and nanodevices [148]. In this case, by applying these PB-NO nanocubes to the wound site and irradiating them with NIR light, the NO was liberated by this thermo-induced stimulus, and went on to do its effect on the tissues, namely, according to the authors, improve angiogenesis and collagen deposition, in a controlled manner [138].

Among the many applications of porphyrins, its oxygen sensor properties can prove to be fairly useful in a tissue regeneration and engineering setting. Oxygen, being quite involved in the wound healing process, can be regarded as a healing marker, and its monitoring can be a useful clinical tool. However, most known oxygen-sensing porphyrins are hydrophobic, resulting in difficult

functionality in biocompatible supports. Giuntini *et al.* describe in their study the synthesis of water soluble functionalized Pt (II) and Pd(II) porphyrin complexes (5-(4-Carboxyphenyl)-10,15,20-tris(4-methylpyridinium)porphyrinatoplatinum(II) trichloride, 5-(4-Carboxyphenyl)-10,15,20-tris(4-methylpyridinium)porphyrinatopalladium(II) trichloride, 5-(4-Carboxyphenyl)-10,15,20-tris(4-sulfonatophenyl)porphyrinatoplatinum(II) trisodium, 5-(4-Carboxyphenyl)-10,15,20-tris(4-sulfonatophenyl)porphyrinatopalladium(II) trisodium) versatile to conjugate to bio-macromolecules in aqueous solutions and mild conditions. In addition, the compounds displayed oxygen-dependent phosphorescence, proving they can be effective monitors of wound healing processes [149].

Also taking advantage of Pt-porphyrins are Roussakis *et al.* They report the synthesis of an oxygen sensor, namely an alkyne-functionalized cyclohexenyl Pt-porphyrin, and its incorporation into a collagen-dextran oxygen-sensing biocomposite scaffold membrane. The objective, as the authors note, is to 'address and track the progression of wound healing, or deterioration, without removal or reapplication, thus avoiding disruption of the wound bed, promoting tissue regeneration and monitor healing'. This would be their first demonstration of the applicability of this porphyrin in *in vivo* oxygenation imaging, which appears to have been successful. Roussakis *et al.* report a success in the noninvasive and longitudinal measurement of oxygenation *in vivo*, by this biocomposite scaffold membrane, using a model of an excisional skin wound in diabetic mice [150].

Pt-porphyrin complexes have long been described as good oxygen sensing probes [151], so it comes as no surprise that they are still used and improved upon to this day.

**Table 1.5** – Porphyrins in nanocubes used for antibacterial and wound healing applications.

| PS | Support | Purpose | Conditions | Result | Ref |
|---|---|---|---|---|---|
| **Hemin** | PB-Hemin-NO | Facilitate angiogenesis and collagen deposition on wound healing | 1 mL of 0.7 mM of hemin used for preparation of nanocubes 0.5 $Wcm^{-2}$ of NIR irradiation (808 nm) for 10 min | PB-NO colloids can be topically drop on the wound sites, and augmented blood microcirculation can be achieved by irradiation of NIR light; Effective angiogenesis and collagen deposition in wound healing process; | Su *et al.* (2019) [138] |

| | | | | | |
|---|---|---|---|---|---|
| | | | | Single delivery is not sufficient to provide efficacy. | |

**Table 1.6** – Porphyrins used for oxygen sensing in wounds.

| PS | Support | Purpose | Conditions | Result | Ref |
|---|---|---|---|---|---|
| **Pt(II) and Pd(II) porphyrin complexes** | Polyacrylamide nanoparticles | Optical oxygen tension measurement in tissue engineering | Nanoconjugates with loading ratios varying between 11 and 13 nmol $mg^{-1}$; Compressed in rod shaped collagen matrix | Oxygen-dependent phosphorescence of species; Oxygen-sensing behavior maintained when nanoprobes are incorporated in collagen gel | Giuntini *et al.* (2014) [149] |
| **PtEtGluD** | Collagen-dextran biocomposite scaffold membrane | Oxygen sensing in wounds | Scaffold membrane produced with 40 µM of porphyrin | Successful noninvasive and longitudinal measurement of oxygenation in *in vivo* wounds | Roussakis *et al.* (2019) [150] |

## 4.2. Applications of Unsupported Porphyrins

### 4.2.1. *SOD Mimetics*

Superoxide dismutase (SOD) is a metalloprotein, which directly scavenges free radicals, acting as a first line of defense against ROS-mediated cell injury and of which mammalians have three forms: Cu/ZnSOD, MnSOD and ECSOD [152],[153]. In a wound healing setting, at the inflammatory stage, immune cells are drawn to the lesion site and secrete pro-inflammatory cytokines, while inflammatory cells produce large amounts of ROS. While this has a protective nature, defending the body against an infection, their presence in excess can lead to damage to the surrounding cells, which is why the amount of circulating ROS must always be kept in check [154]. This is done naturally by the human body,

however, in settings of underlying pathological conditions, such as diabetes, or cancer, there can be an unbalance of these factors which may need external intervention.

SOD mimetics are low molecular weight molecules that can mimic the SOD's natural function. Since using native SODs in therapy have major drawbacks, such as their large molecular size, limited cell permeability, and limited half-life in the body, SOD mimetics can provide a functional alternative to circumvent these limitations [153]. The use of SOD mimetics has been reported in neoplastic studies, since its ability to augment the cell's natural antioxidant defenses has been found beneficial on models of neoplastic and non-neoplastic diseases, where oxidative stress is involved [155].

Aiding in the maintenance of redox balance in mitochondria is MnSOD, which detoxifies the major by-product of mitochondrial respiration, the free radical superoxide ($O_2^-$) [152],[156]. Bellot *et al.* see the potential of using a MnSOD mimetic, specifically the Mn(II) complex of 5,10,15,20-tetrakis (1-ethylpyridinium-2-yl)porphyrin (MnTE-2-PyP, MnE) in wound healing. The authors postulate that the topical application of MnE may achieve the same beneficial effects of Negative Pressure Wound Therapy (NPWT), a therapy which using gauze or foam, employs negative pressure by intermittent or continuous application to the wound [157],[158]. MnTE-2-PyP, a potent SOD mimic, has been previously described to provide beneficial effects treating cardiac arrythmias [159], radiation-induced lung damage [160] and radiation proctitis [161]. And here, a new potential application may have been tapped, as the authors report improved wound healing upon the topical application of MnE, having wound closure advance in two days, in rodent models [162].

Also adjudicating for MnSOD mimetics are Cui *et al.,* however with a different metalloporphyrin choice, 5,10,15,20-tetrakis (4-carboylphenyl) porphyrin manganese (III) chloride (MnTBAP, or Mn(III)TCPP). Their aim was to understand the protective effects that a SOD mimetic may have on liver graft function, growth and survival in a rat small-size graft liver transplantation model study. The treatment with Mn(III)TCPP seemed to result in reduction of serum levels of alanine amino transferase (ALT) (an enzyme which shows elevated activity in severe graft damage), reduced apoptotic cell counts, improved histologic condition, increased serum SOD activity and lower liver malondialdehyde (MDA) contents. Overall, the application of this porphyrin derivative exhibited antioxidant effects, seems to improve graft results and may have a clinical use in the transplant area [163].

ROS, apart from being the main responsible for the antimicrobial and antitumoral effect, are also an important factor in ischemia and reperfusion (I/R)

injury in many organs, including the kidneys. Which leads us to Kim *et al.*'s hypothesis that 'ROS performs differently on the proliferation of tubular epithelial cells and interstitial fibroblasts in the kidneys after I/R injury.' Part of their study is the treatment with Mn(III) complex of the 5,10,15,20-tetrakis (1-methyl-pyridinium-4-yl) porphyrin (Mn(III)TMPyP) as a SOD mimetic. Earlier and longer treatment with Mn(III)TMPyP more deeply reduced ROS generation when compared with later and shorter treatments. Furthermore, their antioxidant intervention, removing ROS, proved to accelerate the proliferation of tubular epithelial cells and attenuate the proliferation of interstitial cells, evidencing a difference of action by cell type. The authors postulate that this anti-oxidative strategy may be an important step to prevent acute kidney injury and consequent complications [164].

**Table 1.7** – Porphyrins used as SOD mimetics for wound healing applications.

| PS | Purpose | Conditions | Result | Ref |
|---|---|---|---|---|
| **MnTE-2-PyP** | Mimic MnSOD activity and accelerate wound healing through NPWT | 500µL MnE (5µM diluted in PBS) was applied topically for 10 min<br>Not irradiated. | Topical aplication of MnE improved wound healing. | Bellot *et al.* (2019) [162] |
| **MnTBAP/ Mn(III)TCPP** | Mimic SOD to improve function, growth, and survival of liver grafts | Mn(III)TCPP injected intraperitoneally at 10 mg/kg, 4 hr before transplant in donor rats and once daily until sacrifice in recipient rats<br>Not irradiated. | MnTCPP reversed the pathological changes of SFS-associated graft failure. | Cui *et al.* (2012) [163] |
| **Mn(III)TMPyP** | Understanding role of ROS in cell proliferation in kidneys after ischemia and reperfusion | MnTMPyP administered intraperitoneally mice, 5 mg/kg body wt<br>Not irradiated. | Earlier and longer treatment with MnTMPyP reduced superoxide generation more than later and shorter treatments, and attenuated the proliferation of interstitial myofibroblasts, but accelerates tubular epithelial cell proliferation.<br>The removal of ROS accelerated the proliferation of tubular epithelial cells, but attenuates the proliferation of interstitial cells. | Kim *et al.* (2010) [164] |

### *4.2.2. Porphyrins in PDT*

PDT has been associated with wound healing and regeneration as far as 1996, at least, when Kübler *et al.* tested the effects of this therapy on rat's skin flap healing after surgery, with Photofrin® as the PS. In this case, however, the authors do not report a positive effect, rather the opposite. They found evidence of epidermal necrosis at the flap, the site of surgery, and decreased wound tensile strength. They go so far as to say that the use of PDT may delay healing. [165] Nevertheless, many studies since then have disproved this, and demonstrated beneficial effects of PDT in wound healing, as have here been discussed.

One aspect of this, as we have previously discussed is how PDT has made significant contributions in battling infected wounds. Lambrechts *et al.* demonstrate the use of 5-phenyl-10,15,20-tris(1-methyl-pyridinium-4-yl)porphyrin chloride (TriMPyP), against *S. aureus* infected burn wounds, while Grinholc *et al.* use protoporphyrin diarginate (PP-IX$Arg_2$) against *S.aureus* in human dermal fibroblasts. Both studies showed promising results, as the PDT enabled for inactivation of the microorganism, leaving however, room for improvement, such as full cytotoxic characterizations of the PS, or adjustment of light doses to best promote wound healing [166], [167]. Lyapina *et al.* attempted this adjustment by using low-intensity laser irradiation of pheophorbide *a* (Pheo *a*) and PP-IX on rats' skin wound healing (Table 9). They found that the introduction of the PSs produced an anti-inflammatory effect upon irradiation. However, the authors did not observe a substantial difference in healing between the study and control groups, apart from a less pronounced scar in the study group [168]. Even so, since then, the effects of low-intensity laser irradiation or low-level laser light therapy have gained more interest in the field of wound healing, and of which some informative literature may be found [169]–[174].

**Table 1.8** – Exogeneous porphyrinic PSs used in PDT for wound healing applications.

| PS | Purpose | Conditions | Result | Ref |
|---|---|---|---|---|
| **Photofrin®** | Healing of Rat Skin Flap | 5mg/kg of Photofrin injected intraperitoneal Irradiation with 75 mW $cm^{-2}$ of 630 nm light (three different fluencies applied: 25 J | Detrimental effect of PDT on wound healing in rat groin flap model. | Kubler *et al.* (1996) [165] |

| | | | | |
|---|---|---|---|---|
| | | $cm^{-2}$, 50 J $cm^{-2}$ and 75 J $cm^{-2}$) | | |
| **TriMPyP** | Antibacterial effect in infected burn wounds | *In vitro:* 1.56 µM TriMPyP solution Irradiation with red light (635 nm) at 10 mW $cm^{-2}$ for 1-2 min (0.6-1.5 J $cm^{-2}$) *In vivo:* 500 µM of TriMPyP Irradiation with red light (635 nm) with 84 mW cm-2 for 42 and 84 min (211 and 423 J $cm^{-2}$, respectively) | The healing of burn wound differed from dark to PDT groups: The groups that received no treatment needed 6.2 less days to heal than the groups who received some sort of treatment. The bacterial numbers in burn wound were reduced after PDT, and more rapidly than standard burn therapy. Bacterial re-growth after PDT is observed. Illumination alone exerted damaging effect. | Lambrechts *et al.* (2005) [167] |
| **PP-IXArg$_2$** | Antibacterial effect and understand effect on human dermal fibroblasts | PP-IXArg$_2$ tested at range from 0-25 µM Red light irradiation (624 nm) at 3.33 mW $cm^{-2}$ for 30 min (6 J $cm^{-2}$) | PP-IXArg$_2$ exhibited antibacterial activity against *S. aureus;* Fibroblasts were still viable after illumination. | Grinholc *et al.* (2008) [166] |
| **PP-IX and Pheo *a*** | Improve skin wound healing through Low-Intensity Laser Irradiation | Pheo *a* and PP- IX at 3 mg/kg Red light irradiation (632.8 nm) at 2.87 mW $cm^{-2}$, total light dose of of 1.72 J $cm^{-2}$ | Presence of exogeneous PS caused anti-inflammatory effect upon laser irradiation. Wound healing was accompanied by less pronounced cicatrization. | Lyapina *et al.* (2010) [168] |

## 5. Aim of this Thesis

Porphyrins have demonstrated their great potential in wound healing studies, however, so far, their application in diabetic wounds has not been evidenced. With the increasing interest of the light therapies and their applications, and the ongoing need to develop treatment options and improve the quality of life of diabetic patients, it is the aim of this thesis to inspect the potential of starch films with incorporated porphyrins in treating infections commonly found in diabetic wounds and furthermore, evaluate the beneficial properties these films may have in tissue healing and regeneration, under light irradiation.

For this purpose 5,10,15,20-tetrakis(pentafluorophenyl)porphyrin (**TPP5F**) and 5,10,15,20-tetrakis(1-methylpyridinium-4-yl)porphyrin tetra-iodide (Tetra-$Py^{+}$-Me, or **TMPyP**) were prepared in the laboratory and incorporated in starch films, which were later applied in cultures of *S. aureus* and *P. aeruginosa* and irradiated under with white light at an irradiance of 50 mW $cm^{-2}$. These assays were done *in vitro* and *ex vivo* (porcine skin). Furthermore, these porphyrin/starch materials were also used to evaluate their cytotoxicity, photocytotoxicity and wound healing capacity, ROS formation and cell adhesion in two cell lines (endothelial cells and fibroblasts) by application of a red light (5 mW $cm^{-2}$). The work steps are represented in Fig.1.6.

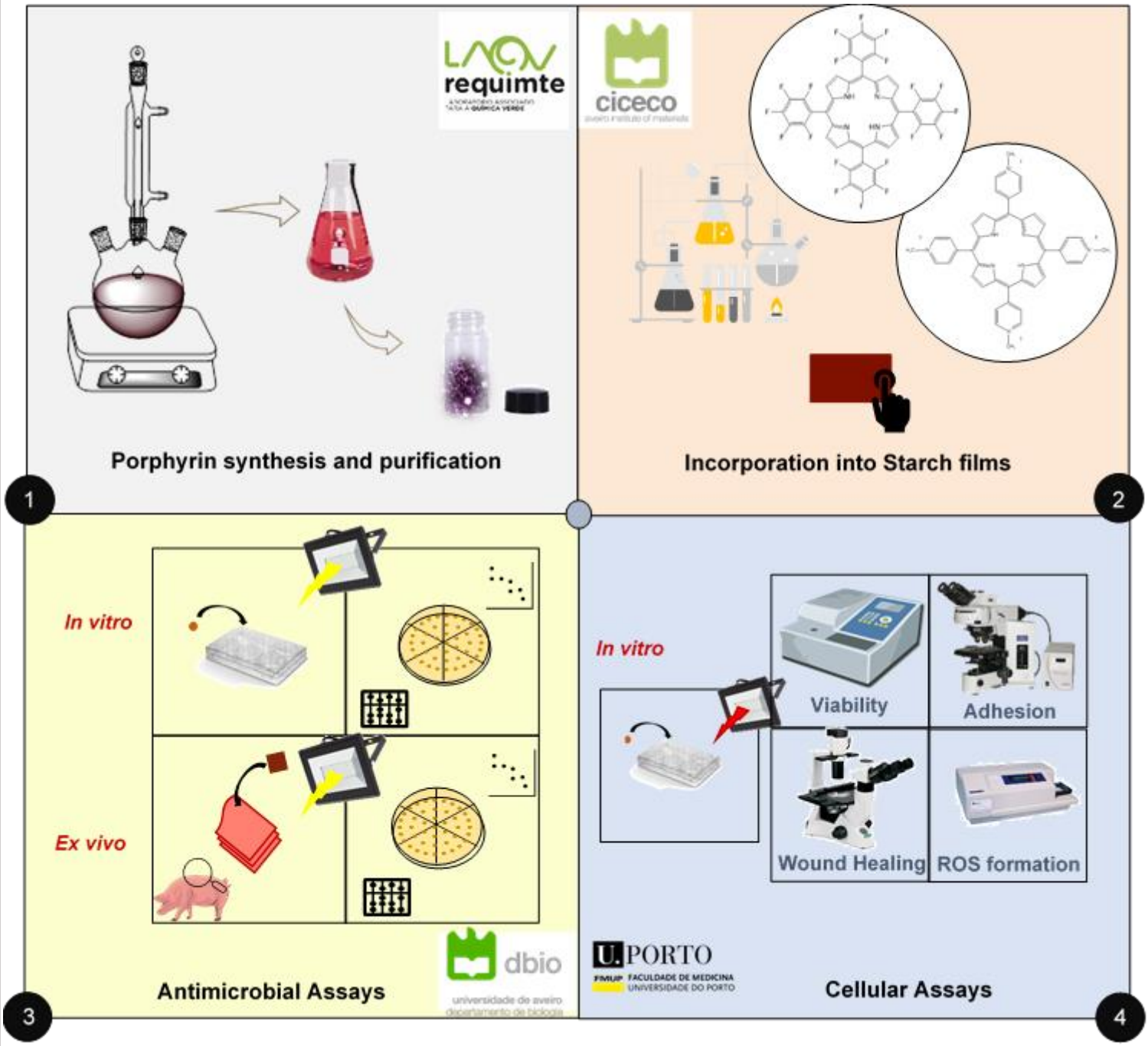


**Fig. 1.6** – Representation of the work steps in this thesis.

# 6. References


[1] R. Lakhtakia, “The History of Diabetes Mellitus,” *Textb. Diabetes Fourth Ed.*, vol. 13, no. August, pp. 368–370, 2013.

[2] J. Casqueiro, J. Casqueiro, and C. Alves, “Infections in patients with diabetes mellitus : A review of pathogenesis,” vol. 16, pp. 27–36, 2012.

[3] W. Fan, “Epidemiology in diabetes mellitus and cardiovascular disease,” *Cardiovasc. Endocrinol.*, pp. 8–16, 2017.

[4] “World Health Organization, General Information on Diabetes. Available at: https://www.who.int/.”

[5] S. Y. Tan *et al.*, “Type 1 and 2 diabetes mellitus: A review on current treatment approach and gene therapy as potential intervention,” *Diabetes Metab. Syndr. Clin. Res. Rev.*, vol. 13, no. 1, pp. 364–372, 2019.

[6] M. A. Weiss, *The Structure and Function of Insulin: Decoding the TR Transition*, 1st ed., vol. 80, no. C. Elsevier Inc., 2009.

[7] S. D. De Ferranti *et al.*, “Type 1 Diabetes Mellitus and Cardiovascular Disease,” *AHA/ASA Journals*, pp. 1110–1130, 2014.

[8] A. B. Olokoba, O. A. Obateru, and L. B. Olokoba, “Type 2 Diabetes Mellitus: A Review of Current Trends,” vol. 27, no. 4, pp. 269–273, 2012.

[9] J. F. Plows, J. L. Stanley, P. N. Baker, C. M. Reynolds, and M. H. Vickers, “The Pathophysiology of Gestational Diabetes Mellitus,” *Int. J. Mol. Sci.*, pp. 1–21, 2018.

[10] J. . Bunza and A. J. Alhassan, “Complications Of Diabetes Mellitus : An Insight In To Biochemical Basis,” *Eur. J. Pharm. Med. Res.*, vol. 6, no. February, pp. 114–120, 2019.

[11] H. Ebrahimzadeh Leylabadlo, S. Sanaie, F. Sadeghpour Heravi, Z. Ahmadian, and R. Ghotaslou, “From role of gut microbiota to microbial-based therapies in type 2-diabetes,” *Infect. Genet. Evol.*, vol. 81, p. 104268, 2020.

[12] H. D. Nickerson and S. Dutta, “Diabetic Complications : Current Challenges and Opportunities,” *J. Cardiovasc. Transl. Res.*, pp. 375–379, 2012.

[13] K. Alexiadou and J. Doupis, “Management of Diabetic Foot Ulcers,” *Diabetes Ther.*, vol. 3, no. 1, p. 4, 2012.

[14] “International Diabetes Federation, Complications of Diabetes, Available at: https://www.idf.org/.”

[15] N. Houreld, “Healing effects of photobiomodulation on diabetic wounds,” *Appl. Sci.*, vol. 9, no. 23, pp. 1–19, 2019.

[16] C. Machado *et al.*, “Evolutionary trends in bacteria isolated from moderate and severe diabetic foot infections in a Portuguese tertiary center,” *Diabetes Metab. Syndr. Clin. Res. Rev.*, vol. 14, no. 3, pp. 205–209, 2020.

[17] T. C. Goh, M. Y. Bajuri, S. C Nadarajah, A. H. Abdul Rashid, S. Baharuddin, and K. S. Zamri, “Clinical and bacteriological profile of diabetic foot infections in a tertiary care,” *J. Foot Ankle Res.*, vol. 13, no. 1, p. 36, 2020.

[18] J. J. Marín-Peñalver, I. Martín-Timón, C. Sevillano-Collantes, and F. J. del Cañizo-Gómez, “Update on the treatment of type 2 diabetes mellitus,” *World J. Diabetes*, vol. 7, no. 17, p. 354, 2016.

[19] M. Siavash, A. Najjarnezhad, N. Mohseni, S. M. Abtahi, A. Karimy, and M. H. Sabzevari, “Efficacy of Maggot Debridement Therapy on Refractory Atypical Diabetic Foot Ulcers: An Open-Label Study,” *Int. J. Low. Extrem. Wounds*, vol. May, no. 5, p. 1534734620920403, 2020.

[20] M. S. Buğday and E. Öksüz, “A new approach at diabetic foot treatment: Phosphodiesterase 5 inhibitors,” *Med. Hypotheses*, vol. 141, no. March, 2020.

[21] K. Saeed *et al.*, “Hot topics in diabetic foot infection,” *Int. J. Antimicrob. Agents*, vol. 55, no. 6, p. 105942, 2020.

[22] M. J. Renwick, V. Simpkin, and E. Mossialos, *Targeting innovation in antibiotic drug discovery and development*, 45th ed. London, United Kingdom: Observatory Studies Series, 2016.

[23] F. Cieplik, D. Deng, W. Crielaard, W. Buchalla, A. Al-ahmad, and T. Maisch, “Antimicrobial photodynamic therapy – what we know and what we don ’ t,” *Crit. Rev. Microbiol.*, vol. 44, no. 5, pp. 571–589, 2018.

[24] M. C. Issa and M. Manela-Azulay, “Photodynamic therapy : a review of the literature and image documentation,” *An. Bras. Dermatol.*, vol. 85, no. 4, pp. 501–511, 2010.

[25] U. Kubitscheck, *Fluorescence Microscopy: From Principles to Biological Applications*. 2012.

[26] H. Abrahamse and M. R. Hamblin, “New photosensitizers for photodynamic therapy,” *Biochem. J.*, no. 473, pp. 347–364, 2016.

[27] V. Pérez-Laguna *et al.*, “Combination of photodynamic therapy and antimicrobial compounds to treat skin and mucosal infections: a systematic review.,” *Photochem. Photobiol. Sci.*, 2019.

[28] L. Costa, M. A. F. Faustino, M. G. P. M. S. Neves, Â. Cunha, and A. Almeida, “Photodynamic Inactivation of Mammalian Viruses and Bacteriophages,” *Viruses*, no. i, pp. 1034–1074, 2012.

[29] M. Q. Mesquita, C. J. Dias, M. G. P. M. S. Neves, A. Almeida, and M. A. F. Faustino, “Revisiting current photoactive materials for antimicrobial photodynamic therapy,” *Molecules*, vol. 23, no. 10, p. 2424, 2018.

[30] W. Xuan *et al.*, “Amphiphilic tetracationic porphyrins are exceptionally active antimicrobial photosensitizers: in vitro and in vivo studies with the free- base and Pd-Chelate,” *J. Biophotonics*, vol. 12, no. 8, p. e201800318, 2019.

[31] R. R. Allison, G. H. Downie, R. Cuenca, X. Hu, C. J. H. Childs, and C. H. Sibata, “Photosensitizers in clinical PDT,” *Photodiagnosis Photodyn. Ther.*, vol. 1000, pp. 7–9, 2004.

[32] A. Garcia-Sampedro, A. Tabero, I. Mahamed, and P. Acedo, “Multimodal use of the porphyrin TMPyP : From cancer therapy to antimicrobial applications,” *J. Porphyr. Phthalocyanines*, vol. 23, no. February, pp. 1–17, 2019.

[33] E. Fagadar-cosma, L. Cseh, V. Badea, G. Fagadar-cosma, and D. Vlascici, “Combinatorial Synthesis and Characterization of New Asymmetric Porphyrins as Potential Photosensitizers in Photodynamic Therapy,” *Comb. Chem. High Throughput Screen.*, vol. 10, no. 6, pp. 466–472, 2007.

[34] R. Giovannetti, “The Use of Spectrophotometry UV-Vis for the Study of Porphyrins,” *Macro to Nano Spectrosc.*, pp. 87–108, 2012.

[35] A. P. J. Maestrin *et al.*, “A novel chlorin derivative of meso-tris(pentafluorophenyl)-4-pyridylporphyrin: Synthesis, photophysics and photochemical properties,” *J. Braz. Chem. Soc.*, vol. 15, no. 6, pp. 923–930, 2004.

[36] Y. Liu, T. H. Lee, S. H. Lee, J. Li, W. K. Lee, and I. Yoon, “Mitochondria-Targeted Water-Soluble Organic Nanoparticles of Chlorin Derivatives for Biocompatible Photodynamic Therapy,” *ChemNanoMat*, vol. 6, no. 4, pp. 610–617, 2020.

[37] B. Pucelik, A. Sułek, and J. M. Dąbrowski, “Bacteriochlorins and their metal complexes as

NIR-absorbing photosensitizers: properties, mechanisms, and applications," *Coord. Chem. Rev.*, vol. 416, no. 1 Aug, p. 213340, 2020.

[38] Y. Chen, G. Li, and R. Pandey, "Synthesis of Bacteriochlorins and Their Potential Utility in Photodynamic Therapy (PDT)," *Curr. Org. Chem.*, vol. 8, no. 12, pp. 1105–1134, 2005.

[39] D. Wöhrle, G. Schnurpfeil, S. G. Makarov, A. Kazarin, and O. N. Suvorova, "Practical Applications of Phthalocyanines – from Dyes and Pigments to Materials for Optical, Electronic and Photo-electronic Devices," *Macroheterocycles*, vol. 5, no. 3, pp. 191–202, 2012.

[40] M. Lan, S. Zhao, W. Liu, C. S. Lee, W. Zhang, and P. Wang, "Photosensitizers for Photodynamic Therapy," *Adv. Healthc. Mater.*, vol. 8, no. 13, pp. 1–37, 2019.

[41] T. Furuyama, K. Satoh, T. Kushiya, and N. Kobayashi, "Design, synthesis, and properties of phthalocyanine complexes with main-group elements showing main absorption and fluorescence beyond 1000 nm," *J. Am. Chem. Soc.*, vol. 136, no. 2, pp. 765–776, 2014.

[42] L. El-Khordagui, N. El-Sayed, S. Galal, H. El-Gowelli, H. Omar, and M. Mohammed, "Photosensitizer-eluting nano fi bers for enhanced photodynamic therapy of wounds : A preclinical study in immunocompromized rats," *Int. J. Pharm.*, vol. 520, no. 1–2, pp. 139–148, 2017.

[43] C. Spagnul, L. C. Turner, and R. W. Boyle, "Immobilized Photosensitisers for antimicrobial applications," *J. Photochem. Photobiol. B Biol.*, vol. 150, no. Sep, pp. 11–30, 2015.

[44] A. Valkov, F. Nakonechny, and M. Nisnevitch, "Polymer-Immobilized Photosensitizers for Continuous Eradication of Bacteria," *Int. J. Mol. Sci.*, pp. 14984–14996, 2014.

[45] M. Q. Mesquita, C. J. Dias, S. Gamelas, M. Fardilha, M. G. P. M. S. Neves, and M. A. F. Faustino, "An insight on the role of photosensitizer nanocarriers for photodynamic therapy," *An. Acad. Bras. Cienc.*, vol. 90, no. 1, pp. 1101–1130, 2018.

[46] L. An *et al.*, "Energy Transfer from CdSe Quantum Dots to Porphyrin via Two-Photon Excitation," *J. Nanosci. Nanotechnol.*, vol. 13, pp. 1368–1371, 2013.

[47] S. Singh *et al.*, "DNA mediated assembly of quantum dot – protoporphyrin IX FRET probes and the effect of FRET efficiency on ROS generation," *Phys. Chem. Chem. Phys.*, vol. 17, no. 8, pp. 5973–81, 2015.

[48] Z. Youssef *et al.*, "The application of titanium dioxide , zinc oxide , fullerene , and graphene nanoparticles in photodynamic therapy," *Cancer Nanotechnol.*, 2017.

[49] Y. Li *et al.*, "Porphyrin-Based Carbon Dots for Photodynamic Therapy of Hepatoma," *Adv. Healthc. Mater.*, vol. 6, no. 1, 2016.

[50] P. V. Peplow, T.-Y. Chung, and G. D. Baxter, "Photodynamic Modulation of Wound Healing : A Review of Human and Animal Studies," *Photomed. Laser Surg.*, vol. 30, no. 3, pp. 118–148, 2012.

[51] V. Falanga, "Wound healing and its impairment in the diabetic foot," *Lancet*, vol. 366, pp. 1736–1743, 2005.

[52] S. Guo and L. A. DiPietro, "Factors Affecting Wound Healing," *J. Dent. Res.*, no. Mc 859, pp. 219–229, 2010.

[53] A. C. de O. Gonzalez, Z. de A. Andrade, T. F. Costa, and A. R. A. P. Medrado, "Wound healing - A literature review," *An. Bras. Dermatol.*, vol. 91, no. 5, pp. 614–620, 2016.

[54] L. I. F. Moura, A. M. A. Dias, E. Carvalho, and H. C. De Sousa, "Recent advances on the development of wound dressings for diabetic foot ulcer treatment — A review," *Acta Biomater.*, vol. 9, no. 7, pp. 7093–7114, 2013.

[55] P. Avci *et al.*, "Low-level laser (light) therapy (LLLT) in skin: stimulating, healing, restoring.," *Semin. Cutan. Med. Surg.*, vol. 32, no. 1, pp. 41–52, 2014.

[56] A. M, S. Ummer V, A. G. Maiya, and M. Hande, “Low level laser therapy for the patients with painful diabetic peripheral neuropathy - A systematic review,” *Diabetes Metab. Syndr. Clin. Res. Rev.*, vol. 13, no. 4, pp. 2667–2670, 2019.

[57] Y. Chen, X. L. Chen, X. L. Zou, S. Z. Chen, J. Zou, and Y. Wang, “Efficacy of low-level laser therapy in pain management after root canal treatment or retreatment : a systematic review,” *Lasers Med. Sci.*, vol. 34, no. 7, pp. 1305–1316, 2019.

[58] S. Mirza, N. Rehman, A. Alrahla, W. R. Alamri, and F. Vohra, “Efficacy of photodynamic therapy and low level laser therapy against steroid therapy in the treatment of erosive-atrophic oral lichen planus,” *Photodiagnosis Photodyn. Ther.*, vol. Mar, no. 21, pp. 404–408, 2018.

[59] G. Oubiña *et al.*, “Low level laser therapy (LLLT) modulates ovarian function in mature female mice,” *Prog. Biophys. Mol. Biol.*, vol. Aug, no. 145, pp. 10–18, 2018.

[60] H. B. Cotler, R. T. Chow, M. R. Hamblin, and J. Carroll, “The Use of Low Level Laser Therapy (LLLT) For Musculoskeletal Pain,” *MOJ Orthop. Rheumatol.*, vol. 2, no. 5, p. 00068, 2016.

[61] J. T. Hopkins, T. A. Mcloda, J. G. Seegmiller, and G. D. Baxter, “Low-Level Laser Therapy Facilitates Superficial Wound Healing in Humans: A Triple-Blind, Sham-Controlled Study,” *J. Athl. Train.*, vol. 39, no. 3, pp. 223–229, 2004.

[62] B. M. Kajagar, A. S. Godhi, A. Pandit, and S. Khatri, “Efficacy of Low Level Laser Therapy on Wound Healing in Patients with Chronic Diabetic Foot Ulcers — A Randomised Control Trial,” *Indian J. Surg.*, vol. 74, no. October, pp. 359–363, 2012.

[63] R. Samaneh, Y. Ali, J. Mostafa, N. A. Mahmud, and R. Zohre, “Laser Therapy for Wound Healing : A Review of Current Techniques and Mechanisms of Action,” *Biosci. Biotechnol. Res. Asia*, vol. 12, no. March, pp. 217–223, 2015.

[64] M. Bagheri *et al.*, “Effects of photobiomodulation on degranulation and number of mast cells and wound strength in skin wound healing of streptozotocin-induced diabetic rats,” *Photomed. Laser Surg.*, vol. 36, no. 8, pp. 415–423, 2018.

[65] R. Kouhkheil *et al.*, “Impact of Photobiomodulation and Condition Medium on Mast Cell Counts, Degranulation, and Wound Strength in Infected Skin Wound Healing of Diabetic Rats,” *Photobiomodulation, Photomedicine, Laser Surg.*, vol. 37, no. 11, pp. 706–714, 2019.

[66] V. R. da Silva Oliveira, R. A. Santos-Eichler, and C. S. Dale, “Photobiomodulation increases cell viability via AKT activation in an in vitro model of diabetes induced by glucose neurotoxicity,” *Lasers Med. Sci.*, vol. 35, no. 1, pp. 149–156, 2020.

[67] S. W. Jere, N. N. Houreld, and H. Abrahamse, “Effect of photobiomodulation on cellular migration and survival in diabetic and hypoxic diabetic wounded fibroblast cells,” *Lasers Med. Sci.*, no. 36, pp. 365–374, 2020.

[68] D. R. Mokoena, N. N. Houreld, S. S. Dhilip Kumar, and H. Abrahamse, “Photobiomodulation at 660 nm Stimulates Fibroblast Differentiation,” *Lasers Surg. Med.*, vol. 52, no. 7, pp. 671–681, 2019.

[69] L. Gong, Z. Zou, L. Huang, S. Guo, and D. Xing, “Photobiomodulation therapy decreases free fatty acid generation and release in adipocytes to ameliorate insulin resistance in type 2 diabetes,” *Cell. Signal.*, vol. 67, p. 109491, 2020.

[70] F. I. Barbosa, P. V. Araújo, L. J. C. Machado, C. S. Magalhães, M. M. M. Guimarães, and A. N. Moreira, “Effect of photodynamic therapy as an adjuvant to non-surgical periodontal therapy: Periodontal and metabolic evaluation in patients with type 2 diabetes mellitus,” *Photodiagnosis Photodyn. Ther.*, vol. 22, pp. 245–250, 2018.

[71] M. F. Elsadek, B. M. Ahmed, D. M. Alkhawtani, and A. Zia Siddiqui, “A comparative clinical, microbiological and glycemic analysis of photodynamic therapy and Lactobacillus reuteri in the treatment of chronic periodontitis in type-2 diabetes mellitus patients,” *Photodiagnosis Photodyn. Ther.*, vol. 29, no. September 2019, p. 101629, 2020.

[72] S. Mirza, A. A. Khan, A. A. Al-Kheraif, S. Z. Khan, and S. S. Shafqat, “Efficacy of adjunctive photodynamic therapy on the clinical periodontal, HbA1c and advanced glycation end product levels among mild to moderate chronic periodontal disease patients with type 2 diabetes mellitus: A randomized controlled clinical trial,” *Photodiagnosis Photodyn. Ther.*, vol. 28, no. June, pp. 177–182, 2019.

[73] M. Asghari *et al.*, “The effect of combined photobiomodulation and metformin on open skin wound healing in a non-genetic model of type II diabetes,” *J. Photochem. Photobiol. B Biol.*, vol. 169, pp. 63–69, 2017.

[74] M. Bagheri *et al.*, “Combined effects of metformin and photobiomodulation improve the proliferation phase of wound healing in type 2 diabetic rats,” *Biomed. Pharmacother.*, vol. 123, no. 109776, 2020.

[75] L. Chengnan *et al.*, “Near-infrared light activatable hydrogels for metformin delivery,” *Nanoscale*, vol. 11, no. 34, pp. 15810–15820, 2019.

[76] R. Ebrahimpour-Malekshah *et al.*, “Combined therapy of photobiomodulation and adipose-derived stem cells synergistically improve healing in an ischemic, infected and delayed healing wound model in rats with type 1 diabetes mellitus,” *BMJ Open Diabetes Res. Care*, vol. 8, no. 1, p. e001033, 2020.

[77] R. Kouhkheil *et al.*, “The effect of combined pulsed wave low-level laser therapy and mesenchymal stem cell-conditioned medium on the healing of an infected wound with methicillin-resistant Staphylococcal aureus in diabetic rats,” *J. Cell. Biochem.*, vol. 119, no. 7, pp. 5788–5797, 2018.

[78] A. Amini *et al.*, “Stereological and gene expression examinations on the combined effects of photobiomodulation and curcumin on wound healing in type one diabetic rats,” *J. Cell. Biochem.*, vol. 120, no. 10, pp. 17994–18004, 2019.

[79] C. A. Ivanaga, D. M. J. Miessi, M. A. A. Nuernberg, M. M. Claudio, V. G. Garcia, and L. H. Theodoro, “Antimicrobial photodynamic therapy (aPDT) with curcumin and LED, as an enhancement to scaling and root planing in the treatment of residual pockets in diabetic patients: A randomized and controlled split-mouth clinical trial,” *Photodiagnosis Photodyn. Ther.*, vol. 27, no. June, pp. 388–395, 2019.

[80] H. Soleimani *et al.*, “The effect of combined photobiomodulation and curcumin on skin wound healing in type I diabetes in rats,” *J. Photochem. Photobiol. B Biol.*, vol. 181, no. January, pp. 23–30, 2018.

[81] H. Soleimani *et al.*, “Combined effects of photobiomodulation and curcumin on mast cells and wound strength in wound healing of streptozotocin-induced diabetes in rats,” *Lasers Med. Sci.*, vol. 36, no. 2, pp. 375–386, 2020.

[82] A. Rübsam, S. Parikh, and P. E. Fort, “Role of inflammation in diabetic retinopathy,” *Int. J. Mol. Sci.*, vol. 19, no. 4, pp. 1–31, 2018.

[83] D. S. Fong *et al.*, “Retinopathy in Diabetes,” *Diabetes Care*, vol. 27, no. SUPPL. 1, 2004.

[84] M. V. Da Silva Leal *et al.*, “Effect of Modified Laser Transcutaneous Irradiation on Pain and Quality of Life in Patients with Diabetic Neuropathy,” *Photobiomodulation, Photomedicine, Laser Surg.*, vol. 38, no. 3, pp. 138–144, 2020.

[85] Y. Cheng, Y. Du, H. Liu, J. Tang, A. Veenstra, and T. S. Kern, “Photobiomodulation inhibits long-term structural and functional lesions of diabetic retinopathy,” *Diabetes*, vol. 67, no.

2, pp. 291–298, 2018.

[86] S. Li *et al.*, “Efficacy of low-level light therapy for treatment of diabetic foot ulcer : A systematic review and meta- analysis of randomized controlled trials,” *Diabetes Res. Clin. Pract.*, vol. 143, pp. 215–224, 2018.

[87] R. K. Mathur, K. Sahu, S. Saraf, P. Patheja, and F. Khan, “Low-level laser therapy as an adjunct to conventional therapy in the treatment of diabetic foot ulcers,” *Lasers Med. Sci.*, vol. 32, no. 2, pp. 275–282, 2016.

[88] J. De Alencar, F. Santos, M. Barbosa, D. Campelo, R. A. De Oliveira, and R. A. Nicolau, “Effects of Low-Power Light Therapy on the Tissue Repair,” vol. 36, no. 6, pp. 298–304, 2018.

[89] I. Frangez, T. Nizic-Kos, and H. B. Frangez, “Phototherapy with LED Shows Promising Results in Healing Chronic Wounds in Diabetes Mellitus Patients : A Prospective Randomized Double-Blind Study,” *Photomed. Laser Surg.*, vol. 36, no. 7, pp. 377–382, 2018.

[90] C. N. Tchanque-Fossuo *et al.*, “A systematic review of low-level light therapy for treatment of diabetic foot ulcer,” *Wound Repair Regen.*, vol. 24, no. 2, pp. 418–426, 2016.

[91] E. Merigo, L. Tan, Z. Zhao, J. P. Rocca, and C. Fornaini, “Auto-Administered Photobiomodulation on Diabetic Leg Ulcers Treatment: A New Way to Manage It?,” *Case Rep. Med.*, vol. 2020, pp. 10–13, 2020.

[92] R. Raizman and L. Gavish, “At-Home Self-Applied Photobiomodulation Device for the Treatment of Diabetic Foot Ulcers in Adults With Type 2 Diabetes: Report of 4 Cases,” *Can. J. Diabetes*, vol. 44, no. 5, pp. 375–378, 2020.

[93] P. M. Carrinho, D. I. K. Andreani, V. D. A. Morete, S. Iseri, R. S. Navarro, and A. B. Villaverde, “A Study on the Macroscopic Morphometry of the Lesion Area on Diabetic Ulcers in Humans Treated with Photodynamic Therapy Using Two Methods of Measurement,” *Photomed. Laser Surg.*, vol. 36, no. 1, pp. 44–50, 2018.

[94] J. P. Tardivo *et al.*, “Is surgical debridement necessary in the diabetic foot treated with photodynamic therapy?,” *Diabet. Foot Ankle*, vol. 8, no. 1, p. 1373552, 2017.

[95] E. Brocco *et al.*, “Photodynamic Topical Antimicrobial Therapy for Infected Diabetic Foot Ulcers in Patients With Diabetes: A Case Series,” *Int. J. Low. Extrem. Wounds*, 2020.

[96] L. P. Rosa *et al.*, “Application of photodynamic therapy, laser therapy, and a cellulose membrane for calcaneal pressure ulcer treatment in a diabetic patient: A case report,” *Photodiagnosis Photodyn. Ther.*, vol. 19, pp. 235–238, 2017.

[97] R. Fekrazad, A. Sarrafzadeh, K. A. Kalhori, I. Khan, P. R. Arany, and A. Giubellino, “Improved Wound Remodeling Correlates with Modulated TGF-beta Expression in Skin Diabetic Wounds Following Combined Red and Infrared Photobiomodulation Treatments,” *Photochem. Photobiol. Sci.*, vol. 94, no. 4, pp. 775–779, 2018.

[98] M. Salvi, D. Rimini, F. Molinari, G. Bestente, and A. Bruno, “Effect of low-level light therapy on diabetic foot ulcers: a near-infrared spectroscopy study,” *J. Biomed. Opt.*, vol. 22, no. 3, p. 038001, 2017.

[99] S. A. Tantawy, W. K. Abdelbasset, D. M. Kamel, and S. M. Alrawaili, “A randomized controlled trial comparing helium-neon laser therapy and infrared laser therapy in patients with diabetic foot ulcer,” *Lasers Med. Sci.*, vol. 33, no. 9, pp. 1901–1906, 2018.

[100] E. Alves, M. A. F. Faustino, M. G. P. M. S. Neves, Â. Cunha, H. Nadais, and A. Almeida, “Potential Applications of Porphyrins in Photodynamic Inactivation beyond the Medical Scope,” *J. Photochem. Photobiol.*, vol. 22, no. Mar, pp. 34–57, 2014.

[101] H. Shy *et al.*, “Two-step Mechanochemical Synthesis of Porphyrins,” *Faraday Discuss.*,

vol. 170, pp. 59–69, 2015.

[102] M. Imran, M. Ramzan, A. K. Qureshi, M. Azhar Khan, and M. Tariq, “Emerging applications of porphyrins and metalloporphyrins in biomedicine and diagnostic magnetic resonance imaging,” *Biosensors*, vol. 8, no. 4, pp. 1–17, 2018.

[103] H. Zhang *et al.*, “Fluorinated cryptophane-A and porphyrin-based theranostics for multimodal imaging-guided photodynamic therapy,” *Chem. Commun.*, vol. 56, no. 25, pp. 3617–3620, 2020.

[104] D. Fan *et al.*, “A 64Cu-porphyrin-based dual-modal molecular probe with integrin αvβ3 targeting function for tumour imaging,” *J. Label. Compd. Radiopharm.*, vol. 63, no. 5, pp. 212–221, 2020.

[105] Y. Zhang *et al.*, “Porphyrin-terminated nanoscale fluorescent polyrotaxane as a biodegradable drug carrier for anticancer research,” *Nanotechnology*, no. May, pp. 0–30, 2020.

[106] G. L. Yang, S. F. Zhao, N. Y. Chen, and S. Li, “Design and syntheses of novel fluoroporphyrin - Anthraquinone complexes as antitumor agents,” *Chem. Pharm. Bull.*, vol. 64, no. 9, pp. 1310–1314, 2016.

[107] R. Paolesse, S. Nardis, D. Monti, M. Stefanelli, and C. Di Natale, “Porphyrinoids for Chemical Sensor Applications,” *Chem. Rev.*, vol. 117, no. 4, pp. 2517–2583, 2017.

[108] L. Lvova, P. Galloni, B. Floris, I. Lundström, R. Paolesse, and C. Di Natale, “A Ferrocene-porphyrin ligand for multi-transduction chemical sensor development,” *Sensors (Switzerland)*, vol. 13, no. 5, pp. 5841–5856, 2013.

[109] M. X. You, Y. X. Wang, H. Wang, and R. H. Yang, “Fluorescent detection of singlet oxygen: Amplifying signal transduction and improving sensitivity based on intramolecular FRET of anthryl appended porphyrins,” *Chinese Sci. Bull.*, vol. 56, no. 31, pp. 3253–3259, 2011.

[110] M. Saleem, M. H. Sayyad, K. S. Karimov, M. Yaseen, and M. Ali, “Cu(II) 5,10,15,20-tetrakis(4′-isopropylphenyl) porphyrin based surface-type resistive-capacitive multifunctional sensor,” *Sensors Actuators, B Chem.*, vol. 137, no. 2, pp. 442–446, 2009.

[111] S. Iordache, R. Cristescu, A. C. Popescu, C. E. Popescu, G. Dorcioman, and I. N. Mihailescu, “Functionalized porphyrin conjugate thin films deposited by matrix assisted pulsed laser evaporation,” *Appl. Surf. Sci.*, vol. 278, pp. 207–210, 2013.

[112] S. Boufi, M. R. Vilar, V. Parra, A. M. Ferraria, and A. M. B. do Rego, “Grafting of Porphyrins on Cellulose Nanometric Films,” *Langmuir*, vol. 24, no. 14, pp. 7309–7315, 2008.

[113] B. Mai *et al.*, “Smart hydrogel-based DVDMS / bFGF nanohybrids for antibacterial phototherapy with multiple damaging-sites and accelerated wound healing,” *ACS Appl. Mater. Interfaces*, vol. 12, no. 9, pp. 10156–10169, 2020.

[114] C. Mao *et al.*, “A Repeatable Photodynamic Therapy with Triggered Signaling Pathways of Fibroblast Cell Proliferation and Differentiation to Promote Bacteria-Accompanied Wound Healing,” *ASC Nano*, vol. 12, no. 2, pp. 1747–1759, 2018.

[115] P. E. Donnelly, T. Chen, A. Finch, C. Brial, S. A. Maher, and P. A. Torzilli, “Photocrosslinked tyramine-substituted hyaluronate hydrogels with tunable mechanical properties improve immediate tissue-hydrogel interfacial strength in articular cartilage,” *J. Biomater. Sci. Polym. Ed.*, vol. 28, no. 6, pp. 582–600, 2017.

[116] C. R. Fontana, D. S. dos Santos Junior, J. M. Bosco, D. M. Spolidorio, and R. A. C. Marcantonio, “Evaluation of Chitosan Gel as Antibiotic and Photosensitizer Delivery,” *Drug Deliv.*, vol. 15, pp. 417–422, 2008.

[117] J. H. Ryu, Y. Lee, W. H. Kong, T. G. Kim, T. G. Park, and H. Lee, “Catechol-Functionalized Chitosan / Pluronic Hydrogels for Tissue Adhesives and Hemostatic Materials †,”

*Biomacromolecules*, vol. 12, pp. 2653–2659, 2011.

[118] M. A. Aziz, J. D. Cabral, H. J. L. Brooks, S. C. Moratti, and L. R. Hanton, “Antimicrobial Properties of a Chitosan Dextran-Based Hydrogel for Surgical Use,” *Antimicrob. Agents Chemother.*, vol. 56, no. 1, pp. 280–7, 2012.

[119] K. Richter *et al.*, “Deferiprone and Gallium-Protoporphyrin Have the Capacity to Potentiate the Activity of Antibiotics in Staphylococcus aureus Small Colony Variants,” *Front. Cell. Infect. Microbiol.*, vol. 7, no. June, pp. 1–10, 2017.

[120] F. J. O’Brien, “Biomaterials & scaffolds for tissue engineering,” *Mater. Today*, vol. 14, no. 3, pp. 88–95, 2011.

[121] C. Ferroni *et al.*, “Wool keratin 3D scaffolds with light-triggered antimicrobial activity,” *Biomacromolecules*, vol. 17, no. 9, pp. 2882–2890, 2016.

[122] M. M. Steward, A. Sridhar, and J. S. Meyer, “Neural Regeneration,” *Curr. Top. Microbiol. Immunol.*, vol. 367, pp. 163–191, 2013.

[123] C. C. Hsu, A. Serio, N. Amdursky, C. Besnard, and M. M. Stevens, “Fabrication of Hemin-Doped Serum Albumin-Based Fibrous Scaffolds for Neural Tissue Engineering Applications,” *ACS Appl. Mater. Interfaces*, vol. 10, no. 6, pp. 5305–5317, 2018.

[124] H. Shrestha, R. Bala, and S. Arora, “Lipid-Based Drug Delivery Systems,” *J. Pharm.*, vol. 2014, no. 8081820, p. 10, 2014.

[125] T. Ben-mordechai *et al.*, “Targeting and modulating infarct macrophages with hemin formulated in designed lipid-based particles improves cardiac remodeling and function,” *J. Control. Release*, vol. 10, no. 257, pp. 21–31, 2017.

[126] H. Furukawa, K. E. Cordova, M. O’Keeffe, and O. M. Yaghi, “The chemistry and applications of metal-organic frameworks,” *Science (80-. ).*, vol. 341, no. 6149, 2013.

[127] F. Cui, Q. Deng, and L. Sun, “Prussian blue modified metal-organic framework MIL-101(Fe) with intrinsic peroxidase-like catalytic activity as a colorimetric biosensing platform,” *RSC Adv.*, vol. 5, no. 119, pp. 98215–98221, 2015.

[128] D. Han *et al.*, “Enhanced photocatalytic activity and photothermal effects of cu-doped metal-organic frameworks for rapid treatment of bacteria-infected wounds,” *Appl. Catal. B Environ.*, vol. 261, no. August, p. 118248, 2020.

[129] G. Borkow, “Using Copper to Improve the Well-Being of the Skin,” *Curr. Chem. Biol.*, vol. 8, no. 2, pp. 89–102, 2015.

[130] G. Ximing, G. Bin, W. Yuanlin, and G. Shuanghong, “Preparation of spherical metal–organic frameworks encapsulating ag nanoparticles and study on its antibacterial activity,” *Mater. Sci. Eng. C*, vol. 80, pp. 698–707, 2017.

[131] Y. Luo *et al.*, “Dual Metal-Organic Framework Heterointerface,” *ACS Cent. Sci.*, vol. 5, no. 9, pp. 1591–1601, 2019.

[132] A. F. Wright, C. F. Chakarova, M. M. Abd El-Aziz, and S. S. Bhattacharya, “Photoreceptor degeneration: Genetic and mechanistic dissection of a complex trait,” *Nat. Rev. Genet.*, vol. 11, no. 4, pp. 273–284, 2010.

[133] J. F. Martin and R. A. Poché, “Awakening the regenerative potential of the mammalian retina,” *Co. Biol.*, vol. 146, no. 23, 2019.

[134] Y. Wang *et al.*, “The application of methylprednisolone nanoscale zirconium-porphyrin metal-organic framework (MPS-NPMOF) in the treatment of photoreceptor degeneration,” *Int. J. Nanomedicine*, vol. 14, pp. 9763–9776, 2019.

[135] S. Huh, S. J. Kim, and Y. Kim, “Porphyrinic metal-organic frameworks from custom-designed porphyrins,” *CrystEngComm*, vol. 18, no. 3, pp. 345–368, 2016.

[136] Y. Zhao, Y. Kuang, M. Liu, J. Wang, and R. Pei, “Synthesis of Metal-Organic Framework

Nanosheets with High Relaxation Rate and Singlet Oxygen Yield," *Chem. Mater.*, vol. 30, no. 21, pp. 7511–7520, 2018.

[137] J. D. Luo and A. F. Chen, "Nitric oxide: A newly discovered function on wound healing," *Acta Pharmacol. Sin.*, vol. 26, no. 3, pp. 259–264, 2005.

[138] C. H. Su *et al.*, "Enhancing Microcirculation on Multitriggering Manner Facilitates Angiogenesis and Collagen Deposition on Wound Healing by Photoreleased NO from Hemin-Derivatized Colloids," *ACS Nano*, vol. 13, no. 4, pp. 4290–4301, 2019.

[139] M. R. Schäffer, U. Tantry, P. A. Efron, G. M. Ahrendt, F. J. Thornton, and A. Barbul, "Diabetes-impaired healing and reduced wound nitric oxide synthesis: A possible pathophysiologic correlation," *Surgery*, vol. 121, no. 5, pp. 513–519, 1997.

[140] P. Tessari *et al.*, "Nitric oxide synthesis is reduced in subjects with type 2 diabetes and nephropathy," *Diabetes*, vol. 59, no. 9, pp. 2152–2159, 2010.

[141] B. S. Dellamea, C. B. Leitão, R. Friedman, and L. H. Canani, "Nitric oxide system and diabetic nephropathy," *Diabetol. Metab. Syndr.*, vol. 6, no. 1, pp. 1–6, 2014.

[142] J. Beck-Ripp, M. Griese, S. Arenz, C. Köring, B. Pasqualoni, and P. Bufler, "Changes of exhaled nitric oxide during steroid treatment of childhood asthma," *Eur. Respir. J.*, vol. 19, no. 6, pp. 1015–1019, 2002.

[143] A. D. Smith *et al.*, "Exhaled nitric oxide: A predictor of steroid response," *Am. J. Respir. Crit. Care Med.*, vol. 172, no. 4, pp. 453–459, 2005.

[144] G. M. Anstead, B. Chandrasekar, Q. Zhang, and P. C. Melby, "Multinutrient undernutrition dysregulates the resident macrophage proinflammatory cytokine network, nuclear factor-κB activation, and nitric oxide production," *J. Leukoc. Biol.*, vol. 74, no. 6, pp. 982–991, 2003.

[145] G. Wu, N. E. Flynn, S. P. Flynn, C. A. Jolly, and P. K. Davis, "Dietary Protein or Arginine Deficiency Impairs Constitutive and Inducible Nitric Oxide Synthesis by Young Rats," *J. Nutr.*, vol. 129, no. 7, pp. 1347–1354, 1999.

[146] J. S. Beckman, W. H. Koppenol, R. Of, N. Oxide, and P. In, "Regulation of Nitric Oxide Production in Health and Disease," *Curr. Opin. Clin. Nutr. Metab. Care*, vol. 13, no. 5 Pt 1, pp. 97–104, 2011.

[147] J. M. Sippel *et al.*, "Exhaled nitric oxide levels correlate with measures of disease control in asthma," *J. Allergy Clin. Immunol.*, vol. 106, no. 4, pp. 645–650, 2000.

[148] A. Klinkova *et al.*, "Structural and optical properties of self-assembled chains of plasmonic nanocubes," *Nano Lett.*, vol. 14, no. 11, pp. 6314–6321, 2014.

[149] F. Giuntini *et al.*, "Conjugatable water-soluble Pt(ii) and Pd(ii) porphyrin complexes: Novel nano- and molecular probes for optical oxygen tension measurement in tissue engineering," *Photochem. Photobiol. Sci.*, vol. 13, no. 7, pp. 1039–1051, 2014.

[150] E. Roussakis *et al.*, "Theranostic biocomposite scaffold membrane," *Biomaterials*, vol. 212, no. May, pp. 17–27, 2019.

[151] L. M. Mink *et al.*, "Platinum(II) and platinum(IV) porphyrin complexes: Synthesis, characterization, and electrochemistry," *Polyhedron*, vol. 16, no. 16, pp. 2809–2817, 1997.

[152] G. E. O. Borgstahl and R. E. Oberley-Deegan, "Superoxide dismutases (SODs) and SOD mimetics," *Antioxidants*, vol. 7, no. 11, pp. 7–9, 2018.

[153] R. Bonetta, "Potential Therapeutic Applications of MnSODs and SOD-Mimetics," *Chem. - A Eur. J.*, vol. 24, no. 20, pp. 5032–5041, 2018.

[154] T. Kurahashi and J. Fujii, "Roles of antioxidative enzymes in wound healing," *J. Dev. Biol.*, vol. 3, no. 2, pp. 57–70, 2015.

[155] R. Thomas and N. Sharifi, "SOD mimetics: A Novel Class of Androgen Receptor Inhibitors

that Suppreses Castration-Resistant Growth of Prostate Cancer," *Mol. Cancer Ther.*, vol. 1, pp. 87–97, 2012.

[156] D. Candas and J. J. Li, "MnSOD in oxidative stress response-potential regulation via mitochondrial protein influx," *Antioxidants Redox Signal.*, vol. 20, no. 10, pp. 1599–1617, 2014.

[157] H. Arti, M. Khorami, and V. Ebrahimi-Nejad, "Comparison of negative pressure wound therapy (NPWT) & conventional wound dressings in the open fracture wounds," *Pakistan J. Med. Sci.*, vol. 32, no. 1, pp. 65–69, 2016.

[158] C. Huang, T. Leavitt, L. R. Bayer, and D. P. Orgill, "Effect of negative pressure wound therapy on wound healing," *Curr. Probl. Surg.*, vol. 51, no. 7, pp. 301–331, 2014.

[159] A. M. Barbosa *et al.*, "Redox-Active Drug, MnTE-2-PyP5+, Prevents and Treats Arrhythmias Preserving Heart Contractile Function," *Oxid. Med. Cell. Longev.*, vol. 21, no. 2020, p. 4850697, 2020.

[160] B. Gauter-Fleckenstein *et al.*, "Early and late administration of MnTE-2-PyP5+ in mitigation and treatment of radiation-induced lung damage," *Free Radic. Biol. Med.*, vol. 48, no. 8, pp. 1034–1043, 2010.

[161] J. O. Archambeau, A. Tovmasyan, R. D. Pearlstein, J. D. Crapo, and I. Batinic-Haberle, "Superoxide dismutase mimic, MnTE-2-PyP5+ ameliorates acute and chronic proctitis following focal proton irradiation of the rat rectum," *Redox Biol.*, vol. 1, no. 1, pp. 599–607, 2013.

[162] G. L. Bellot *et al.*, "MnSOD is implicated in accelerated wound healing upon Negative Pressure Wound Therapy (NPWT): A case in point for MnSOD mimetics as adjuvants for wound management," *Redox Biol.*, vol. 20, pp. 307–320, 2019.

[163] Y. Y. Cui *et al.*, "SOD mimetic improves the function, growth, and survival of small-size liver grafts after transplantation in rats," *Transplantation*, vol. 94, no. 7, pp. 687–694, 2012.

[164] J. Kim, K. J. Jung, and K. M. Park, "Reactive oxygen species differently regulate renal tubular epithelial and interstitial cell proliferation after ischemia and reperfusion injury," *Am. J. Physiol. - Ren. Physiol.*, vol. 298, no. 5, 2010.

[165] A. Kübler, R. K. Finley, I. A. Born, and T. S. Mang, "Effect of photodynamic therapy on the healing of a rat skin flap and its implication for head and neck reconstructive surgery," *Lasers Surg. Med.*, vol. 18, no. 4, pp. 397–405, 1996.

[166] M. Grinholc, A. Kawiak, J. Kurlenda, A. Graczyk, and K. P. Bielawski, "Photodynamic effect of protoporphyrin diarginate (PPArg2) on methicillin-resistant Staphylococcus aureus and human dermal fibroblasts," *Acta Biochim. Pol.*, vol. 55, no. 1, pp. 85–90, 2008.

[167] S. a G. Lambrechts, T. N. Demidova, M. C. G. Aalders, T. Hasan, and M. R. Hamblin, "Photodynamic therapy for Staphylococcus aureus infected burn wounds in mice," *Photochem. Photobiol. Sci.*, vol. 4, pp. 503–509, 2005.

[168] E. A. Lyapina, T. V. Machneva, E. A. Larkina, E. P. Tkachevskaya, A. N. Osipov, and A. F. Mironov, "Effect of photosensitizers pheophorbide a and protoporphyrin IX on skin wound healing upon low-intensity laser irradiation," *Biophysics (Oxf).*, vol. 55, no. 2, pp. 296–300, 2010.

[169] P. Gál *et al.*, "Should open excisions and sutured incisions be treated differently? A review and meta-analysis of animal wound models following low-level laser therapy," *Lasers Med. Sci.*, vol. 33, no. 6, pp. 1351–1362, 2018.

[170] D. P. Kuffler, "Photobiomodulation in promoting wound healing: a review," *Regen. Med.*, vol. 11, no. 1, pp. 107–22, 2015.

[171] V. Nesi-Reis *et al.*, "Contribution of photodynamic therapy in wound healing: A systematic

review," *Photodiagnosis Photodyn. Ther.*, vol. 21, pp. 294–305, 2018.

[172] D. S. Pellosi, P. da C. C. De Jesus, and A. C. Tedesco, "Spotlight on the delivery of photosensitizers: different approaches for photodynamic-based therapies," *Expert Opin. Drug Deliv.*, vol. 14, no. 12, pp. 1395–1406, 2017.

[173] K. Shanmugapriya, H. Kim, Y. W. Lee, and H. W. Kang, "Multifunctional heteropolysaccharide hydrogel under photobiomodulation for accelerated wound regeneration," *Ceram. Int.*, vol. 46, no. 6, pp. 7268–7278, 2020.

[174] S. R. Tsai and M. R. Hamblin, "Biological effects and medical applications of infrared radiation," *J. Photochem. Photobiol. B Biol.*, vol. 170, no. December 2016, pp. 197–207, 2017.

# Chapter 2. Inactivation of *Staphylococcus aureus* and *Pseudomonas aeruginosa*

## 1. General remarks

### 1.1. Gram-positive Bacteria

As previously stated, *Staphylococcus aureus* and *Pseudomonas aeruginosa* are among the bacteria most implicated in the infection and formation of biofilms in chronic wounds. These are prime examples of gram-positive bacteria, in the case of *S. aureus,* and gram-negative bacteria, in the case of *P.aeruginosa*, which differ mainly in their wall structural composition. The gram-positive bacteria exhibit a thicker cell wall that consists primarily of a single type of molecule, the peptidoglycan. Peptidoglycan is a polysaccharide composed of two sugar derivatives – *N acetylglucosamine* and *N-acetylmuramic acid* and a few amino acids [1]. In gram-positive bacteria, such as *S. aureus,* peptidoglycan takes up as much as 90% of the cell wall, often organizing itself into layers. Through these layers of peptidoglycan, anionic glycopolymers containing phosphodiester-linked polyol repeat units may be found, called teichoic acids, which possess many functions including cations homeostasis, and influence in rigidity and porosity of the cell wall [2]. They are intimately involved in many aspects of cell division and are essential for maintaining cell shape in rod-shaped organisms [3].

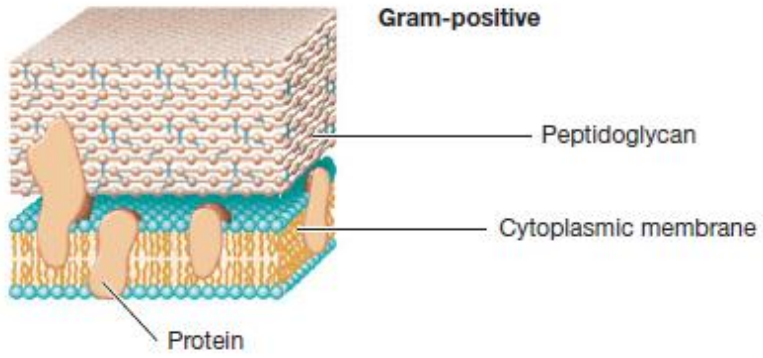


**Fig. 2.1 -** Cell wall structure of a gram-positive bacterium, adapted from [1].

*S. aureus* is a member of the *Staphylococcaceae* family. It colonizes on skin or mucosal surfaces (often the nasal passages), and this is made especially easy by immunosuppressed systems, which makes diabetic patients ideal candidates for infection. *S. aureus* is the most common bacterial isolate reported

from occidental countries in diabetic foot infections (DFI), and after initial infection, the persistence and wound adherence is enhanced by virulence factors (being sometimes responsible for fever, sickness and even death), making early diagnosis and proper treatment very important in avoiding a foot amputation [4]. If in the past, the existence of an infection was immediately eradicated with antibiotics, over the years, the use of antibiotics, leads to the appearance of antibiotic resistant bacterial strains. Since the medical use of penicillin began, in 1942, bacteria have evolved to produce a penicillinase enzyme, which hydrolyzes the antibiotic rendering it ineffective [5]. Although a penicillinase-resistant penicillin was synthesized, the methicillin, after it started being used to treat *S. aureus'* infections, a methicillin-resistant *S. aureus* (MRSA) strain was isolated. This strain differs from methicillin-sensitive *S. aureus* by the presence of a large stretch of foreign DNA (40-60 Kb) referred to as the *mec* element and the presence of the *mecA* gene that encodes the 76 KDa penicillin-binding protein, PBP2a, an essential protein in conferring methicillin resistance [6]. Although initially these infections seemed to be a problem mostly limited to hospitals and health care units (hospital acquired infections), their spread and prevalence increased [7].

### 1.2. Gram-negative Bacteria

The cell wall of the gram-negative bacteria, when compared with the gram-positive one, have an additional layer besides the peptidoglycan layer and are generally more complex. In contrast to gram-positive bacteria, in gram-negative bacteria the peptidoglycan represents only 10% of their cell wall, having instead most of its composition attributed to an outer membrane. This outer membrane functions essentially as a second lipid bilayer and one of its most important biological activities is its toxicity to animals. Some gram-negative pathogenic bacteria can account their effects and symptoms to their toxic outer membrane components [1]. The highly organized system of gram-negative's cell wall, and its heterogeneous composition, makes the entrance of large exogenous molecules very difficult, providing these class of bacteria an added protection against exogenous factors [8]. Thus, gram-negative bacteria tend to be more difficult to treat infection-wise, and are generally more resistant to antibiotics than gram-positive bacteria, *Pseudomonas* is a good example of this [2].

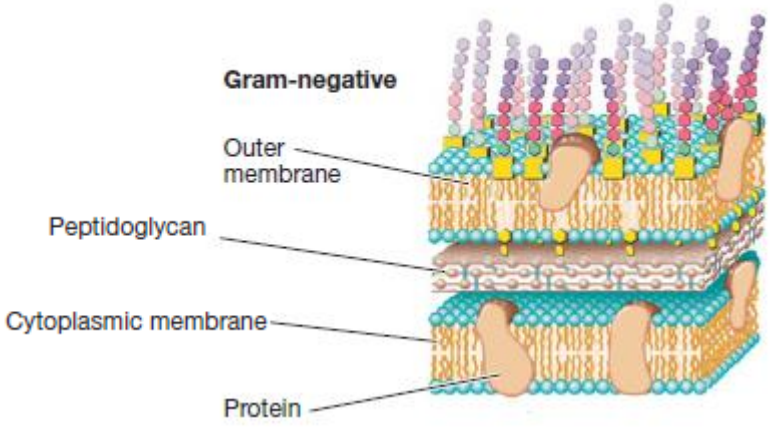


**Fig. 2.2**- Cell wall structure of a gram-negative bacterium, adapted from [1].

*P. aeruginosa* belongs to the *Pseudomonadaceae* family, a member of γ-proteobacteria. It is an ubiquitous organism which can be found in many living sources, such as plants, animals and humans. It can also be found in surfaces and community reservoirs (such as swimming pools and hot tubs, soil and even vegetables) [9]. *Pseudomonas*, however, is not generally found in the normal human microbiota. It can cause multiple infections in humans, which can vary from local to systemic, and from benign to life threatening. Hospitalization is a common transmission, with increased risk for patients with trauma or a break in their cutaneous or mucosal barriers, as well as in patients with impaired immunity [9], [10]. *P. aeruginosa* has manifold virulence factors which helps it to survive and thrive and which vary from strain to strain [11]. This species of bacteria has also developed mechanisms of resistance to antibacterial agents like antibiotics. This resistance mechanisms can be developed by acquiring resistance genes on mobile genetic elements (like plasmids) or through mutational processes that alter the typical expression and function of some of their mechanisms. The main resistance mechanism found is due to the differential gene expression under stress conditions, that leads to the encoding of genes responsible for resistance to β-lactam antibiotics [9], [10]. *P. aeruginosa* also form biofilms to protect itself from a hostile exterior environment (including antibiotic treatment), making its elimination even more challenging.

Without the means to effectively treat the diseases caused by these resistant strains, this problem will become more serious for the general population. Consequently, the objective of this study was to evaluate the potential of starch films loaded with two different porphyrin derivatives in the treatment of skin infections. The porphyrins selected to incorporate in the starch films were the tetracationic 5,10,15,20-tetrakis(1-methylpyridinium-4-yl)porphyrin tetraiodide

(**TMPyP**) which has already revealed good antimicrobial properties including inactivation of *S. aureus* and *P. aeruginosa* in solution and the neutral 5,10,15,20-tetrakis(pentafluorophenyl)porphyrin (**TPP5F**). The efficiency of **TPP5F** in bacteria photoinactivation in solution is reduced mainly due to the fact that when is aqueous solution, the high hydrophobicity leads to an high aggregation rate, reducing dramatically the singlet oxygen generation, the main responsible for the photodynamic effect.

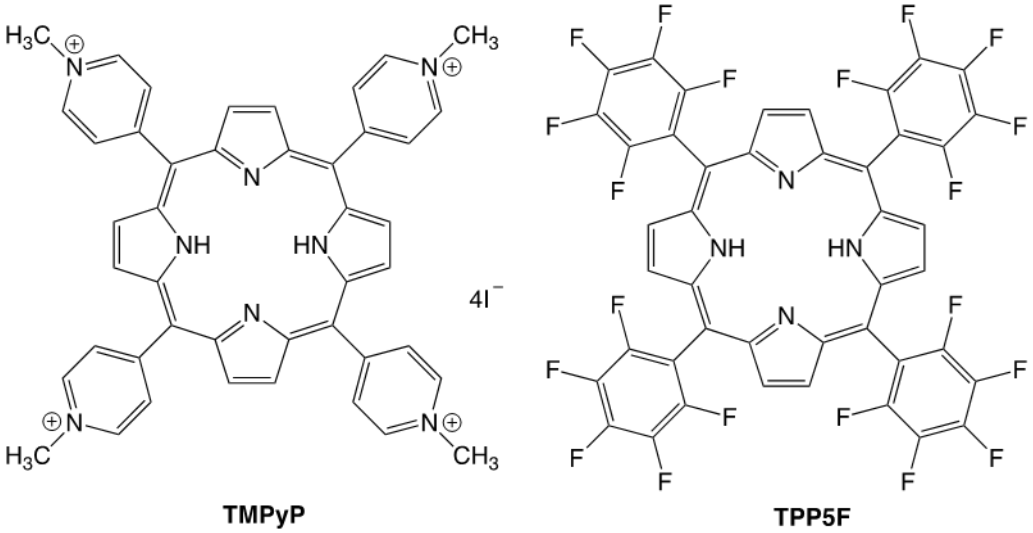


**Fig. 2.3 -** Molecular structures of the porphyrin PS used in this study to incorporate in starch films.

## 2. Material and Methods

### 2.1. Synthesis of 5,10,15,20-tetrakis(pentafluorophenyl)porphyrin (TPP5F) and 5,10,15,20-tetrakis(1-methylpyridinium-4-yl)porphyrin (TMPyP)

The porphyrinic photosensitizers 5,10,15,20-tetrakis(pentafluorophenyl)-porphyrin (**TPP5F**) and 5,10,15,20-tetrakis(1-methylpyridinium-4-yl)porphyrin tetra-iodide (**TMPyP**), (Fig. 2.3), were synthetized according to previously described procedures [12], [13]. The tetracationic **TMPyP** was prepared by methylation of the corresponding neutral 5,10,15,20-tetrapyridylporphyrin (**TPyP**). The neutral porphyrins, **TPP5F** and **TPyP**, were obtained from the Rothemund reaction of pyrrole and the 5,10,15,20-tetrakis(pentafluorophenyl)porphyrin or pyridine-4-carbaldehyde respectively.

The cationization of **TPyP** was carried out using a large excess of methyl iodide and dry dimethylformamide (DMF) as solvent at 40 °C, overnight, in a

closed flask. The reactional mixture was cooled to room temperature and diethyl ether was added to precipitate the **TMPyP**. The solid obtained was filtered, washed with diethyl ether and redissolved in methanol/water being after concentration, reprecipitated in methanol/acetone. Porphyrins purity were confirmed by thin layer chromatography and by $^{1}$H NMR spectroscopy [14], [15].

### 2.2. Starch/ porphyrin films

The starch-based materials used in this work were kindly provided by Idalina Gonçalves group from CICECO which incorporate the **TPP5F** and **TMPyP**. These materials were based on the formulation: starch recovered from industrial potato washing slurries (45% wt.), glycerol (30% wt.), water (25% wt.) The tetracationic **TMPyP** represented 0.5% of dry starch weight meanwhile **TPP5F** represented 0.05 % of the starch film. All components including the PS were combined, melt-mixed, granulated, and further hot-pressed as thermoplastic starch (TPS)/PS-based films. TPS-based formulation without **TMPyP** or **TPP5F** was used as reference/control.

**Fig. 2.4**- Starch/porphyrin-based material (TPS/**TMPyP**).

### 2.3. Characterization of bacterial strains and culture conditions

Two bacterial species were used in this study, *S. aureus (*strain DSM 25693), a Gram-positive bacterium, and *P. aeruginosa*, a Gram-negative bacterium. The *S. aureus* DSM 25693 is a methicillin-resistant strain (MRSA) with six staphylococcal enterotoxins A, C, H, G, I and Toxic Shock Syndrome Toxin 1 (TSST-1) isolated from sputum [16]. The *P. aeruginosa* strain was isolated from a patient of the Hospital of Matosinhos, in a previous work from our research group [17]. This *P. aeruginosa* strain is resistant to: lactams **Cefoxitin** (30 µg) (9018, Liofilchem, Italy), **Amoxycillin** (25 µg) (CT0061B, Oxoid, United

Kingdom), **Imipenem** (10 µg) (CT0455B, Oxoid, United Kingdom), and **Ampicillin** (10 µg) (CT0003B, Oxoid, United Kingdom); for the second generation fluoroquinolone **Ciprofloxacin** (5 µg) (CT0425B, Oxoid, United Kingdom); for the carboxylic acids and derivatives **Penicillin G** (10 µg) (CT0043B, Oxoid, United Kingdom), **Piperacillin** (100 µg)/**Tazobactam** (10 µg) (CT0725B, Oxoid, United Kingdom), **Piperacillin** (100 µg) (CT0199B, Oxoid, United Kingdom), for the benzene derivative **Chloramphenicol** (30 µg) (CT0013B, Oxoid, United Kingdom); and for the **Tetracycline** (10 µg) (CT0053B, Oxoid, United Kingdom).

The two bacteria were grown aerobically in Tryptic Soy Broth (TSB, Liofilchem, Italy) at 37 °C for 18-24 h, under horizontal shaking at 120 rpm, until reaching a concentration of ≈$10^9$ colony forming units per mL (CFU $mL^{-1}$). For each assay, an aliquot of the overnight inoculum was transferred to 30 mL of fresh TSB and incubated under the same conditions.

## 2.4. Light source

The artificial white light was provided by a LED (light-emitting diodes) projector (ELMARK®, United Kingdom) (20 W operate at ~230 V of voltage, and ~50 Hz). In the Fig. 10 is shown the spectral range of the white light emitted by the LED projector. For each assay, the light irradiance was measured and adjusted to 50 mW $cm^{-2}$ with a power and energy meter (model FieldMaxII-Top from Coherent, USA) connected to a high-sensitivity sensor (model PS19Q, Coherent, USA).

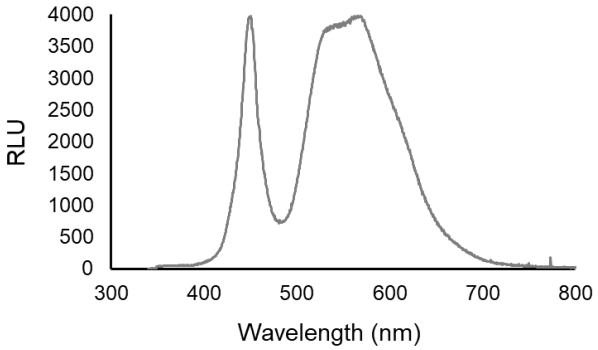


**Fig. 2.5 -** LED output. In the graph is shown the spectral range of the white light emitted by the LED projector used. The data are shown as relative light units (RLU) vs. wavelength in nm.

## 2.5. Antimicrobial Photodynamic Therapy (aPDT) treatments

### 2.5.1. *In vitro* aPDT assays

For each assay, a bacterial suspension from the overnight inoculum (with a bacterial load of ≈$10^9$ CFU $mL^{-1}$) was ten-fold diluted in PBS to reach the bacterial concentration of ≈$10^8$ CFU $mL^{-1}$. A final volume of 5.0 mL was added to each well of a 6-well plate, correspondent to each sample. A disc of each starch material (TPS/PS) film) with a diameter of 6 mm (Ø 6 mm, 28.27 $mm^2$), [material without PS (TPS film control), material with **TMPyP** (0.5%) or with **TPP5F** (0.05%)] was added to the correspondent well, and were incubated in the dark for 10 min, at room temperature, with magnetic stirring (100 rpm). Light (LC) and Dark (DC) controls were prepared along with the samples LC bacteria, LC TPS film, Sample light film **TMPyP** 0.5%, Sample light film **TPP5F** 0.05%, and DC bacteria, DC TPS film, DC film **TMPyP** 0.5%, DC film **TPP5F** 0.05%. After a dark incubation period, dark controls were protected from light with aluminium foil; samples and light controls (LC Bacteria and LC film) were exposed to white light at an irradiance of 50 mW $cm^{-2}$ for a total irradiance time of 60 min. Periodically (0, 15, 30 and 45 min) aliquots of 100 µL were collected, successive ten-fold dilutions in PBS were performed, and 3 droplets of 10 µL were plated per dilution, by the surface plating method, in Petri dishes with TSA medium. Then, the plates were incubated at 37 °C for 24 h. The number of colony forming units (CFU) were counted and the concentration of bacterial cells were expressed as CFU $mL^{-1}$.

Three independent assays in triplicate were performed for each condition tested.

### *2.5.2. Ex vivo* aPDT assays in porcine skin

Porcine skin samples were first prepared and disinfected. The protocol of preparation and disinfection was adapted from previous works done in our research group [18], [19]. The fresh skin samples were acquired from a local supermarket, and, once in the laboratory, the layer of adipose tissue beneath the dermis layer was removed with a surgical scalpel. Then, the skin samples were cut into 9.0 $cm^2$ (3.0 x 3.0 cm), and a small area of 1.0 $cm^2$ was defined in the skin surface. For the sterilization procedure, the prepared skin samples were placed in Petri dishes and sprayed with 70% ethanol in a way that ensures that all the skin sample surface was covered with ethanol and incubated for 30 min. After that, the skin samples were abundantly washed with sterile PBS and, with the open Petri dishes, subjected to UV-C light (100 – 280 nm) for a period of 30 min (Fig. 2.6)

Following the decontamination procedure, one of two different methodologies were practiced, herein named Methodology A and Methodology B.

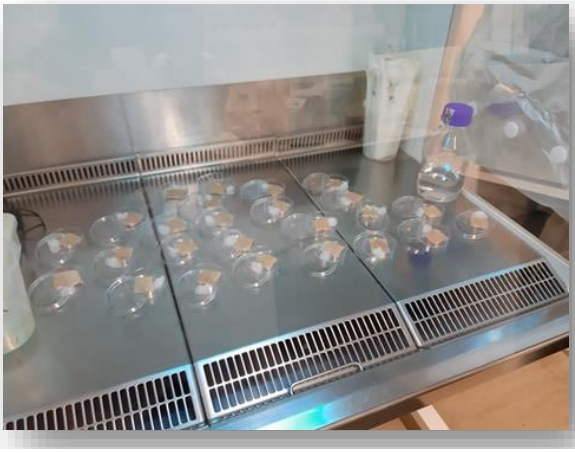

**Fig. 2.6**- Porcine skin samples being subjected to UV-C light for sterilization.

**Methodology A**

After the disinfection procedure, in the delimited area of 1.0 $cm^2$, the surface of the skin was contaminated with a sterile cotton swab from a bacterial suspension of *S. aureus* with a concentration of ≈$10^8$ CFU $cm^{-2}$, in PBS. The TPS/PS film was then placed above the same area, covering the delimited area of the skin samples. After 30 min of dark incubation, the skin samples with or without the starch films on top, were exposed to artificial white light at an irradiance of 50 mW $cm^{-2}$, for periods of time of 60,150, 180, or 360 min. At the irradiation period end, the film was removed and the amount of bacteria remaining below the starch film was determined by collecting with the aid of a sterile cotton swab into an Eppendorf with 1.0 mL of sterile PBS (30 x). Successive ten-fold dilutions were performed and 3 droplets of 10 µL were plated per dilution, by the surface plating method, in Petri dishes with TSA medium. Then, the plates were incubated at 37 °C for 24 h. The number of colony forming units (CFU) were counted and the concentration of bacterial cells were expressed as CFU $mL^{-1}$.
Also for the ex vivo assays, dark (DC) and light (LC) controls were performed along with the samples: LC/DC skin (irradiated/non-irradiated controls where no bacteria nor starch film (TPS) were added to this skin sample), LC/DC bacteria (irradiated/non-irradiated controls with the addition of bacteria to the skin surface), LC/DC film (irradiated/non-irradiated controls with bacteria to the skin surface and starch film on top), Sample light/dark film TPS/**TMPyP** 0.5% (irradiated/non-irradiated samples with bacteria to the skin surface and film loaded with the PS **TMPyP** at 0.5% added on top), and Sample light/dark film

TPS/**TPP5F** 0.05% (irradiated/non-irradiated samples with bacteria to the skin surface and film loaded with the PS **TPP5F** at 0.05% added on top).

Three independent assays in triplicate were performed for each condition tested.

**Methodology B**

After the disinfection procedure, in the delimited area of 1.0 it was placed the correspondent starch film (TPS) with the same area, covering the delimited area of the skin samples. The surface of the starch films (TPS) was contaminated with an aliquot of 10 µL of bacterial suspension, previously prepared with a concentration of ≈$10^8$ CFU $mL^{-1}$, in PBS. After a dark incubation period of 60 min, the samples were exposed to artificial white light at an irradiance of 50 mW $cm^{-2}$, for period of time of 6, 12 and 24 h. Then, the starch film (TPS) was collected, and its surface (above) was washed with 1.0 mL of sterile PBS (30 x) into an Eppendorf. The collection of the amount of bacteria remaining below the starch film was also done to evaluate if the microorganisms' community under the film was affected – this collection was performed with the aid of a sterile cotton swab into another Eppendorf with 1.0 mL of sterile PBS (30 x). Successive ten-fold dilutions were performed and 3 droplets of 10 µL were plated per dilution, by the surface plating method, in Petri dishes with TSA medium. Then, the plates were incubated at 37 °C for 24 h. The number of colony forming units (CFU) were counted and the concentration of bacterial cells were expressed as CFU $mL^{-1}$.
Also for the ex vivo assays, dark and light controls were performed along with the samples: LC/DC skin (irradiated/non-irradiated controls where no bacteria nor film were added to this skin sample), LC/DC bacteria (irradiated/non-irradiated controls with the addition of bacteria to the skin surface), LC/DC starch film (irradiated/non-irradiated controls with starch film (TPS) added to the skin surface and bacteria added to the starch film top), and Sample light/dark film TPS/**TMPyP** 0.5% (irradiated/non-irradiated samples with film loaded with the PS **TMPyP** at 0.5% added to the skin surface and bacteria added to the film top).

Three independent assays in triplicate were performed for each condition tested.

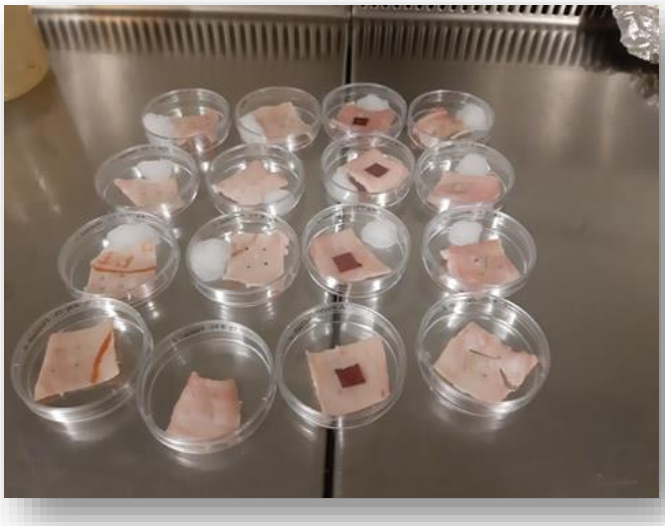

**Fig. 2.7-** Porcine skin samples with controls (bacteria, skin and starch film) and applied treatment sample (TPS/**TMPyP** film).

## 2.6. Statistical analysis

Statistical analysis of the obtained data was carried out by GraphPad Prism® 7.04 (GraphPad Software, CA, USA). Normal distribution of the data was checked by the Shapiro-Wilk normality test. The significance of bacterial concentrations between treatments, and along the experiments, was tested using two-way ANOVA analysis of variance and the Tukey's multiple comparison test was used for a pairwise comparison of the means. For different treatments, the significance of differences was evaluated by comparing the results obtained in the test samples after treatment with the results obtained for the correspondent test samples before treatment. A $p$ value < 0.05 value was considered statistically significant. At least, three independent assays in triplicate were performed for each condition tested.

## 3. Results and Discussion

Porphyrins have been known to conjugate to various different supports, however, this is the first time these TPS/porphyrin -based materials are tested for antimicrobial applicability, in the photoinactivation of *S.aureus* and *P.aeruginosa* both *in vitro* and *ex vivo.*

### 3.1. *In Vitro* Assay

#### 3.1.1. *Staphylococcus aureus* and *Pseudomonas aeruginosa* photoinactivation

To first assess the antimicrobial response of the starch/porphyrin based films (TPS/**TMPyP** and TPS/**TPP5F**), a liquid medium assay (in PBS) was performed. In this medium it was expected that the porphyrinic PS present in the starch films will be released into the liquid medium being available to generate reactive oxygen species to efficiently destroy the bacterial cells. The results (depicted in Fig. 2.8 A.) demonstrate neither the starch film without PS nor the films TPS/**TMPyP** and TPS/**TPP5F** are cytotoxic to the *S. aureus* strain in the absence of light. Upon light activation it is not observed any phototoxicity induced by light nor by the starch film or by the **TPS/TPP5F** at 0.05% towards *S. aureus* (Fig. 2.8. B). However, a significant inactivation effect ($p<0.0001$) was found for the TPS/**TMPyP** film, where a reduction of 7 log of CFU $mL^{-1}$ was observed after 60 min of irradiation. The starch materials with the well-known PS **TMPyP** incorporated showed effectiveness in the photoinactivation of *S. aureus*, notwithstanding, when the neutral porphyrin **TPP5F** was the PS molecule incorporated in the starch film, the photoinactivation of the *S. aureus* was not well succeeded. It is known that charge is an important parameter in photodynamic inactivation of bacteria, and it may affect the ability of the PS to bind to the bacteria [20]. A positively charged PS is generally more likely to bind to the bacteria wall than a neutral one [21]. A **TMPyP** is a positively charged PS and a higher inactivation of *S. aureus* was observed when compared with the **TPP5F**. However, it has been reported in the literature an effective inactivation of *S. aureus* with **TPP5F**, albeit conjugated with a methacrylic unit [22]. It is worth to refer that, in this study, the **TPP5F** concentration in the starch film is ten times lower to the **TMPyP** in the starch film and lower to the effective concentration reported in the literature. Also, the irradiance of white light used in previous studies was 156 mW $cm^{-2}$, while in this study the irradiance was 50 mW $cm^{-2}$, a much lower light irradiance.

**A.**

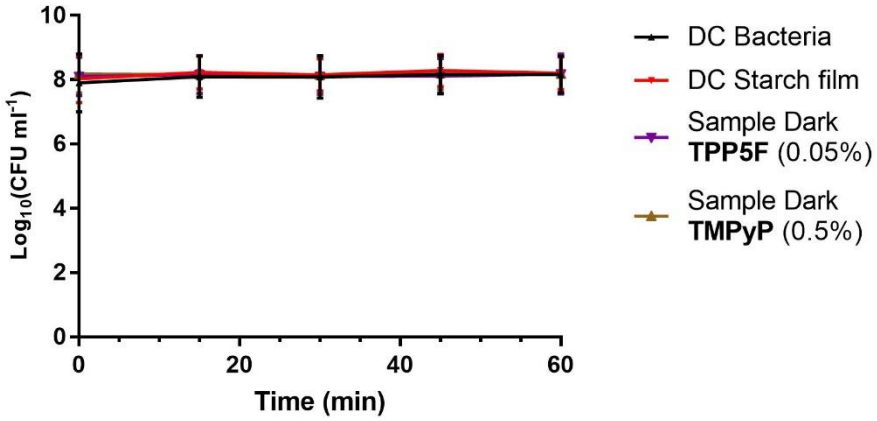


**B.**

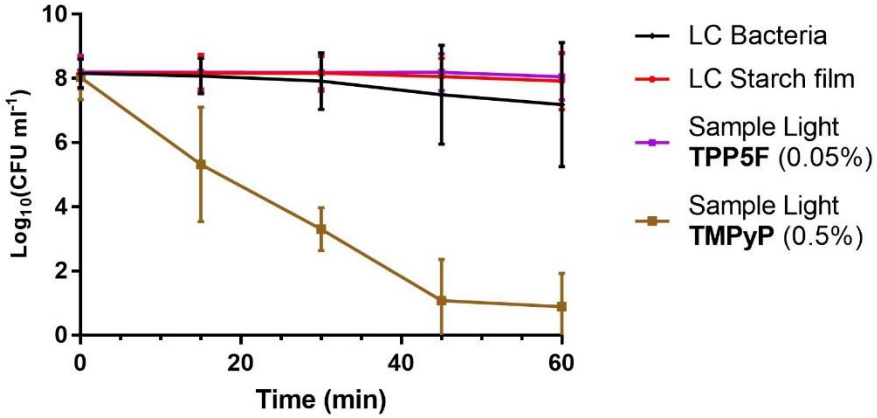


**Fig. 2.8-** *S. aureus* viability represented by colony forming units (CFU) per mL, in the dark (**A**) or under irradiation with white light at an irradiance of 50 mW $cm^{-2}$ (**B**), for bacteria and starch film controls and samples for both starch films with **TMPyP** and **TPP5F**. Values represent the mean of three independent experiments, and the bars the standard deviation.

Similarly, the experimental conditions were applied to the *P. aeruginosa* strain inactivation, however, in this case, no inactivation was observed in any conditions, even after 60 min of irradiation (Fig. 2.9).

Even though no significant inactivation was observed, a slight decrease by **TMPyP** after 60 min of irradiation was detected, and so, the experiments were extended to a period of 120 min (Fig.2.10). Even so, after 120 min of white light irradiation at an irradiance of 50 mW $cm^{-2}$, no inactivation of *P. aeruginosa* was observed in the presence of any of the starch based films with the incorporated porphyrins. As previously stated, *P. aeruginosa* belongs to the class of bacteria described as gram-negative, and as such has a more complex cell wall than

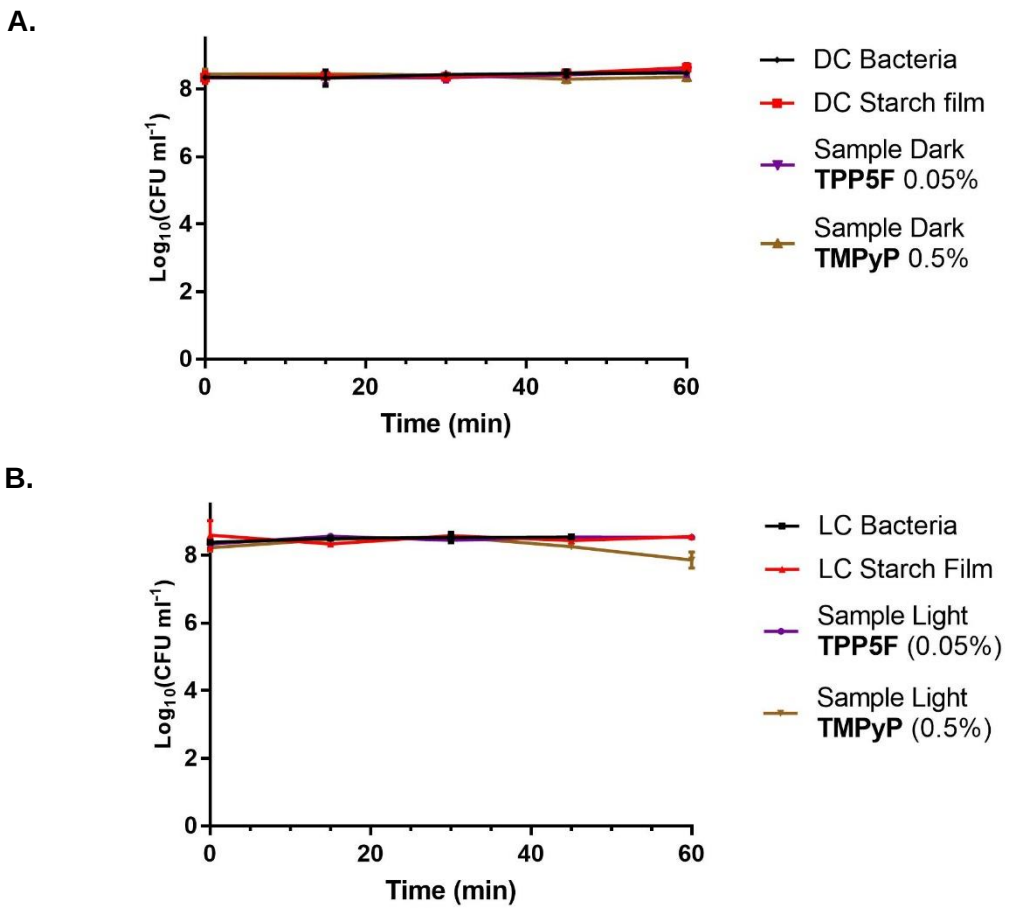


**Fig. 2.9 -** *P.aeruginosa* represented by colony forming units (CFU) per mL, in the dark (**A**) or under 60 min irradiation with white light at an irradiance of 50 mW $cm^{-2}$ (**B**), for bacteria and starch film controls and samples for both starch films with **TMPyP** and **TPP5F**. Values represent the mean of three independent experiments, and the bars the standard deviation.

gram-positive bacteria. This complexity grants this kind of bacteria an extra protection. Considering that the positive charge on the PS seems to be essential to the well succeeded photodynamic inactivation, and the **TPP5F** has no ionic charge, the inefficiency of **TPS/TPP5F** film to photoinactivate the *P. aeruginosa* strain wasn't unexpected. In regard to **TMPyP**, cationic PSs seem to be more efficient to inactivate gram-negative bacteria [23], [24], even if not as easily as gram-positive bacteria [25]. However, in this study it is possible that the **TMPyP** concentration in the starch film in combination with the light irradiance was not enough to photoinactivate *P. aeruginosa.* Further experiments using films with a higher concentration of PS are needed. Having into account these results, the next *ex-vivo* experiments were done with the gram-positive bacterium.

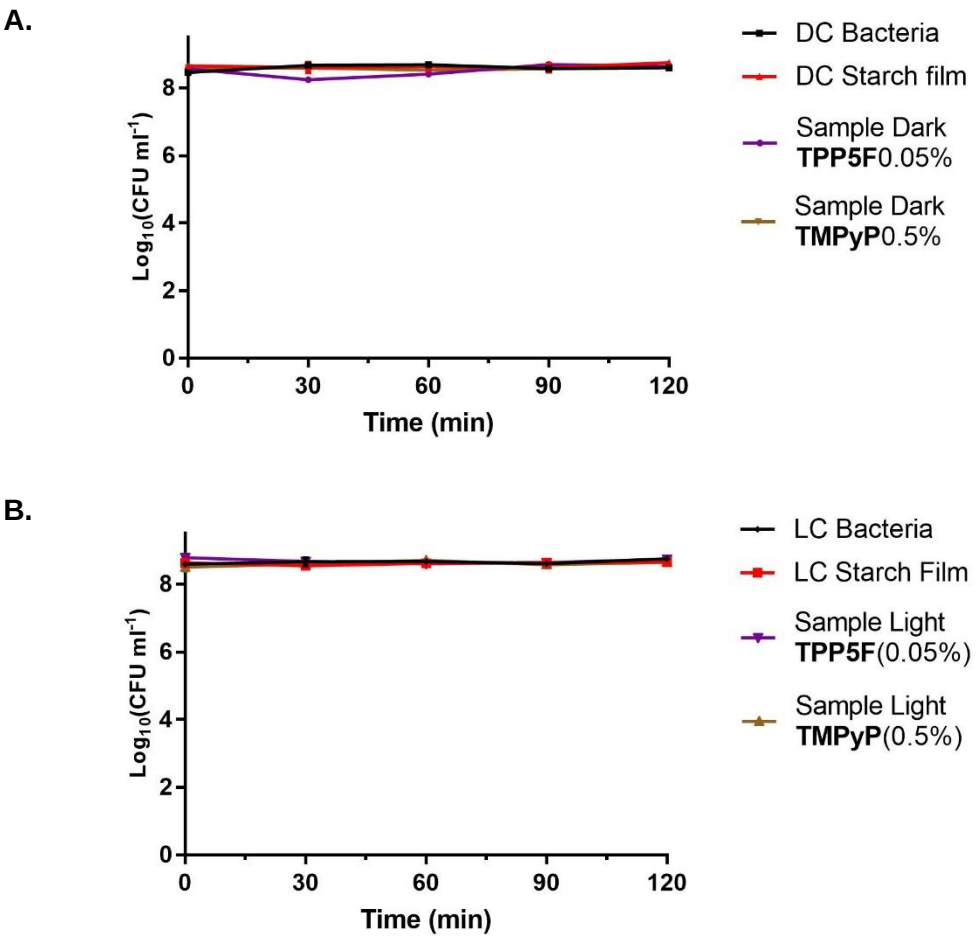


**Fig. 2.10-** *P.aeruginosa* represented by colony forming units (CFU) per mL, in the dark (**A**) or under 120 min irradiation with white light at an irradiance of 50 mW $cm^{-2}$ (**B**), for bacteria and starch film controls and samples for both starch films with **TMPyP** and **TPP5F**. Values represent the mean of three independent experiments, and the bars the standard deviation.

### 3.1.2. *Ex Vivo* assay on porcine skin

At first, methodology A, was followed, and a preliminary study was designed with only three time points (0, 60 and 150 min) to examine the photoinactivation tendencies and analyze the best photoinactivation conditions (Fig. 2.11). The experimental results point out that after 150 min of white light irradiation at an irradiance of 50 mW $cm^{-2}$ in the presence of the starch films incorporated with porphyrins, no photoinactivation or decrease in the bacterial abundance was found neither in controls nor in samples. Despite skin decontamination before the assay, some of the native microorganisms remain in the skin (Fig. 2.13), including gram-positive, gram-negative bacteria and fungi, which seem to difficult the photoinactivation of *S. aureus*. However, the controls remained stable, and no significant variations were found during the experiment.

While in PBS experiments almost all of the porphyrin incorporated in the starch film released itself from the film, in the case of the skin experiments, the release seems lower, which difficults the contact of the PS with the bacterial cells.

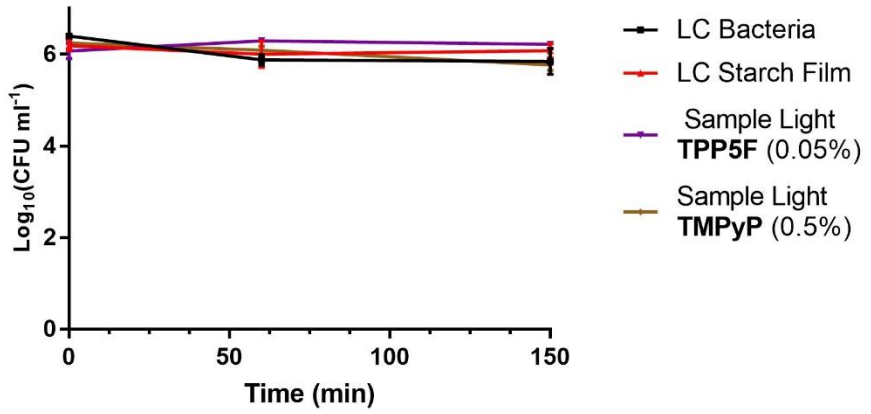


**Fig. 2.11-** Viability of *S. aureus* in porcine skin (methodology A) represented by colony forming units (CFU) per mL, during 150 min irradiation with white light at an irradiance of 50 mW $cm^{-2}$, for light controls, and samples light for both films with **TMPyP** and **TPP5F**. Values represent the mean of three independent experiments, and the bars the standard deviation.

Once again, it was decided to extend the time of irradiation (to 360 min), as well as the preliminary dark incubation time (to 60 min), in order to promote the porphyrinic PS release from the starch film, increasing its contact with the bacterial cells. Furthermore, to provide a wet atmosphere, a PBS embedded piece of cotton was placed in the plates close to the pieces of skin. For this assay, the time points were 0, 180 and 360 min (Fig. 2.12). No *S.aureus* photoinactivation was found even after 360 min (6h) of white light irradiation, indicating either that time is not enough to promote photoinactivation or that other factors are implicated in the inactivation process. In similar studies of this, using a formulation constituted by a mixture of porphyrins, *S.aureus* inactivation was observed, but the PS formulation was tested in solution, not supported or incorporated in any support or film [19]. Moreover, in this study, the starch film can also affect the bacterial inactivation as it may difficult the light penetration in the skin where the bacterial cells were inoculated. To test this hypothesis further studies are needed.

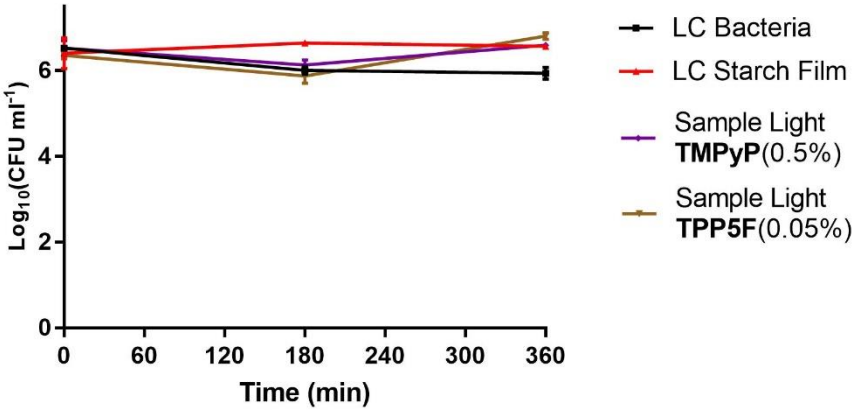


**Fig. 2.12-** Viability of *S. aureus* in porcine skin (methodology A) represented by colony forming units (CFU) per mL, during 360 min irradiation with white light at an irradiance of 50 mW $cm^{-2}$, for light controls, and samples light, for both films with **TMPyP** and **TPP5F**. Values represent the mean of three independent experiments, and the bars the standard deviation.

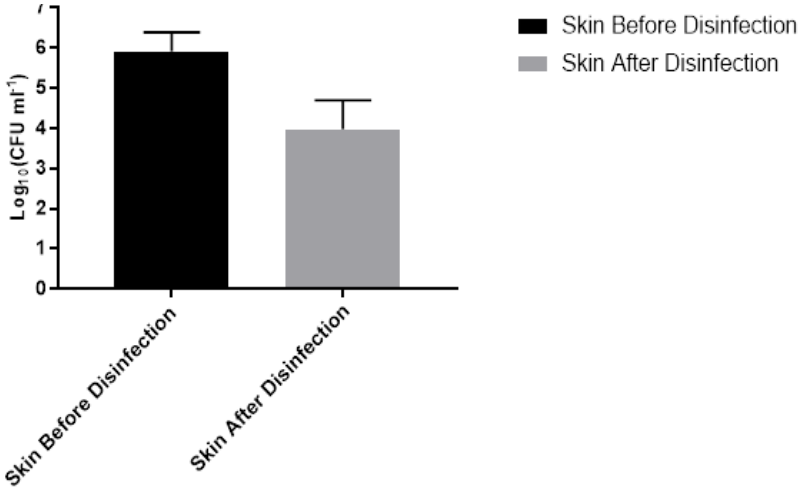


**Fig. 2.13-** Efficiency of skin disinfection pre-assay. The value represents the mean from three independent experiments, and the bar the standard deviation.

The methodology B was also tested with **TMPyP** films, but this time to test if this approach can prevent infection, that is, the procedure was planned in order to avoid biofilm formation. The period of irradiation was once again extended, this time to 24 h, and samples were collected at 0, 6, 12 and 24 h. In the non-irradiated experimental samples, no significant bacterial abundance reductions were found either for control or samples (Fig. 2.14 A.). However, dissimilar behavior was found after the white light irradiation of skin samples. The bacteria abundance below the film did not increase during the irradiation period, as occurred slightly

in the dark conditions, and the number of bacteria above the film decrease significantly after 6h of white light irradiation (Fig. 2.14 B.). The analysis of the experimental controls [skin infected with bacteria (Control Bacteria) and the Control Skin (without added bacteria)], show an increase in bacterial concentration in the experimental time course. This behavior suggests that during that 24 h period the bacteria multiply still, possibly due to nutrients still present in the dead skin. Contrarily, in the samples with **TPS/TMPyP** films, both below and above the film, the bacterial concentration decrease. This is particularly significant above the film ($p < 0.005$), where the inactivation is of 3.77 log of CFU

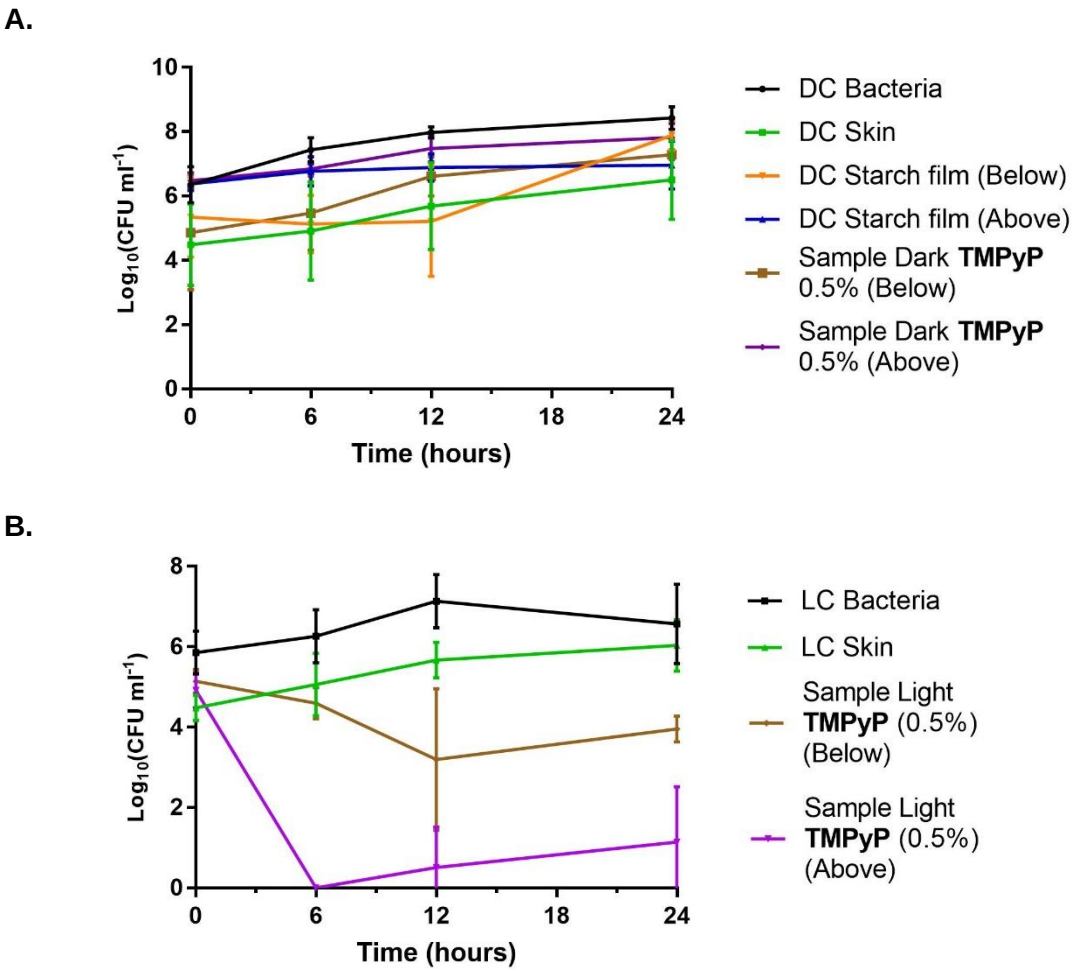


**Fig. 2.14-** Viability of *S. aureus* in porcine skin represented by colony forming units (CFU) per mL, during 24 h in the dark, for the film with **TMPyP** and dark controls (**A**), and irradiation of 50 mW $cm^{-2}$ (white light), for light controls and sample light for the film with **TMPyP** (**B**). The values represent the mean of three independent experiments and the bars show the standard deviation.

$mL^{-1}$ after 24 h of PDT treatment.

Regarding the starch film without PS incorporated (Starch Film), below the film its behavior exhibits a very similar tendency as the control without film and

bacteria (Control Skin), which suggest that these bacteria belong to the native bacteria of the porcine skin. (Fig. 2.15 A.) Above the film, however, a decrease in bacteria was also found. However, this decrease is not as pronounced as the one found for the starch film with **TMPyP** (Fig. 2.15 B.), suggesting that the starch film when irradiated by light may contribute to the inactivation of the bacteria. In this case, however, it must be noted that variability is high maybe due to the high variability of the native bacteria of the skin.

**A.**

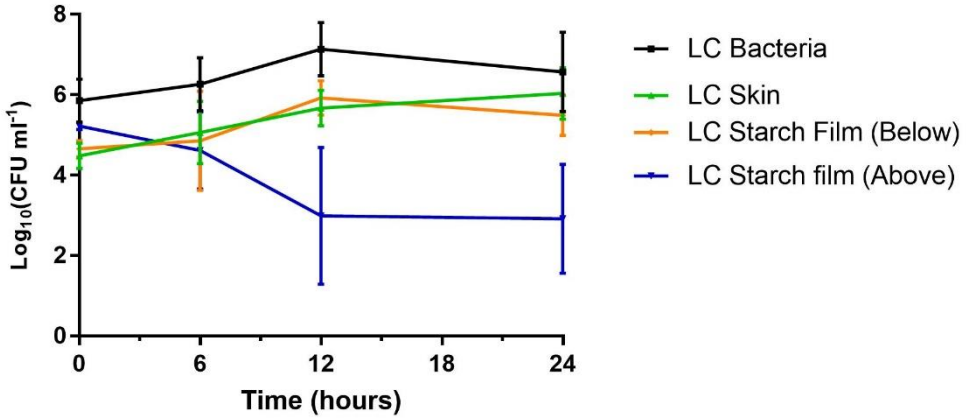


**B.**

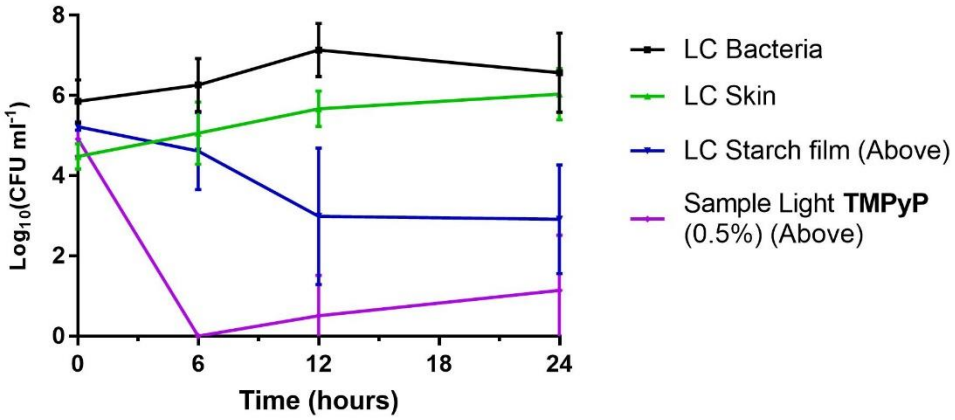


**Fig. 2.15-** Viability of *S. aureus* in porcine skin represented by colony forming units (CFU) per mL during 24 h of white light irradiation with irradiance of 50 mW $cm^{-2}$ for the Starch film and controls (**A**), and for film with **TMPyP** and starch film, above the film (**B**). The values represent the mean of three independent experiments and the bars show the standard deviation.

Below the starch films, the bacterial concentration followed a tendency similar to the skin control, although in the case of the starch films doped with **TMPyP**, a slight tendency to bacterial concentration decrease over time was observed, namely after 12 h ($p < 0.05$, *vs* controls bacteria and skin) (Fig. 2.16).

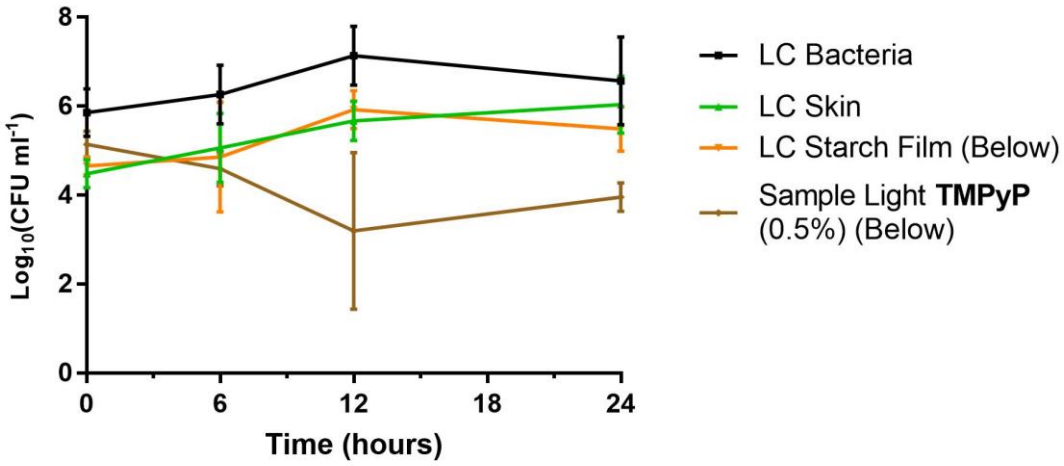


**Fig. 2.16-** Viability of *S. aureus* in porcine skin represented by colony forming units (CFU) per mL, during 24 h irradiation of white light with irradiance of 50 mW $cm^{-2}$ for the light controls (bacteria, skin and film) and sample **TMPyP** (below film). The values represent the mean of three independent experiments and the bars show the standard deviation.

## 4. Conclusions

When considering clinical applicability, one must ponder what the best delivery system might be. Porphyrins have been identified as good antimicrobial agents through photodynamic therapy, however, their delivery in a solution may not prove practical in treating a wound. Porphyrins can be incorporated into solid supports and maintain their activity, such as starch-based films used in this work. These prove to not inactivate bacteria in the dark, affording them a controllable effect, and only in the presence of the porphyrin PS and light the antimicrobial effect can be observed. The results suggest that these starch films doped with **TMPyP** can be effectively used as antimicrobial materials against gram-positive bacteria, such as *S.aureus*. However, these starch films doped with **TMPyP** under the tested conditions are not effective against gram-negative bacteria. Further studies using higher concentrations of **TMPyP** incorporated in the starch film should be addressed. The *ex vivo* assays results suggest that these films seem to filter the light that was meant to reach the skin surface. Overall, the

results indicate the tetracationic porphyrinic starch films may be used as a safe dressing that prevents infection in wounds.

## 5. References


[1] M. T. Madigan, *Brock Biology of Microorganisms*, vol. XXXIII, no. 2. 2012.

[2] T. J. Silhavy, D. Kahne, and S. Walker, "The Bacterial Cell Envelope," *Cold Spring Harb. Perspect. Biol.*, vol. 2, no. 5, p. a000414, 2010.

[3] S. Brown, J. P. Santa Maria Jr, and S. Walker, "Wall Teichoic Acids of Gram-Positive Bacteria," *Annu. Rev. Microbiol.*, vol. 67, no. 1, pp. 1–7, 2013.

[4] K. Shettigar and T. S. Murali, "Virulence factors and clonal diversity of Staphylococcus aureus in colonization and wound infection with emphasis on diabetic foot infection," *Eur. J. Clin. Microbiol. Infect. Dis.*, vol. 39, no. 12, pp. 2235–2246, 2020.

[5] C. Arjyal, J. Kc, and S. Neupane, "Prevalence of Methicillin-Resistant Staphylococcus aureus in Shrines," *Int. J. Microbiol.*, vol. 2020, no. Feb 29, p. 7981648, 2020.

[6] P. D. Stapleton and P. W. Taylor, "Methicillin Resistance in Staphylococcus aureus: mechanisms and modulation," *Sci. Prog.*, vol. 85, no. Pt 1, pp. 225–235, 2002.

[7] G. Ippolito, S. Leone, F. N. Lauria, E. Nicastri, and R. P. Wenzel, "Methicillin-resistant Staphylococcus aureus: the superbug," *Int. J. Infect. Dis.*, vol. 14, no. SUPPL. 4, pp. 7–11, 2010.

[8] G. A. Meerovich *et al.*, "Photodynamic inactivation of Pseudomonas aeruginosa bacterial biofilms using new polycationic photosensitizers," *Laser Phys. Lett.*, vol. 16, no. 11, p. 115603, 2019.

[9] P. D. Lister, D. J. Wolter, and N. D. Hanson, "Antibacterial-resistant Pseudomonas aeruginosa: Clinical impact and complex regulation of chromosomally encoded resistance mechanisms," *Clin. Microbiol. Rev.*, vol. 22, no. 4, pp. 582–610, 2009.

[10] A. J. Rocha, M. R. De Oliveira Barsottini, R. R. Rocha, M. V. Laurindo, F. L. L. De Moraes, and S. L. Da Rocha, "Pseudomonas aeruginosa: Virulence factors and antibiotic resistance Genes," *Brazilian Arch. Biol. Technol.*, vol. 62, pp. 1–15, 2019.

[11] B. Tümmler and J. Klockgether, "Recent advances in understanding Pseudomonas aeruginosa as a pathogen," *F1000Research*, vol. 6, no. 0, 2017.

[12] C. M. B. Carvalho *et al.*, "Photoinactivation of bacteria in wastewater by porphyrins: Bacterial β-galactosidase activity and leucine-uptake as methods to monitor the process," *J. Photochem. Photobiol. B Biol.*, vol. 88, no. 2–3, pp. 112–118, 2007.

[13] C. M. B. Carvalho *et al.*, "Antimicrobial photodynamic activity of porphyrin derivatives : potential application on medical and water disinfection," *J. Porphyrins Phtalocyanines*, vol. 13, pp. 574–577, 2009.

[14] C. Simões *et al.*, "Photodynamic inactivation of Escherichia coli with cationic meso-tetraarylporphyrins - The charge number and charge distribution effects," *Catal. Today*, vol. 266, pp. 197–204, 2016.

[15] K. A. D. F. Castro *et al.*, "Control of Listeria innocua biofilms by biocompatible photodynamic antifouling chitosan based materials," *Dye. Pigment.*, vol. 137, no. February, pp. 265–276, 2017.

[16] Leibniz Institute. DSMZ-German Collection of Microorganisms and Cell Cultures GmbH, "Leibniz Institute DSMZ," *Staphylococcus aureus DSM 25693*. .

[17] A. Vieira, Y. J. Silva, Â. Cunha, N. C. M. Gomes, H. W. Ackermann, and A. Almeida, "Phage therapy to control multidrug-resistant Pseudomonas aeruginosa skin infections: In vitro and ex vivo experiments," *Eur. J. Clin. Microbiol. Infect. Dis.*, vol. 31, no. 11, pp. 3241–3249, 2012.

[18] T. M. Branco *et al.*, "Single and combined effects of photodynamic therapy and antibiotics to inactivate Staphylococcus aureus on skin," *Photodiagnosis Photodyn. Ther.*, vol. 21, pp. 285–293, 2018.

[19] M. Braz *et al.*, "Photodynamic inactivation of methicillin-resistant Staphylococcus aureus on skin using a porphyrinic formulation," *Photodiagnosis Photodyn. Ther.*, vol. 30, no. January, p. 101754, 2020.

[20] O. E. Akilov *et al.*, "The Role of Photosensitizer Molecular Charge and Structure on the Efficacy of Photodynamic Therapy against Leishmania Parasites," *Chem. Biol.*, vol. 13, no. 8, pp. 839–847, 2006.

[21] J. Ghorbani, D. Rahban, S. Aghamiri, A. Teymouri, and A. Bahador, “Photosensitizers in antibacterial photodynamic therapy: An overview,” *Laser Ther.*, vol. 27, no. 4, pp. 293–302, 2018.
[22] K. A. D. F. Castro *et al.*, “Synthesis and characterization of photoactive porphyrin and poly(2-hydroxyethyl methacrylate) based materials with bactericidal properties,” *Appl. Mater. Today*, vol. 16, pp. 332–341, 2019.
[23] E. Alves, M. A. F. Faustino, M. G. P. M. S. Neves, Â. Cunha, H. Nadais, and A. Almeida, “Potential Applications of Porphyrins in Photodynamic Inactivation beyond the Medical Scope,” *J. Photochem. Photobiol.*, 2014.
[24] C. Ramos Camargo, V. Da Conceição, A. Martins, A. Maria De Guzzi Plepis, and J. R. Perussi, “Photoinactivation of Gram-Negative Bacteria in Circulating Water Using Chitosan Membranes Containing Porphyrin,” *Biol. Chem. Res.*, vol. 2014, no. December 2014, pp. 67–75, 2014.
[25] A. Hanakova *et al.*, “The application of antimicrobial photodynamic therapy on S. aureus and E. coli using porphyrin photosensitizers bound to cyclodextrin,” *Microbiol. Res.*, vol. 169, no. 2–3, pp. 163–170, 2014.

# Chapter 3. Skin Wound healing: *In Vitro* assays

## 1. General Remarks

### 1.1. Characterization of the Human Skin

The human skin is the barrier that separates our interior from the harshness of the external environment. As such it serves the very important function of being a primary source of defense against the abrasiveness of outside agents, protecting us from infection, UV radiation, physical trauma, harmful chemical exchanges and overall contributing to the homeostasis of the human body. To do all this, the skin must have an efficient structure capable of performing its functions. The skin is composed by different layers, and it extends approximately 2 $m^2$ in area, has around 2.5 mm of thickness and an average density of 1.1 [1]. It is conventionally described as having two main tissue layer types: the epidermis and the dermis (Figs. 3.1 and 3.2). The epidermis is the most external tissue, a stratified and non-vascularized epithelium. This is a thin protective coat that keeps moisture inside the body [2]. This layer is mostly consisted of keratinocytes (about 95% of cells), highly specialized epithelial cells that have the ability to regenerate via mitosis and repair any defect as long as the underlying layer, the dermis, is not damaged [2]. The other 5% of cells in the epidermis belong to melanocytes, Langerhan's and Merkel's cells. Generally, the epidermis can be observed with four distinct layers: the stratum basale (SB), the stratum spinosum (SS), the stratum granulosum (SGr), and the stratum corneum (SC) (Fig. 3.1) [3], [4]. When encountering a thick skin, another sublayer may be

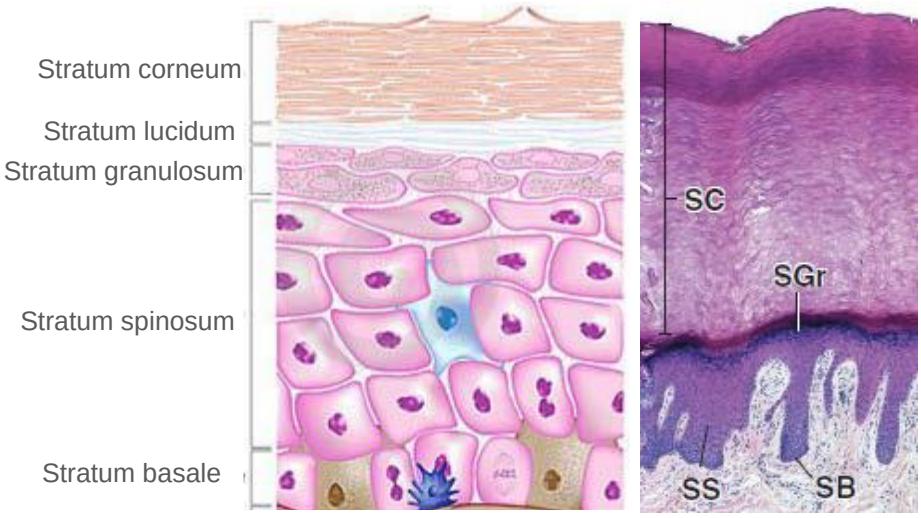


**Fig. 3.1-** Structure of the epidermis layer, adapted from [3] and [4].

found: the stratum lucidum [4]. The dividing cells at the stratum basale gradually push the cells in the overlying layers outward, as they mature, making them flatten. Eventually they become fully matured keratinized cells and are shed from the skin surface [4].

Below the epidermis, a thick layer of connective tissue, called dermis can be found. The dermis is mainly composed by collagen, elastine and glycosaminoglycans and different cells types such as fibroblasts, endothelial cells, mast cells, dermal dendritic cells and lymphocytes [1], [2], [5].

The dermis can be divided in two structurally distinct sublayers, the papillary layer and the reticular layer (Fig 3.2). The papillary layer is the more superficial sublayer, which means it is directly beneath the epidermis. It consists of loose connective tissue, the collagen fibers are not as thick as in the deeper portion and the elastic fibers are threadlike and form an irregular network. This layer is relatively thin and rich in blood vessels and nerve processes [4]. Indeed, the blood supply of the skin derives from a series of vascular plexuses located in the dermis, all interconnected [6]. The reticular layer is deeper, and its thickness varies in different parts of the body, though it is thicker and less cellular than the papillary layer. In this layer the collagen and elastic fibers form regular lines of tension called Langer's lines. Beneath the reticular layer, often layers of adipose tissue may be found. It's presence serves as energy storage and provides insulation [4].

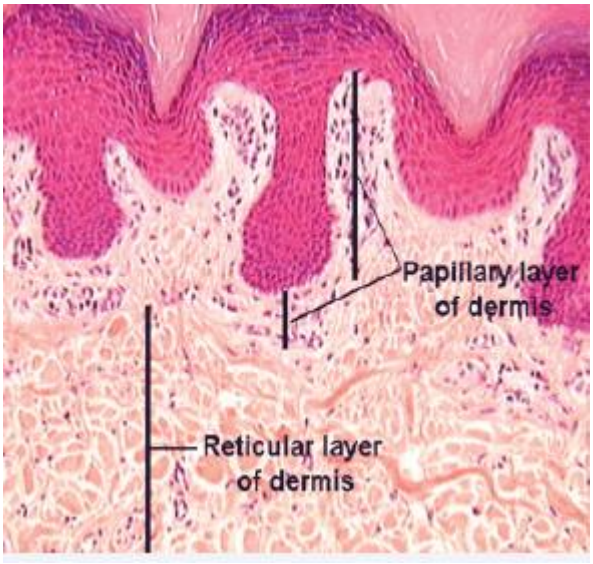


**Fig 3.2-** Structure of the dermis layer, adapted from [3].

Any damage in the layers of skin creates an exposure that, in turn, may lead to very dangerous infections, trauma, and, in some particular instances,

chronic wounds. The wound's microenvironment has inflammatory cells and growth factors that orchestrate the tissue remodeling. In skin wound healing, vascularization tissue remodeling continues to be a challenge for tissue engineering.

### 1.1.1. Endothelial Cells

The vascular system counts with varying types of blood vessels, however, all of them, from the smallest capillary to the largest vein and artery, have in common the presence of the endothelium. The endothelium consists of a smooth, single- celled layer of endothelial cells which is in contact with the flowing blood, as it coats the interior of arteries', capillaries' and veins' walls [7]. Endothelial cells are polarized cells which shape is generally thin and slightly elongated, with dimensions described to be roughly 30-50 μm in length, 10-30 μm wide and thickness of 0.1-10 μm [8]. They can actively transport small molecules, macromolecules and hormones such as insulin, degrade lipoprotein particles, as well as regulate, with smooth muscle cells, the blood flow to tissues, as they are responsive to vasoactive agents [10-11]. In the process of inflammation, the action of the endothelium is key, as it is capable of increasing vessel permeability, vasodilation, increase leukocyte extravasation and alter coagulation control and thrombus formation [8]. In addition, they play a very important role in angiogenesis, in the formation of new blood vessels, important for tissue remodeling and regeneration.

### 1.1.2. Fibroblasts

Fibroblasts are the main cell type of the dermis [1]. They are derived from mesenchymal stem cells within the body and they are migratory cells that make and degrade extracellular matrix (ECM) components. ECM is composed by collagens (mainly types I and III), which are responsible for about 70% of the dry weight of the dermis, while 5% are attributed to elastin and elastic microfibrils. Collagen and elastic fibers are surrounded by ground substance, a gelatinous substance composed of proteoglycans and glycoproteins [5].

When fibroblast differentiate into a myofibroblast, a contractile cell phenotype involved in increased extracellular matrix production and contraction during the tissue repair process. It seems, then, that both fibroblasts and myofibroblasts are important players in the body's response to injury. Contraction occurs when the wound edges move towards each other reducing wound's dimensions. This may be beneficial as less granulation tissue is needed to

replace the lost tissue of the wound and the healing time may be significantly reduced, however scarring may be present [10]. Fibroblasts migrate to a wound area during the healing process and stay there until full epithelialization takes place. After the wound has been remodeled the fibroblast levels return to pre-injury levels [11]. These cells provide to the wound new material and wound contraction required to close it [11].

## 1.2. New Perspectives for Skin Wound Healing

Based on biotechnology development, new medical treatment modalities arise with the advent of novel materials. Concerning wound dressings, for instance, the materials should present biocompatibility, but also be able to protect the wound bed from physical factors as well as infection. The functionalization of materials allows the introduction of biological and therapeutical properties that can be used for applications such as drug delivery. In fact, considering the classical dressings, they can be improved to not only fulfill their protection functionalities but also be able to incorporate molecules that can be released to the wound site and promote healing. Biopolymers, for instance, have been regarded as good possibilities for dressings, due to their low-cost, biocompatibility and ability to impregnate molecules that can be released from the matrix in a controlled fashion to the target site [12]. Porphyrins, as mentioned previously, have the useful ability of being chemically tailored and incorporated into materials. Their antibacterial properties (through aPDT), among other properties described in chapter 1, are advantageous for wound healing. However, their effects on cellular behavior (proliferation, viability, migration, etc.) when applied directly for wound healing purposes are not well explored. It is known that, in general, microorganisms' inactivation occurs at high light irradiances (≥ 50 mW $cm^{-2}$), however lower light irradiances have been suggested as better promoters of wound healing [13], [14].

In this chapter will be studied the influence of 5,10,15,20-tetrakis(pentafluorophenyl) porphyrin (**TPP5F**) and 5,10,15,20-tetrakis(1-methylpyridinium-4-yl) porphyrin (**TMPyP**) incorporated in starch-based materials in cell cultures of human microvascular endothelial cells (HMEC) and human dermal fibroblasts (HDF) when irradiated with a low intensity light and if the starch-based films could be used as a matrix to fill the wound bed. This study entails the evaluation of the metabolic activity, migration, adhesion and ROS formation by the cells.

## 2. Materials and Methods

### 2.1. TPS/Porphyrin-based Films

The starch-based materials used in this work were kindly provided by Idalina Gonçalves' group from CICECO which incorporate the 5,10,15,20-tetrakis(pentafluorophenyl)-porphyrin (**TPP5F)** and 5,10,15,20-tetrakis(1-methylpyridinium-4-yl)porphyrin tetra-iodide (**TMPyP)**, in wt/wt percentages of 0.05% and 0.5%, respectively (described in chapter 2), using a sample without PS for control reference (TPS).

### 2.2. Cell culture

Human dermal fibroblasts (HDF, ATCC) were cultured in Dulbbecco's modified Eagle's medium (DMEM, Invitrogen Life Technologies, Paisley, UK), supplemented with 10% fetal bovine serum (FBS, Invitrogen Life Technologies, Paisley, UK) and 1% penicillin/streptomycin (Invitrogen Life Technologies, Paisley, UK). Cell cultures were maintained in a humidified atmosphere containing 5% $CO_2$ at 37ºC. Cells were used at passages 20-24.

Human microvascular endothelial cells (HMEC, ATCC) were cultured in Roswell Park Memorial Institute 1640 medium (RPMI, Invitrogen Life Technologies, Paisley, UK) supplemented with 10% FBS and 1% penicillin/streptomycin (Invitrogen Life Technologies, Paisley, UK). Cell cultures were used at passages 8-12 and maintained in a humidified atmosphere at 37 ºC and 5% $CO_2$.

Cells were allowed to grow until 70–80% confluence. For sub-culturing attached cells, old medium was removed from the plate and cells were washed with a PBS solution, after which it was removed, and it was added 1 mL of trypsin. After 1 min the trypsin was removed, and the plate was incubated for 5 min at 37 ºC. Complete medium for the respective cell type was added and cells were counted on a Double Neubauer Ruled Metallized Counting Chamber.

### 2.3. Light Source

The artificial illumination was performed using a homemade red light (652 nm $\pm$ 15 nm) LED setup, at an irradiance of 5 mW $cm^{-2}$ for 15 min, corresponding to 4.5 J $cm^{-2}$. The light irradiance was measured with a power and energy meter (model FieldMaxII-Top from Coherent, USA) connected to a high-sensitivity sensor (model PS19Q, Coherent, USA).

**A** **B**

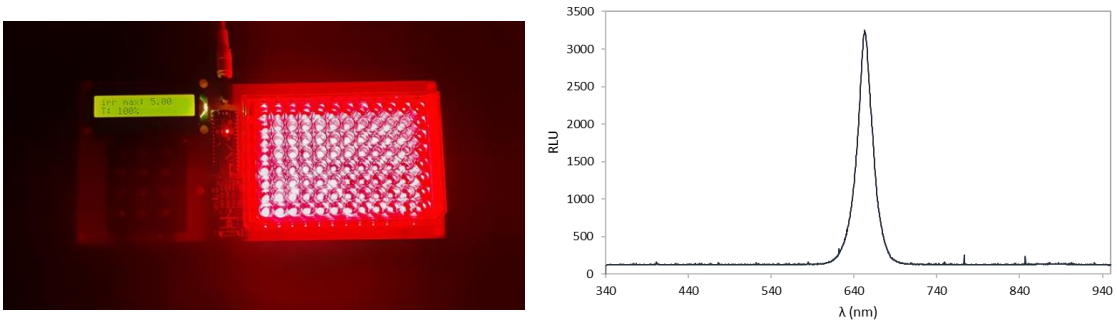


**Fig. 3.3- A.** LED lamp used for the skin wound healing *in vitro* assays; **B.** LED output, shown in relative light units (RLU) vs. wavelength in nm.

## 2.4. Cellular viability assay

In order to evaluate the effect of the TPS/PS films in the metabolic activity of HMEC and HDF cells, a viability assay using 3-(4,5-dimethylthiazol-2-yl)-5-(3-carboxymethoxyphenyl)-2-(4-sulfophenyl)-2H-tetrazolium (MTS, Promega) was performed. HMEC and HDF cells were seeded into 96- well plates culture (1 x104 cells /well) and allowed to adhere overnight in 100 µL of appropriate cell medium. Cells were incubated with the starch-based film without porphyrin incorporated (control TPS Film); starch-based film with 5,10,15,20-tetrakis(pentafluorophenyl)porphyrin incorporated (**TPP5F** film); starch-based film with 5,10,15,20-tetrakis(1-methylpyridinium-4-yl)porphyrin incorporated (**TMPyP** film) and only complete cell medium (control) as evidenced by the schematic presented in Fig. 3.4. The disc films with 28.27 mm2 were obtained using a 6 mm punch to cut the starch-based sheet. It was also used half of the disc film (14.13 mm2) or a quarter of disc film (7.06 mm2).

The 96-well plates were then protected from light and incubated for 30 min at 37ºC prior to irradiation. Red light exposure was performed in one plate for 15 min (5 mW cm-2, or 4.5 J cm-2) while the other plate remained in the dark. Both plates were then incubated in a humidified atmosphere at 37 ºC (5% CO2). After 24h, it was added 20 µL of MTS to each well and incubated for 2 h at 37 ºC. The TPS/PS discs were removed, and the absorbance was measured at 490 nm on a microplate reader (Thermo Electron corporation, multiskan ascent). All samples were assayed in n=5.

Cell viability was then calculated using the formulae:

$$\%\, Cell\ Viability = \frac{Abs_{Sample} - Abs_{Background}}{Abs_{Control} - Abs_{Background}} \times 100 \qquad \textbf{(1)}$$

where $Abs_{Sample}$ refers to the absorbance of the sample, $Abs_{Background}$ refers to the absorbance of the background without cells, and $Abs_{Control}$ refers to the absorbance of the wells with cells without treatment (neither light nor films).

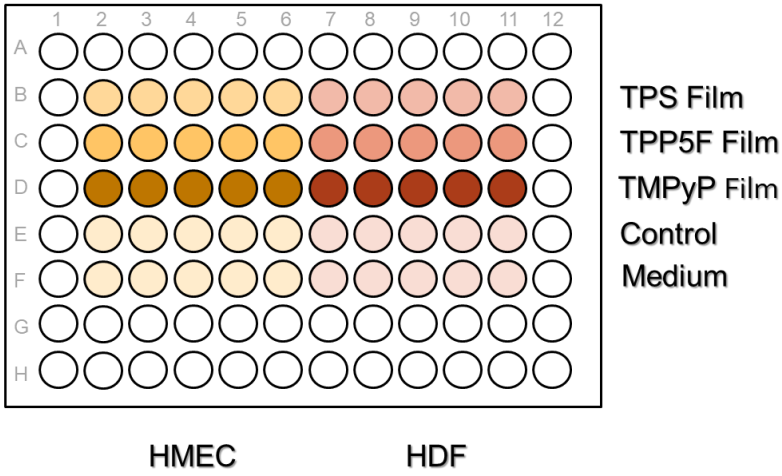


**Fig. 3.4-** Plate schematics for MTS assay.

## 2.5. Cellular adhesion

The discs previously used for the cellular viability assay were replaced in a new 96-well plate and washed with 200 $\mu$L of PBS 1x, then in each well 100 µL of 3,7% paraformaldehyde solution were added and incubated during 15 min at room temperature. The solution was removed, and the wells were washed three more times with 200 µL of PBS 1x. The plates were stored at 4ºC. In order to evaluate the presence or absence of the cells in the films a fluorescent DNA stain were performed. Cell nuclei were counterstained with 1 µg/mL DAPI (Molecular Probes, Germany) in PBS, for 10 min. After washing with PBS, samples were mounted with Gel/Mount (Natutec, Germany) and examined by fluorescence microscope Zeiss AxioImager Z1 (Carl Zeiss, Germany) with camera Axiocam MR ver3.0 (Carl Zeiss, Germany) and processed with software Axiovision 4.9 (Carl Zeiss, Germany).

## 2.6. Wound Healing Assay

In a 24-well culture plate the ibidi® culture-Insert 2 Well for gap formation were used. A suspension of cells with density of $5x10^5$ cells/mL was prepared and 70 µL were added to each side of the insert and incubated for 24 h in a humidified atmosphere at 37 ºC (5% $CO_2$). The insert was removed, and the well was washed with PBS to remove cell debris, after which cell culture medium was added (200 µL). The plates were inspected at an inverted microscope (Nikon,

TMS-F model) with D40X Nikon camera. The different films with 14.13 $mm^2$ were added: TPS film, **TPP5F** and **TMPyP** films. Incubated in the dark for 30 min at 37 ºC (evidenced at Fig. 3.5, a representation of the plate schematic). One plate was then irradiated with red light at an irradiance of 5 mW $cm^{-2}$ for 15 min while another was kept in the dark. Both plates were then incubated in a humidified atmosphere at 37 ºC (5% $CO_2$) for 24 h. Pictures of the gaps were taken at time point 0 and after 24 h. The experiment was performed with a number of replicates of 3 (N=3). Wound closure was measured by gap area with Java-based software program Image J.

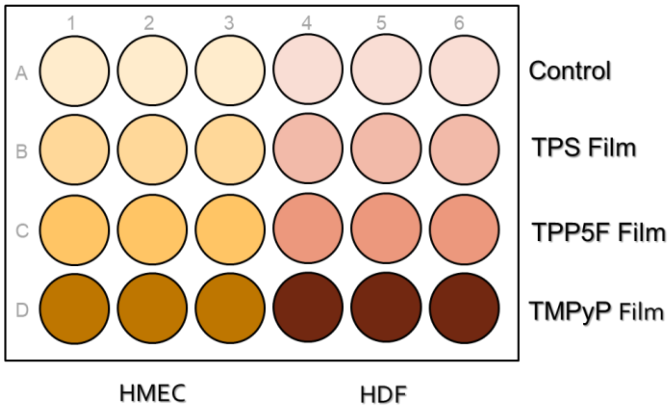


**Fig. 3.5-** Plate schematic for Wound Healing assay, using 14.13 $mm^2$ discs.

## 2.7. ROS Detection Assay

The ROS detection assay was performed using the 2',7'-dichlorofluorescein diacetate (DCFDA) Cellular ROS Detection Assay Kit (abcam). Cells were cultivated into a 96-well plate with black walls and clear bottom (2.5 x $10^4$ cells per well). After incubation for 24h at 37ºC and 5% $CO_2$, the cells were treated with the films (control TPS film, **TPP5F**, and **TMPyP** films) and then incubated at 37 ºC in the dark for 30 min. Once this period was over, one plate was irradiated with red light at an irradiance of 5 mW $cm^{-2}$ for 15 min while another similar plate was left in the dark. The plates were then left again to incubate for 24 h at 37 ºC and 5% $CO_2$. Hydrogen peroxide was added to the positive control wells, 3 h prior to measuring. The DCFDA solution (20 µM) was then added to the wells, except for two non-stain wells to measure the background fluorescence intensity, and left for 30 min. To measure the ROS formation during irradiation, the DCFDA was added 30 min prior to the treatment with films and detection was performed immediately after the irradiation period.

The detection of fluorescence was performed with a fluorometer (spectra max, gemini EM, molecular devices) using an excitation wavelength of 485 nm and emission wavelength of 535 nm. Experimental conditions were tested in replicates of N=3 for control. N=4 for 7.06 $mm^2$ discs, and N=3 for 14.13 $mm^2$ disc. Results are expressed in percentage of control which is considered to be 100%.

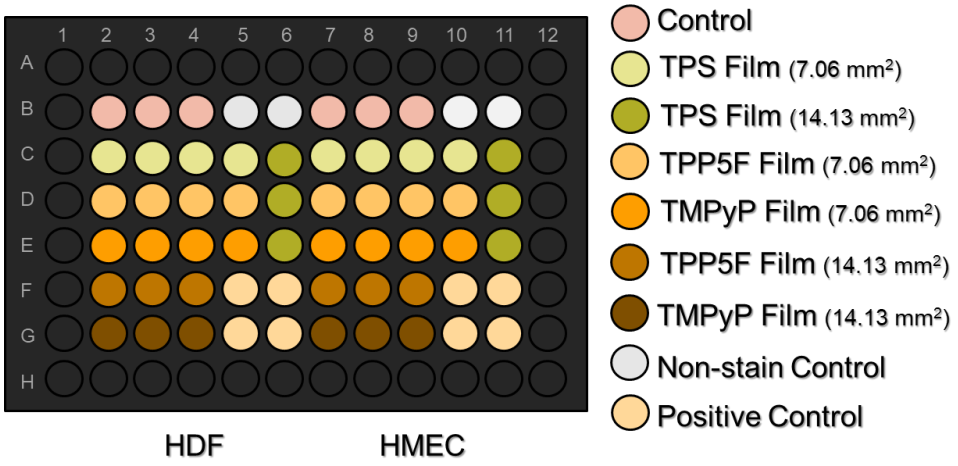


**Fig. 3.6-** Plate schematic for ROS detection assay, using 7.06 $mm^2$ and 14.13 $mm^2$ discs.

### 2.8. Statistical Analysis

Statistical analysis of the obtained data was carried out by GraphPad Prism® 7.04 (GraphPad Software, CA, USA). All primary data are represented as means with standard deviations of the mean. Statistical analysis was performed with a one-way analysis of variance (ANOVA), with a Tukey test for multiple comparisons. A *P* value of <0.05 of the mean comparison between the groups and against the non-irradiated cell control was considered as statistically significant in each experiment.

## 3. Results and Discussion

### 3.1. Effect of the porphyrinic starch films on HDF and HMEC viability

The cellular viability assay using MTS tetrazolium compound is based on the conversion of the tetrazolium salt to a colored formazan dye by NADPH-dependent dehydrogenase enzymes in metabolically active cells. Thus, the measurement of metabolic activity is an indicator of cell viability, cytotoxicity or proliferation. An area of 28.27 $mm^2$ was irradiated or non-irradiated with red light

at irradiance of 5 mW $cm^{-2}$ for 15 min (total light dose of 4.5 J $cm^{-2}$) and the results found are depicted at at Fig. 3.7.

The results point out that in the presence of starch-based films (TPS) with 28.27 $mm^2$, the metabolic activity is significantly reduced when compared with non-treated cells (control group, $p<0.05$), even in the dark (non-irradiated groups). Moreover, the film control group (TPS film without any PS) displays reduced metabolic activity levels, which can mean a direct cytotoxic effect of the TPS films in both cell lines. Additionally, the red-light irradiation of the cells in the presence of **TPS/PS** films did not demonstrate any statistically significant difference on the metabolic activity of HMEC or HDF (when compared to non-irradiated samples, $p>0.05$), which can highlight a negligible photocytotoxic effect by porphyrinic PS.

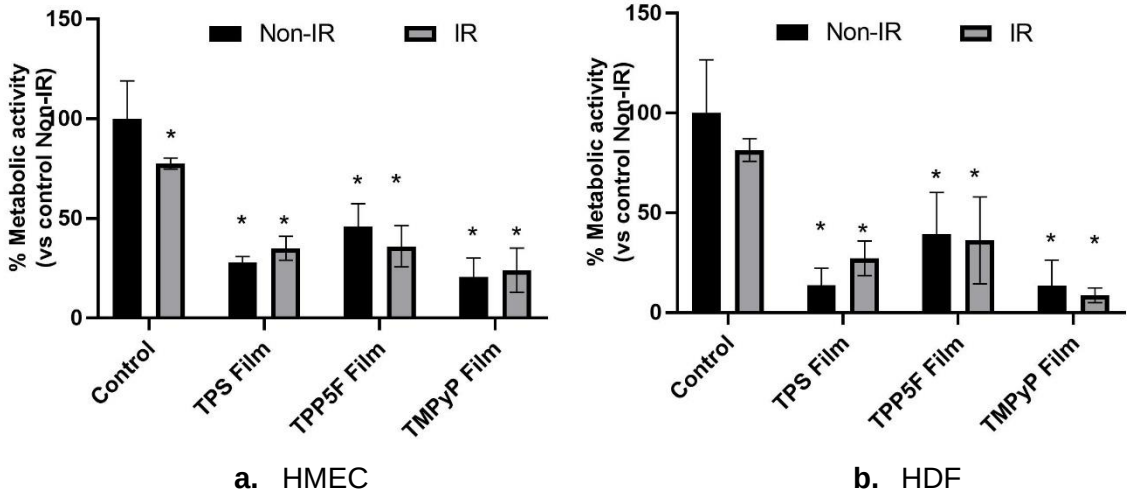


**Fig. 3.7-** Metabolic activity of HMEC **(a.)** and HDF **(b.)**, in percentage, 24 h after treatment with 28.27 $mm^2$ films (**TPS, TPP5F** or **TMPyP)** non-irradiated (Non-IR) or irradiated (IR) with red-light at irradiance of 5 mW $cm^{-2}$ (total light dose of 4.5 J $cm^{-2}$). It was included a cell control with no film applied (control). Results present metabolic activity percentage *versus* control Non-IR mean (SD), n=5, * $p<0.05$ *vs* control Non-IR.

The toxicity exhibited from the TPS film highlights the possibility that the potato collected, the raw material used for starch extraction and applied for the manufacturing of the TPS films, could have contained some impurities, which at these concentrations may also prove to be toxic. Previous studies developed by Salgado *et al.* 2004 and Marques *et al.* 2005, using starch-based materials in cell lines demonstrated excellent biocompatibility [15], [16], although their starch was originated from corn. However, it is also known that depending on the starch sources, the extrusion process that starch undergoes to form materials may alter its physical, chemical and functional properties, significantly [17]. Besides, it has also been found that the degradation of starch inhibits cell growth. Gomes *et al.*

2001 finds that thermal-mechanical degradation of starch materials leads to a release of low-molecular weight chains that can contribute to a decrease in cell proliferation [18]. Thus, it cannot be disregarded the possibility that on the assays performed, a possible leachable toxic content been released by solubilization in the cells medium.

In order to verify the effects of the films' size in cells, TPS films of smaller dimensions were tested (14.13 $mm^2$ and 7.06 $mm^2$), and the PDT assays were repeated in the same experimental conditions as previously. The results are summarized in Figs. 3.8 and 3.9.

Regarding the Figure 3.8, where are summarized the results obtained using **TPS** films with an area of 14.13 $mm^2$, there can be observed differences in terms of metabolic activity in both cell lines. In the case of HMEC, it is observed for the non-irradiated cells, a decrease of the metabolic activity in the presence of all films tested (TPS, **TPP5F, TMPyP**) but the differences are not statistically significant when compared with the control (Fig. 3.8).

For HDF, it is observed for the non-irradiated cells, a significant decrease of the metabolic activity in the presence of all films tested (TPS, **TPP5F, TMPyP)** although less pronounced when compared with the metabolic reduction obtained in the presence of TPS films of 28.27 $mm^2$, which revealed that some film toxicity remains (Fig. 3.8 b.).

On the other hand, it was observed a HMEC stimulus in metabolic activity induced by the red light, manifested by the metabolic activity increase, when compared to non-irradiated cells ($p < 0.05$). This improvement on HMEC proliferation induced by light, although not statistically significant, was observed in the presence of the TPS film control group, as well as in the presence of **TPP5F** and **TMPyP,** when comparing with non-irradiated samples of the same group (Fig. 3.8 a).

Regarding the effect of light on HDF (Fig. 3.8 b), the cell's improvement in metabolic activity is not present, as in HMEC. Furthermore, in the presence of **TMPyP** films and irradiated, the cells exhibit a reduction in the metabolic activity, when compared to the non-irradiated control group ($p < 0.05$). TMPyP is a known good singlet oxygen generator upon illumination by adequate wavelength [19]. There are reports of non-immobilized TMPyP at low concentrations of (0.5-10 µM) being able to significantly decrease viability of different cell lines when irradiated [20]–[23]. In the case of this study, however, there are no significant differences between the irradiated and non-irradiated cells treated with the TPS/TMPyP film, indicating the absence of a phototoxic effect.

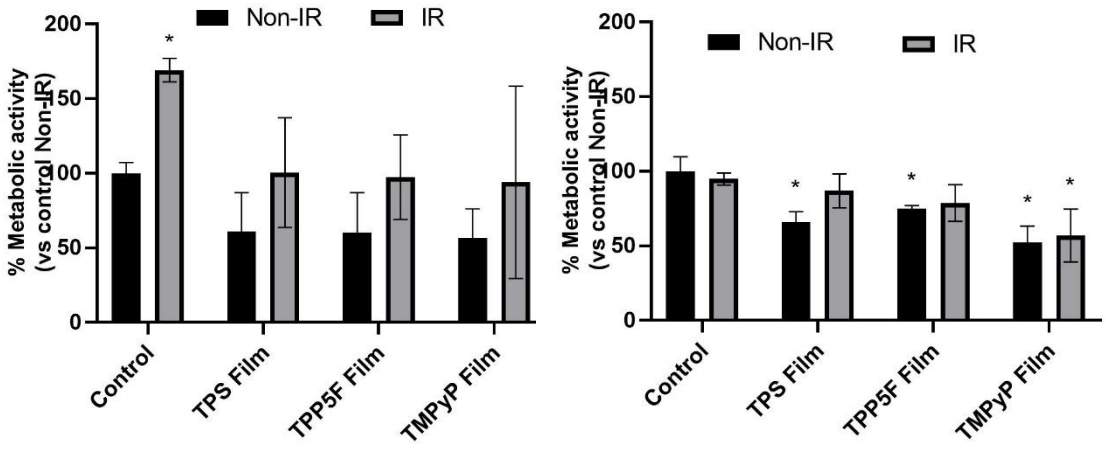


**a.** HMEC **b.** HDF

**Fig. 3.8** - Metabolic activity of HMEC **(a.)** and HDF **(b.)**, in percentage, 24 h after treatment with 14.13 $mm^2$ films (**TPS, TPP5F** or **TMPyP)** non-irradiated (Non-IR) or irradiated (IR) with red-light at irradiance of 5 mW $cm^{-2}$ (total light dose of 4.5 J $cm^{-2}$). It was included a cell control with no film applied (control). Results present metabolic activity percentage *versus* control Non-IR mean (SD), n=5, * $p<0.05$ *vs* control Non-IR.

When the TPS and TPS/PS films' area was reduced for 7.06 $mm^2$ (a quarter of are of the first experiment) the most significant effect for HMEC (Fig. 3.9) was found. It seems that, as observed before, the control group shows cellular viability improvement upon red light irradiation, when compared to the non-irradiated control ($p < 0.05$). Furthermore, at these experimental conditions a significant improvement on the HMEC viability was found upon treatment with **TPP5F** film and irradiated with red light ($p < 0.05$). Nevertheless, no significant differences between the irradiated control and the irradiated cells treated with the **TPP5F** film were found ($p > 0.05$). It seems undeniable, that the low light dose delivered into the cells (in this case, 4.5 J $cm^{-2}$) provides beneficial effects for HMEC and perhaps for the vascularization process too. This effect has indeed been reported in the literature as it has been previously observed that a low light density (4 J $cm^{-2}$) at a wavelength of 635 nm resulted in a significant increase in proliferation of endothelial cells, similar parameters as the ones here tested [24]. Furthermore, LLLT (in similar conditions as these) has also been found to influence the production of growth factors, the vasodilation of the vessels and other interactive components of the tissue remodeling process [25].

Concerning the viability of HDF, neither light nor treatment with TPS/PS films produced a significant effect on the metabolic activity, as the cell metabolic activity did not appear to significantly change after PDT treatment. Regarding

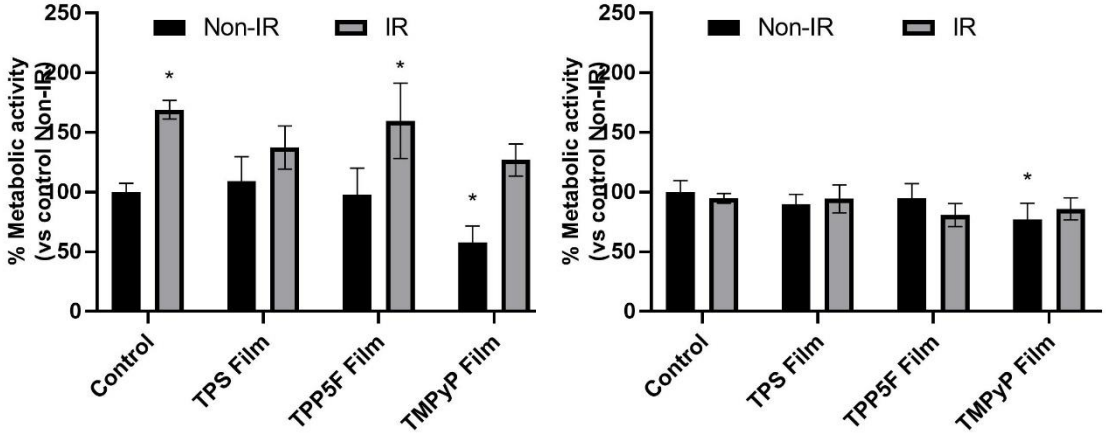


**a.** HMEC **b.** HDF

**Fig. 3.9-** Metabolic activity of HMEC **(a.)** and HDF **(b.)**, in percentage, 24 h after treatment with 7.06 $mm^2$ films (**TPS, TPP5F** or **TMPyP)** non-irradiated (Non-IR) or irradiated (IR) with red-light at irradiance of 5 mW $cm^{-2}$ (total light dose of 4.5 J $cm^{-2}$). It was included a cell control with no film applied (control). Results present metabolic activity percentage *versus* control Non-IR mean (SD), n=5, * $p<0.05$ *vs* control Non-IR.

photobiomodulation in fibroblasts, there seems to be some contradictory studies in the literature [26]. On one hand, Mokoena *et al.* 2019 have reported an increase in cell viability and proliferation after infrared irradiation with light of 830 nm and a total light dose of 5 J $cm^{-2}$ [27]. Similarly Rahbar *et al.* 2020 report an increase in cell viability, proliferation and migration of diabetic human dermal fibroblasts when irradiated with red light of 632.8 nm and a total light dose of 0.5 J $cm^{-2}$ [28]. On another hand, Pansani *et al.* 2017 used a total light dose of of 3 J $cm^{-2}$ at 780 nm and report only a small increase in gingival fibroblasts' viability and proliferation. However, this effect was only noticeable after 72 h, and even then it is not statistically different from the control group at the same time point [29]. It is known that different wavelengths will produce different outcomes, for instance, blue light has been found to inhibit mitochondrial activity, suppress differentiation and decrease migration in fibroblasts [30] which can have applications in reducing tissue fibrosis. And although red light is generally thought to induce cell viability and proliferation, is has also been reported to inhibit fibroblast differentiation into myofibroblasts (0.3 J $cm^{-2}$). [31] Theodoro *et al.* 2020 using red light (635 nm) irradiation and different light doses (ranging from 0.2 J $cm^{-2}$ to 2.91 J $cm^{-2}$) found no differences in cell viability between them after 24 h, and after 3 days of treatment with 1.6 J $cm^{-2}$ found no differences in fibroblast viability between treated and control groups [32]. Thus, the results found in this study seem to be in accordance with these last studies, where red light did not produce a significant effect on fibroblast viability.

Regarding the cells treated only with the TPS/**TMPyP** film (non-irradiated), results show a significant decrease in cell viability for both cell types. In the case of HMEC, it seems that the cells when treated with TPS/**TMPyP**-based film and irradiated reverted the cytotoxic effect of the non-irradiated sample.

To evaluate the possibility of the TPS films retaining the MTS reagent used and, in this way, produce a misleading result, the experimental protocol was modified, and the films were removed from the wells prior to adding the MTS reagent. To perform this experiment, the film area 28.27 $mm^2$ was selected, where the cell metabolic activity had suffered the most significant reduction. The results obtained are displayed in (Fig. 3.10).

The results point out that, in HMEC, the cell metabolic activity decreased when the starch-based films (TPS) are applied, either alone or with PS immobilized ($p < 0.05$). However, in HDF, this decrease is not so marked as previously (Fig. 3.7) or even when compared to the results in HMEC. In fact, no statistical differences were found between the TPS, or TPS/PS treated cells and the HDF control. Indeed, the cell viability remains above 68% in all tested conditions where starch-based films were applied, with **TPP5F**, **TMPyP** or without PS, irradiated or non-irradiated. This is a marked improvement from the first assay, where viability remained below 40% for film-treated groups. In fact, films may have adsorbed either part of the MTS substrate, part of the formazan product formed, or both and therefore resulting in lower detected values of activity which compromise the correct evaluation of the cell's viability. By removing the film's adsorbing effect, we are able to state that HDF cells had metabolic activity above 50%. Even so, HMEC seem to express a higher sensitivity to these starch-base film materials and its metabolic activity dropped despite the absence of the "masking" film effect. In the following experiments, films of smaller dimensions were considered more adequate for the purpose of these assays.

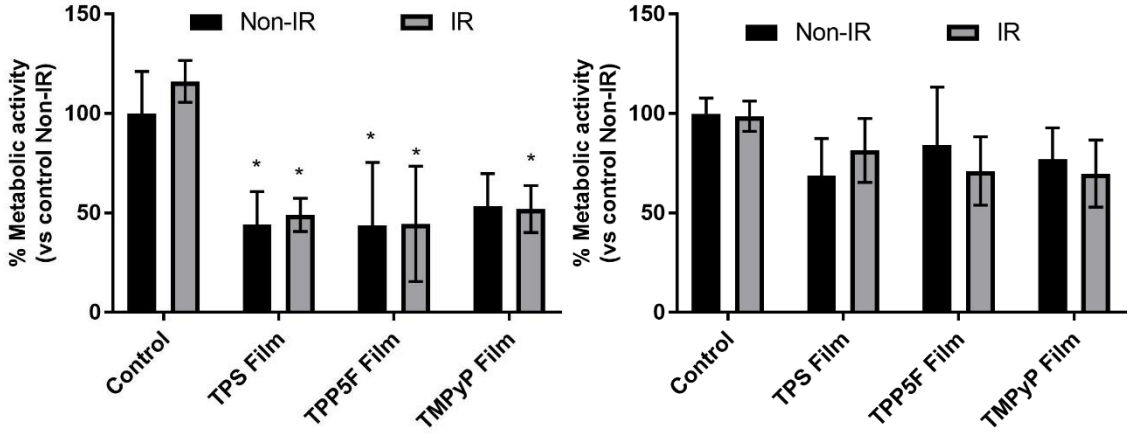


**a.** HMEC **b.** HDF

**Fig. 3.10-** Metabolic activity of HMEC **(a.)** and HDF **(b.)**, in percentage, 24 h after treatment with 28.27 $mm^2$ films (**TPS, TPP5F** or **TMPyP,** removed prior to MTS addition) non-irradiated (Non-IR), or irradiated (IR) with red-light at irradiance of 5 mW $cm^{-2}$ (total light dose of 4.5 J $cm^{-2}$). It was included a cell control with no film applied (control). Results present metabolic activity percentage *versus* control Non-IR mean (SD), n=5, * $p<0.05$ *vs* control Non-IR.

It is known that ROS produced in great quantities *in situ* largely affect cell viability. The same principle is taken by porphyrins when used for PDT of tumors and as antimicrobial agents. This may account for the drop of metabolic activity of live cells in the highest concentrations of TPS/PS films. A small ROS amount, however, may be beneficial to tissues, especially to fight against infections or aiding the inflammatory response. This is a very delicate equilibrium to achieve, and in which many different players are involved, such as inflammatory cells, cytokine levels, tissue oxygenation, among others. Besides this, it seems that in the starch films' composition (TPS and TPS/PS) there may be some component or impurity responsible for the cell toxicity, since HMEC viability was decreased in control (TPS) films and non-irradiated samples (**TPP5F and TMPyP**).

## 3.2. Cellular adhesion on the starch-based films

The cell adhesion is another factor that needs to be evaluated in order to understand if the biomaterial could be used as a matrix to fill the wound bed and allowed cell migration and proliferation in order to enhance the skin wound healing and tissue remodeling. As such, the different films were stained with a fluorescence label for cell nuclei and analyzed through fluorescence microscopy for their ability to accommodate cells. The general matrix of the different films appeared to differ somewhat between them (Fig. 3.11). Overall, the TPS films (without porphyrin) and **TPP5F** films were able to accommodate HMEC and HDF

cells, while in the TPS/**TMPyP** material only a small number of HMEC adhere, and no fibroblasts were observed attached to the film.

Among the three starch-based films under evaluation, the **TPP5F** film displayed the highest abundance of cells adhered, irradiated and non-irradiated, for both cell lines. The TPS film had more positive nuclei-staining for HDF than HMEC. In both **TPP5F** and **TPS** films, the irradiation did not seem to perceptively affect the adherence of the cells to the films. If anything, the irradiated films seemed to contain slightly more cells.

Overall, the structure and composition of these starch/porphyrin-based films allows for the establishment of interactions between cell and films, proving the material to be adherent. The cells presented higher preference for the **TPP5F** film, regardless of irradiation, while not adhering much to the **TMPyP** film. Between different cell lines, the HDF exhibited a higher tendency to adhere to the material than HMEC.

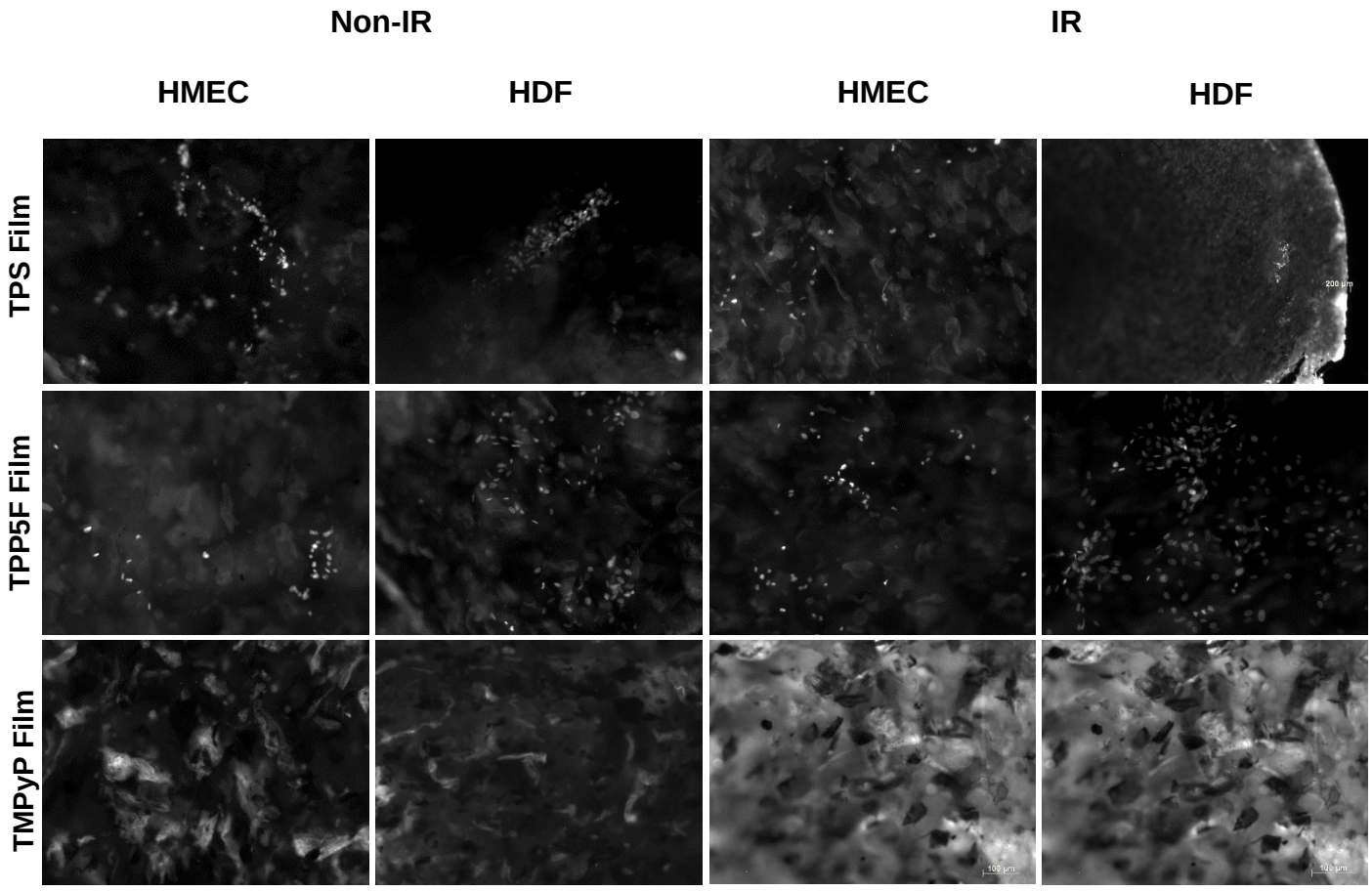


**Fig. 3.11**- Cellular adhesion assay. Representative images of DAPI cell nuclei staining of **TPS** film, **TPP5F** film and **TMPyP** film under 10x magnification, both non-irradiated (Non-IR) and irradiated, with HMEC or HDF cells, n=4 for sample.

### 3.3. The effect of porphyrinic starch films on HMEC and HDF cells migration

To evaluate the effects of the starch/porphyrin films (TPS/PS) and red-light irradiation on cell migration, a migration assay, or *in vitro* wound healing assay, was performed on HMEC and HDF. This assay involves the opening of a gap in the cellular layer which will be closed off by migrating cells. The results obtained, and summarized in Figures 3.12 and 3.13), showed that after 24 h, HDF almost completely close the gap area, with little influence when irradiated while HMEC show a pronounced improvement in migration when the cells were irradiated.

In the presence of films **TPS** and **TPP5F,** HDF cells appear slower, exhibiting an increased gap area regarding the control group, after 24 h. However, when subjected to irradiation, this effect was no longer noticeable.

In the absence of TPS/PS films, the red-light irradiation promoted migration in HMEC ($p > 0.05$), however no statistical difference was found for any other treatment group, irradiated or non-irradiated, against the non-irradiated control ($p > 0.05$).

This data seems to be in accordance with the results obtained from the viability assay. HMEC seem to be more susceptible to light and the cells thrive under the low light dose used. However, when a starch-based film is applied the ability of the cells to migrate seems to diminish. Nevertheless, this effect was only statistically relevant in HDF for the **TPS** film and **TPP5F** which were not irradiated ($p > 0.05$). Considering that no cytotoxicity was found with the MTS assay, at these concentrations of film, the reduction of rate migration could be due to the film somehow interfering by scraping the cells off the plate and impeding the closing of the gap. It is worth to refer that under visual observation, the wells correspondent to these groups exhibited a closed gap in some areas while in others it was wide open, suggesting that there was likely a physical interference.

Overall, irradiated samples displayed a smaller gap area, after 24 h than non-irradiated samples, both in HDF and HMEC, stressing the benefit of red light (Fig. 3.13). The treatment with red light and **TPS/PS**-based films, did not inhibit the wound healing of HDF and HMEC, even if the cell layer was not as homogenous as the control group.

To our knowledge, this is the first *in vitro* skin wound healing study using HDF and HMEC, no cellular migration studies were found in the literature with the two tested porphyrins **TMPyP** and **TPP5F**, either free or conjugated in supports (except for infected models [33]). However, similar studies have been performed for carboxyl group substituted porphyrins in *in vivo* wounds, and been found that treatment with photosensitizer and light favored healing and wound closure. [34]

At the conditions tested in this study, this wound closure effect was not observed, however further optimization of the parameters must be conducted in the future.

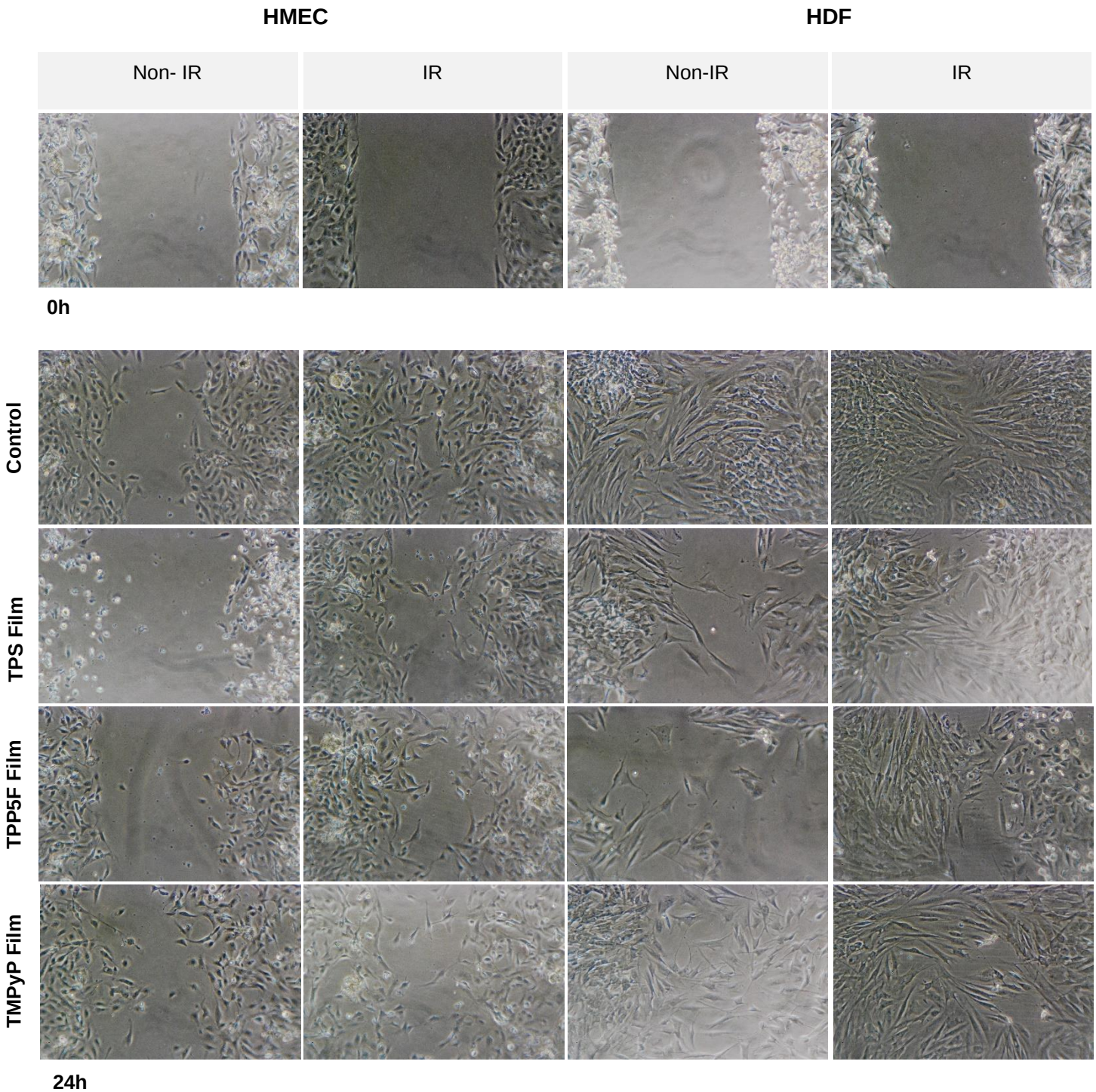


**Fig. 3.12-** Representative images of wound closure in HMEC and HDF cells, at 0h (before treatment) and 24h after treatment with red light irradiation at an irradiance of 5 mW $cm^{-2}$ for 15 min (IR), and non-irradiated (Non-IR) and 14.13 $mm^2$ films (TPS **TPP5F** and **TMPyP)** as well as cellular control (no film applied, Control). Taken with inverted microscope with 100x magnification.

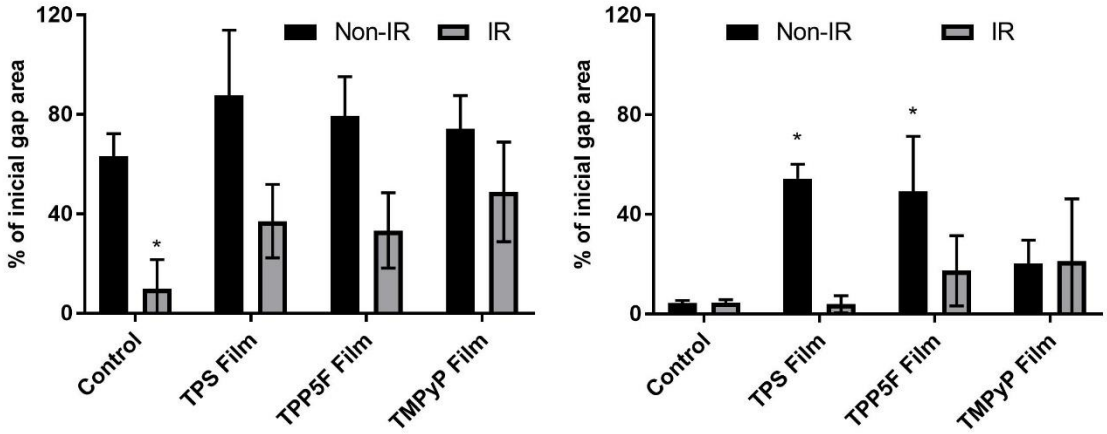


**a.** HMEC **b.** HDF

**Fig. 3.13-** Wound closure in HMEC (**a.)** and HDF **(b.)** cells, in percentage of initial gap area, 24 h after treatment with a total light dose of 4.5 J cm $^{-2}$ of red light at an irradiance of 5 mW cm$^{-2}$ (IR) and not irradiated (Non-IR), and **TPS, TPP5F** and **TMPyP** films with an area of14.13 mm$^2$ as well as cellular control (no film applied). Results present area percentage *versus* initial gap area mean (SD), n=3, * $p$<0.05 *vs* control Non-IR.

### 3.4. The effect of porphyrinic starch films on HMEC and HDF cells ROS production

As it has been previously stated, the irradiation of porphyrin derivatives leads to the production of reactive oxygen species (ROS). In order to evaluate if the production of ROS into the cells treated with the TPS/PS-based films was responsible for their toxicity, the ROS produced in HDF and HMEC cells treated with the starch-based films of 14.13 mm$^2$ and 7.06 mm$^2$ was assessed. The formation of ROS was detected using a 2',7'-dichlorofluorescein diacetate (DCFDA) Cellular ROS Detection Assay Kit. DCFDA is a fluorogenic dye that after diffusion into the cell is deacetylated by cellular esterases to a non-fluorescent compound. When it encounters ROS, it is oxidized into 2',7'-dichlorofluorescein (DCF) which is a highly fluorescence compound. The detection was performed in two moments: immediately after (0 h) light irradiation (Fig. 3.14) and 24 h after irradiation (Fig. 3.15). The two periods of evaluation allow for an understanding of the photodynamic action and if the cells develop oxidative stress.

The results obtained point out that during red light irradiation, in both cell lines, the presence of 14.13 mm$^2$ **TPS** film and TPS/**TPP5F** film did not affect the level of ROS produced into the cells, since the ROS production was similar to the amount of ROS present in the control (Fig. 3.14). The only film that increased the level of ROS produced into the cells was the TPS/**TMPyP** film. In fact, when the

cells were irradiated in the presence of this film, the amount of ROS detected is two times higher. Similar results were obtained for the cells treated with the films with 7.06 $mm^2$ and irradiated with red light (Fig. 3.15). Under these conditions (14.13 $mm^2$ and red light) the TPS/**TMPyP** film seems to produce identical ROS amounts in the two cell lines. However, the ROS production of non-irradiated cells in the presence of 7.06 $mm^2$ of the TPS/**TMPyP** film diminished when compared with the ROS produced when 14.13 $mm^2$ films were used. In the latter case, no

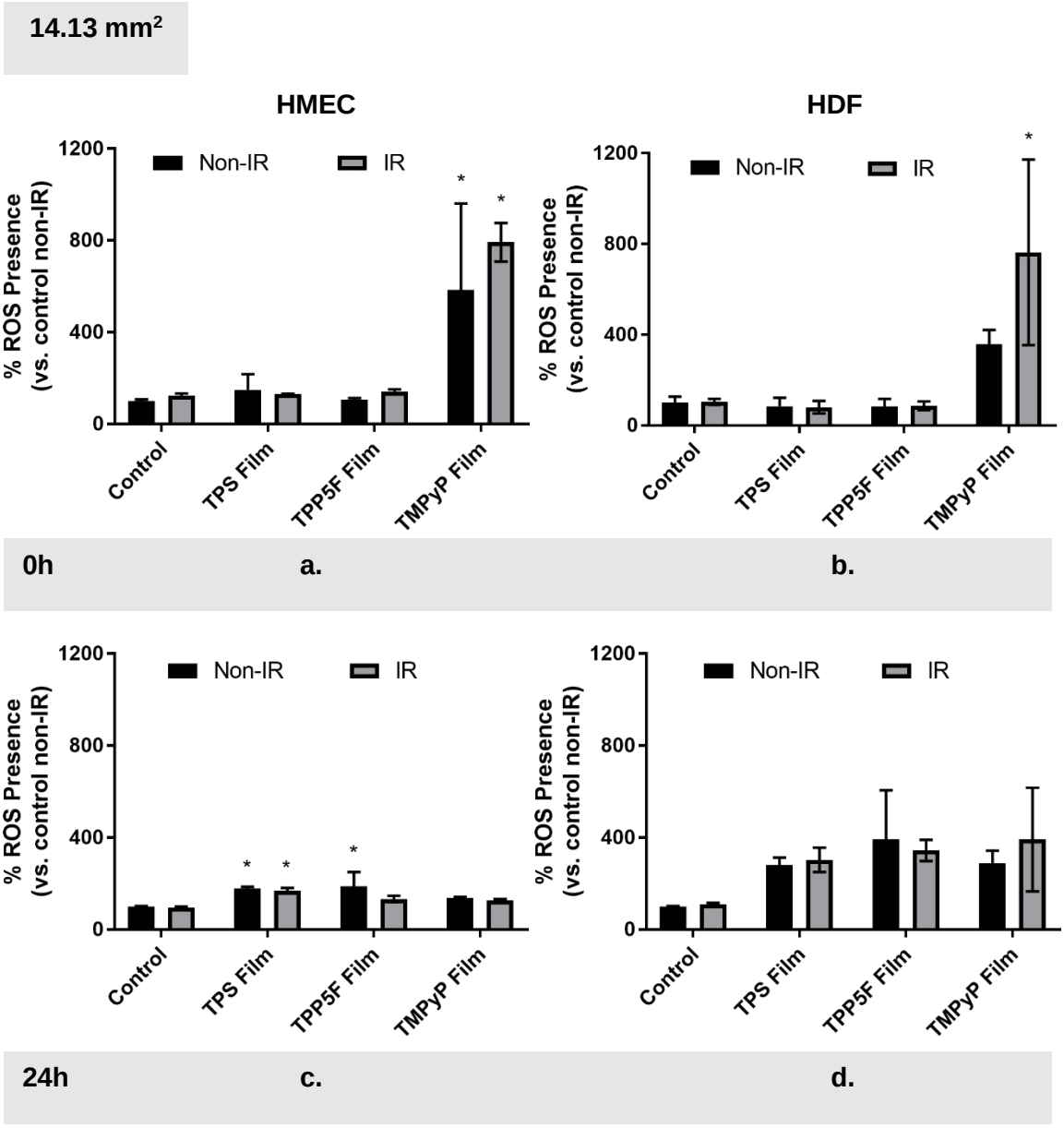


**Fig. 3.14-** ROS detection of HMEC **(a., c.)** and HDF **(b., d.)**, in percentage. Results obtained 0 h (**a., b**.) and 24 h (**c., d**.) after treatment with 4.5 J $cm^{-2}$ of red light (IR) or without red light (Non-IR) and 14.13 $mm^2$ films with porphyrins TPS/**TPP5F** or TPS/**TMPyP** as well as control film (without porphyrin) and control (no film applied). Results present ROS presence percentage *versus* control Non-IR mean (SD), n=3, * $p<0.05$ *vs* control Non-IR.

significant differences were found between the amount of ROS measured in the non-irradiated cells treated with 7.06 $mm^2$ of TPS/**TMPyP** film and the control group. The different results obtained between the irradiated and non-irradiated TPS/**TMPyP** group of cells can be explained by the presence of TMPyP, embedded in the starch-based film. TMPyP is a good singlet oxygen generator, and light is a key factor to generate the photodynamic action which leads to the production of ROS, as porphyrins in the free form absorb light.

**7.06 $mm^2$**

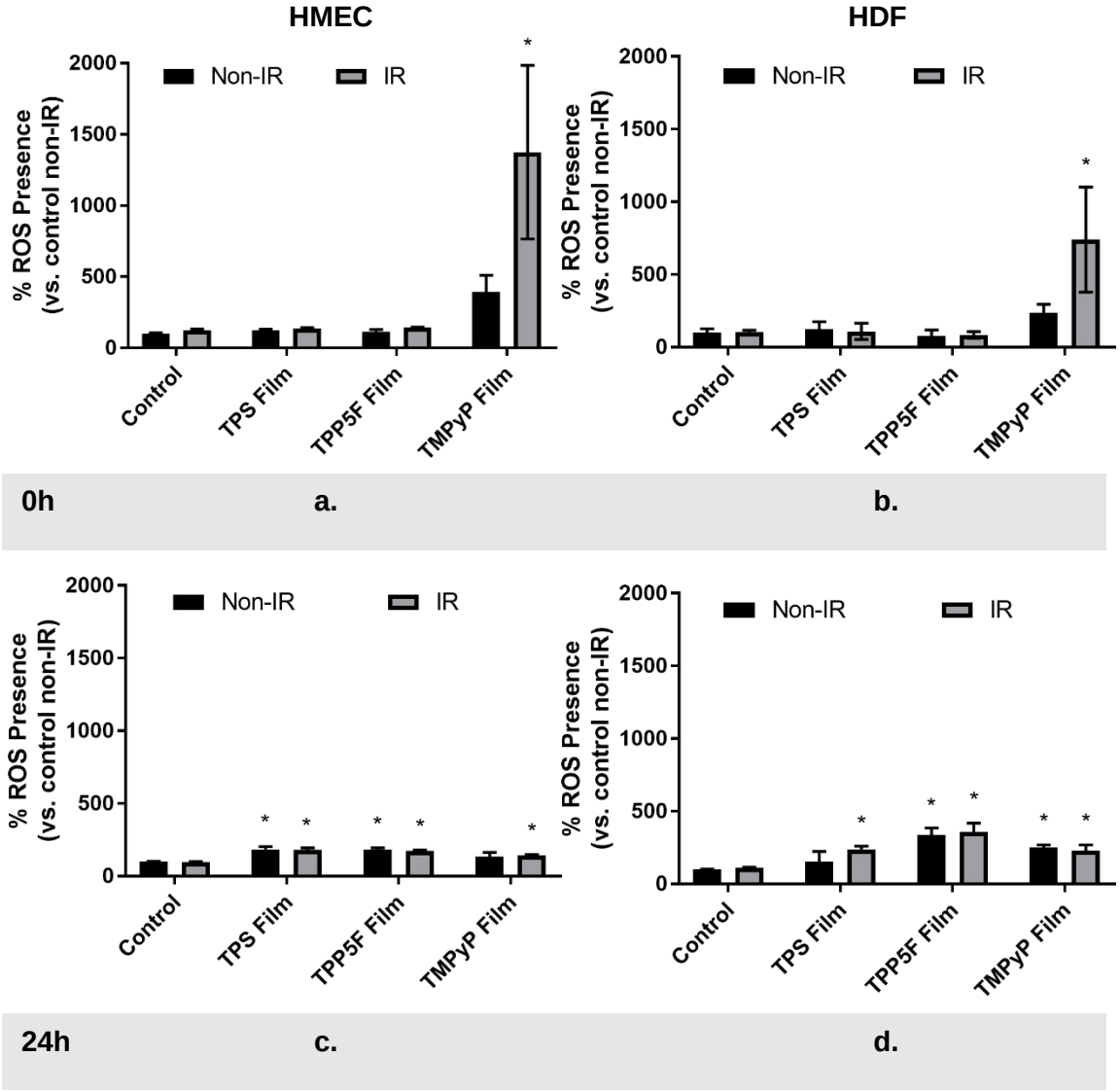


**Fig. 3.15-** ROS detection of HMEC **(a., c.)** and HDF **(b., d.)**, in percentage. Results obtained 0 h (**a., b**.) and 24 h (**c., d**.) after treatment with 4.5 J $cm^{-2}$ of red light (IR) or without red light (Non-IR) and 7.06 $mm^2$ films with porphyrins TPS/**TPP5F** or TPS/**TMPyP** as well as control film (without porphyrin) and control (no film applied). Results present ROS presence percentage *versus* control Non-IR mean (SD), n=3, * $p<0.05$ *vs* control Non-IR.

Furthermore, it can also be observed that the **TPS** film does not directly produce ROS, as both irradiated and non-irradiated samples displayed similar amounts as the control group immediately after irradiation, which can be attributed to the basal ROS production by the cells.

After 24 h of film exposition (and 24 h since light irradiation), in both cell lines and for both film sizes (7.06 $mm^2$ and 14.13 $mm^2$), cells treated with **TPS** film and TPS/**TPP5F** and TPS/**TMPyP** films exhibited, in general, higher ROS production than the control, although this increase in the ROS production was particularly evident in the cells treated with smaller discs (7.06 $mm^2$; $p$ <0.05) (Fig. 3.15). Furthermore, the irradiation of the cells 24 h prior the ROS analysis did not result in a higher presence of ROS in the cells, after this period. In fact, the high amount of ROS found in the cells treated with the TPS/**TMPyP** film and irradiated, immediately after the irradiation, seems to have disappeared and the intracellular levels of ROS were similar or lower than the ones found in the cells treated with other films (**TPS** and TPS/**TPP5F**).

According to these results, it seems unlikely that the beneficial effects in the viability and wound healing assays regarding irradiated samples are due to ROS levels, as they are identical to their non-irradiated counterparts. Similarly, it cannot be held accountable for the toxicity found. For one, the higher amounts of ROS are found in HDF, which seems to suffer less changes in metabolic activity. Secondly, we can also find significantly increased ROS in cells treated with the smaller films, the size that showed better cell viability results.

This increase in ROS presence in the cells does not seem to be a direct result of the PDT treatment, as the ROS levels after irradiation were only higher for the TPS/**TMPyP** film and dropped after irradiation to similar levels as the other film groups. The degradation of the starch can explain the fact that only after 24 h the cells start to exhibit higher levels of ROS, including the TPS film, which has no photosensitizer embedded. Starch is commonly regarded as totally biodegradable since it is constituted by the two major components: amylose, a mostly linear α-D-(1-4)-glucan and amylopectin, an α- D -(1→4)-glucan with α- D -(1→6) linkages at the branch point and contains glucose as monomer. It can be hydrolysed by amylases and glucosidases and generate glucose, maltose or maltotriose. The process of biodegradation, often also generates low molecular mass components that may interfere with physiological activity and/or even display cell toxicity [35]. The starch-based materials are not only starch, but processed starch with additives to form a thermal plastic starch material. The starch processing as well as the chemical composition may affect the cell rate of enzymatic degradation by cells and presence of these low weight “leachable” contents [36]. The efforts of the cells to metabolize the small degradation

products may lead to the generation of ROS as a byproduct of enzymatic activity and account for the higher levels presented in this study, after 24 h. To avoid this possible degradation effect, the films should be replaced after a number of hours of being exposed to the wound. To understand whether this increase leads to oxidative stress in the cells, other studies should be performed, to evaluate the activity of the antioxidant enzymes, among others.

The absence of significant difference between irradiated and non-irradiated groups, found in this assay can be a result of the short lifetime of the singlet oxygen produced by the porphyrins upon irradiation, and after 24 h, the effects of the irradiation were no longer observed. The MTS assay allowed for the understanding that light not only affects porphyrins but the cells as well and it has been found that light wavelength greatly affects ROS production from cells. George *et al.* report that 636 nm (red region) did not stimulate human dermal fibroblasts to form ROS, while a wavelength of 835 nm (near infrared region) greatly increased the number of ROS [37]. In keratinocytes, it has been reported that red light affects antioxidant pathways and stimulates the anti-inflammatory response [38]. It is possible the red light applied in this study stimulated the antioxidant system in HMEC, which would explain the improvement in metabolic activity, observed in the MTS assay, in irradiated against non-irradiated groups of these cells.

With the available collected data, it becomes clear that the toxicity presented in the MTS assay is not in fact a representation of the action of the porphyrins, but of the starch film, as the effects are similar for all three films (TPS film, TPS/**TPP5F** film, and TPS/**TMPyP**), and that light is the sole responsible for the improvement in cell viability and wound healing.

## 4. Conclusions

The starch/porphyrin (TPS/PS) films seemed to exhibit a detrimental effect in the cellular viability of HMEC, detected through the metabolic activity of cells, for films of area 28.27 $mm^2$, while HDF seemed to tolerate the prepared starch-based films. Red light at 652 nm at an irradiance of 5 mW $cm^{-2}$ applied for 15 min proved to increase cellular viability of endothelial cells (HMEC) as well as cellular migration, which is a benefit for angiogenesis during tissue wound healing (Table 3.1). The use of TPS/**TPP5F** and TPS/**TMPyP** films under red light irradiation seems to control the fibroblasts (HDF) migration and proliferation which is important in order to reduce fibrosis in the wound healing process. HMEC showed a higher response to irradiation than HDF. The starch-based films used exhibited toxicity to cells after 24 h, and increased ROS levels. The high level of intracellular

ROS was found in cells exposed to smaller film samples (7.06 $mm^2$), indicating that ROS can be responsible for the activation of pathways involved in metabolic activity, migration and proliferation that should be explored in the future.

In the future, it would be important to understand the origin of the citotoxicity found for the films with 28.27 $mm^2$ and to identify the starch degradation and byproducts resulting from the starch processing. Furthermore, a comparative study with non-immobilized porphyrins should be conducted to evaluate the effects of the PS without the starch films.

This study will allow to move forward to identify potential photoactivatable materials for biomedical purposes and highlights the importance of light in biological processes, including cell viability. In a chronic wound setting, such as diabetic foot ulcers, where vascularization and healing are impaired, a dressing that is able to stimulate angiogenesis, does not impair viability and can also be modulated (by different application of light) to inactivate microorganisms is an important step into improving patients' quality of life and prevent amputations.

**Table 3.1-** Summary of the *in vitro* assays results performed on HMEC and HDF cell cultures, for 7.06 $mm^2$ films. The green arrow pointing up represents an increase on the parameter evaluated (viability, migration, or ROS levels), when compared to non-IR control. On the other way, the red arrow pointing down, represents a decrease. The asterisk next to an arrow represents a statistically significant result ($p$<0.05).

| | | **HMEC** | | | | **HDF** | | | |
|---|---|---|---|---|---|---|---|---|---|
| | | Control | TPS Film | TPS/**TPP5F** Film | TPS/**TMPyP** Film | Control | TPS Film | TPS/**TPP5F** Film | TPS/**TMPyP** Film |
| **Viability** | Non-IR | - | ↑ | = | ↓* | - | ↓ | = | ↓* |
| | IR | ↑* | ↑ | ↑* | ↑ | ↓ | ↓ | ↓ | ↓ |
| **Wound Healing** | Non-IR | - | ↓ | ↓ | ↓ | - | ↓* | ↓* | ↓ |
| | IR | ↑* | ↑ | ↑ | ↑ | = | = | ↓ | ↓ |
| **ROS (0 h)** | Non-IR | - | = | = | ↑ | - | = | = | ↑ |
| | IR | = | = | = | ↑* | = | = | = | ↑* |
| **ROS (24 h)** | Non-IR | - | ↑* | ↑* | ↑ | - | ↑ | ↑* | ↑* |
| | IR | = | ↑* | ↑* | ↑* | ↑ | ↑* | ↑* | ↑* |

## 5. References


[1] D. J. Tobin, “Biochemistry of human skin—our brain on the outside,” *Chem. Soc. Rev.*, vol. 35, no. 1, pp. 52–67, 2006.

[2] L. A. Brodell and K. S. Rosenthal, “Skin structure and function: The body’s primary defense against infection,” *Infect. Dis. Clin. Pract.*, vol. 16, no. 2, pp. 113–117, 2008.

[3] A. Shukla, P. Nandi, and M. Ranjan, “Acellular Dermis as a Dermal Matrix of Tissue Engineered Skin Substitute for Burns Treatment,” *Ann. Public Heal. Res.*, vol. 2, no. 3, p. 1023, 2015.

[4] M. H. Ross and W. Pawlina, *Histology: A Text and Atlas: With Correlated Cell and Molecular Biology, 6th Edition*, 6th Editio., vol. 66. Lippincott Williams & Wilkins, 2012.

[5] J. E. Lai-Cheong and J. A. McGrath, “Structure and function of skin, hair and nails,” *Med. (United Kingdom)*, vol. 41, no. 6, pp. 317–320, 2013.

[6] M. Navarro, J. Ruberte, and A. Carretero, “Common integument,” in *Morphological Mouse Phenotyping: Anatomy, Histology and Imaging*, 1st ed., Elsevier Ltd., 2017, pp. 541–562.

[7] E. P. Widmaier, H. Raff, and K. T. Strang, *Vander’s Human Physiology: The Mechanisms of Body Function, 14th Edition*, 14th Editi. New York: McGraw-Hill Education, 2016.

[8] A. Krüger-Genge, A. Blocki, R. P. Franke, and F. Jung, “Vascular endothelial cell biology: An update,” *Int. J. Mol. Sci.*, vol. 20, no. 18, p. 4411, 2019.

[9] D. Bouïs, G. A. P. Hospers, C. Meijer, G. Molema, and N. H. Mulder, “Endothelium in vitro: A review of human vascular endothelial cell lines for blood vessel-related research,” *Angiogenesis*, vol. 4, no. 2, pp. 91–102, 2001.

[10] S. Porter, “The role of the fibroblast in wound contraction and healing,” *Wounds UK*, vol. 3, no. 1, pp. 33–40, 2007.

[11] P. Bainbridge, “Wound healing and the role of fibroblasts,” *J. Wound Care*, vol. 22, no. 8, pp. 407–412, 2013.

[12] A. M. Smith, S. Moxon, and G. A. Morris, *Biopolymers as wound healing materials*, vol. 2. Elsevier Ltd, 2016.

[13] P. Avci *et al.*, “Low-level laser (light) therapy (LLLT) in skin: stimulating, healing, restoring.,” *Semin. Cutan. Med. Surg.*, vol. 32, no. 1, pp. 41–52, 2014.

[14] M. R. Hamblin, “Photobiomodulation or low-level laser therapy,” *J. Biophotonics*, vol. 9, no. 11–12, pp. 1122–1124, 2016.

[15] A. J. Salgado, O. P. Coutinho, and R. L. Reis, “Novel Starch-Based Scaffolds for Bone Tissue Engineering: Cytotoxicity, Cell Culture, and Protein Expression,” *Tissue Eng.*, vol. 10, no. 3–4, pp. 465–474, 2004.

[16] A. P. Marques, H. R. Cruz, O. P. Coutinho, and R. L. Reis, “Effect of starch-based biomaterials on the in vitro proliferation and viability of osteoblast-like cells,” *J. Mater. Sci. Mater. Med.*, vol. 16, no. 9, pp. 833–842, 2005.

[17] P. Fallahi, K. Muthukumarappan, and K. A. Rosentrater, “Functional and structural properties of corn, potato, and cassava starches as affected by a single-screw extruder,” *Int. J. Food Prop.*, vol. 19, no. 4, pp. 768–788, 2016.

[18] M. E. Gomes, R. L. Reis, A. M. Cunha, C. A. Blitterswijk, and J. D. De Bruijn, “Cytocompatibility and response of osteoblastic-like cells to starch-based polymers: Effect of several additives and processing conditions,” *Biomaterials*, vol. 22, no. 13, pp. 1911–1917, 2001.

[19] A. Garcia-Sampedro, A. Tabero, I. Mahamed, and P. Acedo, “Multimodal use of the porphyrin TMPyP : From cancer therapy to antimicrobial applications,” *J. Porphyr. Phthalocyanines*, vol. 23, no. February, pp. 1–17, 2019.

[20] A. Hanakova *et al.*, “The application of antimicrobial photodynamic therapy on S. aureus and E. coli using porphyrin photosensitizers bound to cyclodextrin,” *Microbiol. Res.*, vol. 169, no. 2–3, pp. 163–170, 2014.

[21] K. Kassab, “Evaluating the antitumor activity of combined photochemotherapy mediated by a meso-substituted tetracationic porphyrin and adriamycin,” *Acta Biochim. Biophys. Sin. (Shanghai).*, vol. 41, no. 11, pp. 892–899, 2009.

[22] V. Cenklová, “Photodynamic therapy with TMPyP – Porphyrine induces mitotic catastrophe and microtubule disorganization in HeLa and G361 cells, a comprehensive view of the action of the photosensitizer,” *J. Photochem. Photobiol. B Biol.*, vol. 173, no. December 2015, pp. 522–537, 2017.

[23] A. Jiménez-Banzo, M. L. Sagristà, M. Mora, and S. Nonell, “Kinetics of singlet oxygen

photosensitization in human skin fibroblasts," *Free Radic. Biol. Med.*, vol. 44, no. 11, pp. 1926–1934, 2008.
[24] J. Szymanska *et al.*, "Phototherapy with low-level laser influences the proliferation of endothelial cells and vascular endothelial growth factor and transforming growth factor-beta secretion," *J. Physiol. Pharmacol.*, vol. 64, no. 3, pp. 387–91, 2013.
[25] F. Colombo, A. de A. P. V. Neto, A. P. C. de Sousa, A. M. T. Marchionni, A. L. B. Pinheiro, and S. R. de A. Reis, "Effect of low-level laser therapy (λ660 nm) on angiogenesis in wound healing: A immunohistochemical study in a rodent model," *Braz. Dent. J.*, vol. 24, no. 4, pp. 308–312, 2013.
[26] N. Tripodi *et al.*, "The effects of photobiomodulation on human dermal fibroblasts in vitro: A systematic review," *J. Photochem. Photobiol. B Biol.*, vol. 214, no. November 2020, p. 112100, 2021.
[27] D. R. Mokoena, N. N. Houreld, S. S. Dhilip Kumar, and H. Abrahamse, "Photobiomodulation at 660 nm Stimulates Fibroblast Differentiation," *Lasers Surg. Med.*, vol. 52, no. 7, pp. 671–681, 2019.
[28] E. R. Layegh *et al.*, "Photobiomodulation therapy improves the growth factor and cytokine secretory profile in human type 2 diabetic fibroblasts," *J. Photochem. Photobiol. B Biol.*, vol. 210, no. September, p. 111962, 2020.
[29] T. N. Pansani, F. G. Basso, D. G. Soares, A. P. da S. Turrioni, J. Hebling, and C. A. de S. Costa, "Photobiomodulation in the Metabolism of LPS-exposed Epithelial Cells and Gingival Fibroblasts," *Photochem. Photobiol.*, vol. 94, no. 3, pp. 598–603, 2017.
[30] L. Y. Chang, S. M. Y. Fan, Y. C. Liao, W. H. Wang, Y. J. Chen, and S. J. Lin, "Proteomic Analysis Reveals Anti-Fibrotic Effects of Blue Light Photobiomodulation on Fibroblasts," *Lasers Surg. Med.*, vol. 52, no. 4, pp. 358–372, 2020.
[31] C. Sassoli *et al.*, "Low intensity 635 nm diode laser irradiation inhibits fibroblast-myofibroblast transition reducing TRPC1 channel expression/activity: New perspectives for tissue fibrosis treatment," *Lasers Surg. Med.*, vol. 48, no. 3, pp. 318–332, 2016.
[32] V. Theodoro *et al.*, "Inhibitory effect of red LED irradiation on fibroblasts and co-culture of adipose-derived mesenchymal stem cells," *Heliyon*, vol. 6, no. 5, p. e03882, 2020.
[33] L. Sun, L. Song, X. Zhang, R. Zhou, J. Yin, and S. Luan, "Poly(γ-glutamic acid)-based electrospun nanofibrous mats with photodynamic therapy for effectively combating wound infection," *Mater. Sci. Eng. C*, vol. 113, no. April, p. 110936, 2020.
[34] J. C. E. Silva *et al.*, "Evaluation of the use of low level laser and photosensitizer drugs in healing," *Lasers Surg. Med.*, vol. 34, no. 5, pp. 451–457, 2004.
[35] M. A. Araújo, A. M. Cunha, and M. Mota, "Enzymatic degradation of starch-based thermoplastic compounds used in protheses: Identification of the degradation products in solution," *Biomaterials*, vol. 25, no. 13, pp. 2687–2693, 2004.
[36] H. S. Azevedo, F. M. Gama, and R. L. Reis, "In vitro assessment of the enzymatic degradation of several starch based biomaterials," *Biomacromolecules*, vol. 4, no. 6, pp. 1703–1712, 2003.
[37] S. George, M. R. Hamblin, and H. Abrahamse, "Effect of red light and near infrared laser on the generation of reactive oxygen species in primary dermal fibroblasts," *J. Photochem. Photobiol.*, vol. 188, no. November, pp. 60–68, 2018.
[38] Q. Sun, H. E. Kim, H. Cho, S. Shi, B. Kim, and O. Kim, "Red light-emitting diode irradiation regulates oxidative stress and inflammation through SPHK1/NF-κB activation in human keratinocytes," *J. Photochem. Photobiol. B Biol.*, vol. 186, pp. 31–40, 2018.

# Chapter 4. Considerations and Future Perspectives

The literature review conducted for the production of this work allowed for the understanding of the potential of light therapies for biomedical applications. Diabetic foot ulcers resulting of the *diabetes mellitus* disease, and the rise of antimicrobial resistance demand increased health care attention. Thus, it is important to consider new ways to both prevent infection and promote healing in patients' wounds. Porphyrins, in combination with light reveal promise in treating infections and have been proposed for wound healing purposes, which was addressed in chapter 1. This work considered the use of porphyrins immobilized in starch-based materials as a dressing to prevent infection and promote tissue regeneration.

The application envisioned for the films used in this work, far extended what was possible to study in the short time that comprised the preparation of this thesis. Despite the information that was gathered in this work, other studies should be performed to achieve a safe biomedical application.

Regarding the antimicrobial studies, the ability of the TPS/TMPyP film to inactivate MRSA was promising, however, the potential of TPS/TPP5F to promote microbial photoinactivation when in higher concentration in the films should be explored. Furthermore, although more challenging, the photoinactivation of gram-negative bacteria, such as *Pseudomonas aeruginosa* should not be put aside, but rather optimized, perhaps with different light dosages, porphyrin concentrations, formulations, and adjuvants like potassium iodide.

Regarding the skin wound healing studies, many other parameters must be characterized to understand the "full picture" of what is happening as an effect of the TPS film + light treatment, such as apoptosis, oxidative stress biomarkers, and proliferation, to name a few. The origin of the toxic TPS films effect on cells must be identified, once it was not clear whether it was due to a toxic component present in the starch films produced by potato raw material, or a result from natural degradation that negatively affect the cells' viability. Furthermore, as this work mainly focused on the treatment of diabetic foot ulcers, *in vitro* assays simulating the conditions found in diabetic patients would be an asset to understand the potential of this treatment.

The studies presented in this work were a result of a first approach to this complex problem that we proposed to tackle, and as such they must all be subjected to further optimization. Still, porphyrins demonstrated tremendous potential in both antimicrobial and skin wound healing studies and are assuredly a path to follow. Although their immobilization into starch-based supports was

successful, their potential goes beyond that, and other supports might prove equally (or even more) interesting for the applicability here presented. Considering all this, the work is definitely not over, and its continuation is certain to bring enrichment for the scientific knowledge and possibly the opening of new horizons in the wound healing field.